DESIGN OF SOLAR WATER HEATING SYSTEMS FOR COLD CLIMATE AND STUDY OF HEAT TRANSFER ENHANCEMENT DEVICES IN FLAT-PLATE SOLAR COLLECTORS

ALIREZA HOBBI

A Thesis

in

The Department

of

Mechanical and Industrial Engineering

Presented in Partial Fulfillment of the Requirements

For the Degree of Master of Applied Science (Mechanical Engineering) at

Concordia University

Montreal, Quebec, Canada

March 2007

Your file Votre référence
ISBN: 978-0-494-28938-9
Our file Notre référence
ISBN: 978-0-494-28938-9

ABSTRACT

Design of Solar Water Heating Systems for Cold Climate and Study of Heat Transfer Enhancement Devices in Flat-Plate Solar Collectors

ALIREZA HOBBI

Solar water heating systems with the flat-plate collectors are studied theoretically and experimentally. In theoretical part of this study, a forced circulation solar water heating systems is designed for domestic hot water requirements of a single family residential unit in Montreal. All necessary design parameters are studied and optimized using TRANSYS simulation program. The solar fraction of the entire system is used as the optimization parameters. The results show that by utilizing solar energy, the designed system could provide 85-100% and 30-40% of the hot water demand in summer and winter, respectively.

The experimental part of this study is focused on the investigation of the effect of heat transfer augmentation devices inside the tubes of a flat-plate solar collector. An indoor experimental facility is developed, and different modules of flat-plate collectors with heat enhancement devices are designed and fabricated. Heat is provided by radiation and local temperature measurements were made at different locations inside and outside the collector over a range of Reynolds numbers from 200 to 5500 and two different incidents radiant heat fluxes. For the entire Reynolds number range, no appreciable heat enhancement is observed due to the heat enhancement devices. The analysis showed that in all cases, the free convection is the dominant mode of heat transfer compared to the forced convection. Thus, the turbulence production due to shear is suppressed by the thermal stratification in the flow. It is concluded that any method of heat enhancement by enhancing the shear-production of turbulence is ineffective in flat plate solar collectors.

ACKNOWLEDGMENT

I would like to express my heartfelt gratitude and thanks to my supervisor Dr. Kamran Siddiqui for his excellent guidance and encouragement throughout this work. I profoundly appreciate his kindness, trust and confidence in me.

My deep appreciation also goes to Mr. Danny Juras, Mr. Alex Berardelli, and Mr. Gilles Huard for their helpful technical assistances in my experimental work.

Finally, I wish to extend my sincere appreciations and extreme thanks to my dedicated parents and brother for their faith in me, and their tremendous and endless support and encouragement, which it made possible for me to accomplish the goal.

TABLE OF THE CONTENTS

LIST OF THE FIGURES

LIST OF THE TABLES

NOMENCLATURE

A_c	Collector area	m^2
C_B	Bond conductance	$hr.m^2K/kJ$
C_p	Specific heat of fluid	kJ/kg°C
$\overline{T}_{amb}$	Average monthly outdoor temperature	°C
$\overline{T}_{main}$	Monthly average inlet water temperature	°C
T_{amb}	Ambient temperature	°C
$T_{p,m}$	Mean absorber plate temperature	°C
$T_{f,in}$	Inlet fluid temperature	°C
$T_{f,out}$	Outlet fluid temperature	°C
T_{set}	Set temperature	°C
$T_{f,avg}$	Average bulk water temperature	
T_{ph}	Panel heater's surface temperature	°C
$T_{f,b}$	Bulk fluid temperature	°C
T_w	Pipe wall temperature	°C
D	Inner diameter of the pipe *(chapter 4)*	m
$D_{r,i}$	Inside diameter of the pipe	m
$D_{r,o}$	Outside diameter of the pipe	m
F	Fin efficiency factor	
F_R	Collector heat removal factor	
F'	Collector efficiency factor	
f	Solar fraction (annual or monthly)	
$F_{ph\text{-}c}$	Shape factor between the absorber plate and panel heater	
G_{sc}	Solar constant	
Gr	Grashof number	
Gr_q	Modified Grashof number	
h_w	Wind heat transfer coefficient	W/m^2 °C
$h_{f,i}$	Heat transfer coefficient between the pipe wall and the circulating fluid	W/m^2 °C
H_t	Tank height	m
$\overline{H}$	Monthly average total daily radiation	kJ/m^2day
$\overline{H}_T$	Monthly average radiation on a tilted surface	kJ/m^2day
$\overline{H}_d$	Monthly average diffuse radiation	kJ/m^2day
$\overline{H}_0$	Extraterrestrial daily insolation	kJ/m^2day
I_T	Solar radiation incident on the collector surface per unit area	W/m^2
$\overline{K}_T$	Monthly average clearness index	
k	Thermal conductivity	W/m^2 °C
k_f	Fluid thermal conductivity	W/m^2 °C

l	Collector length	m
L	Pipe length, test section length	m
$\dot{m}$	Flow rate	kg/sec
n	Number of riser tubes	
N_{day}	Number of days in a month	
Nu	Nusselt number	
Pr	Prandtl number	
Re	Reynolds number	
Ra	Rayleigh number	
Ra_q	Modified Rayleigh number	
Ri	Richardson number	
Ri_q	Modified Gradient Richardson number	
$\overline{R}$	Ratio of the monthly average daily radiation on the tilted surface to that on the horizontal one	
$\overline{R_b}$	Ratio of the monthly average direct (beam) radiation on a tilted surface to that on the horizontal one	
R	Collector aspect ratio, l / w	
S	Absorbed solar energy by the collector (hourly or monthly)	MJ/m^2
t	Thickness	m
q_l	Average heat transfer rate per unit length	W/m^2/m
q'_u	Useful energy gain per area per unit length	W/m^2/m
q_W	Average pipe wall heat flux	W/m^2
q_u	Useful energy	W
Q_{Load}	Total monthly (or annual) energy removed from the system	W
$Q_{Auxiliary}$	Total monthly (or annual) auxiliary energy	W
U	Flow axial velocity (Chapter 4)	m/sec
U_b	Thermal loss from the back side of the collector	W/m^2 ^{o}C
U_{side}	Thermal losses from sides of the collector	W/m^2 ^{o}C
U_L	Collector overall heat loss coefficient	W/m^2 ^{o}C
U_{top}	Collector top heat loss coefficient	W/m^2 ^{o}C
U_{tank}	Tank heat loss coefficient	kJ/hr.m^{2}K
V	Wind speed	m/sec
Vc	Tank volume	m^3
W	Collector's tube spacing	m
w	Collector width, nW	m

Greek Symbols

φ	Latitude angle	Deg
δ	Solar declination angle	Deg
β	Tilt angle	Deg
ω	Hour angle	Deg
ω_s	Solar sunset hour angle	Deg
θ	Incident angle	Deg

ρ	Density of the fluid	kg/m^3
τ	Glass transmittance	
α	Plate absorptance, Thermal diffusivity of the fluid	
$(\tau\alpha)_{avg}$	Average solar-transmittance product	
ε_g	Glass cover emittance	
ε_p	Absorber plate emittance	
λ	Spacing between glass covers	m
η	Collector efficiency	
ε_{HX}	Heat exchanger effectiveness	
δ_p	Absorber plate thickness	m
θ	Dimensionless temperature	
Δ	Difference	
ν	Kinematic viscosity	m^2/sec
β	Thermal expansion coefficient	$^oC^{-1}$

Subscripts

avg	Average
in	Inlet
out	Outlet
e	Effective
n	Normal
p	Plate
g	Glass
f	Fluid
m	mean

CHAPTER 1

INTRODUCTION AND LITERATURE REVIEW

1.1. INTRODUCTION

All signatory countries of the Kyoto Protocol including Canada are obliged to reduce the greenhouse gas emissions. Furthermore, the continuous increase in the energy demand and the depletion of fossil fuel energy resources underscore the significance of the development of energy conservation methods and utilization of the renewable energies. Renewable energies from sun, wind, and geothermal sources are ceaseless and most importantly have much less environmental impact than the conventional fossil-based energy resources. Thus, they have the high potential to substitute fossil fuels as the energy resources in buildings. Solar energy is the most abundant energy source, which can be effectively used to heat or cool the spaces, provide domestic hot water, provide space lightening, and generate electricity without polluting the environment. If solar energy is properly trapped and utilized, it will be able to fulfill the future energy demand of the mankind.

1.2. SOLAR WATER HEATING

Solar domestic water heating, apparently, has been the most successful, extensive and cost-effective application of solar energy hereunto from the fact that domestic water heating represents almost 20% of the total energy consumption of a typical dwelling unit in Canada. Canadian Solar Industries Association (CanSIA) has estimated yearly saving of about $500 for a residential unit in Canada using solar water heating system. This saving could further increase in the future due to the rising energy cost.

Initially developed in early 19th century, the conventional solar water heaters have the capability to fulfill most of the hot water demand for any application in sunny and hot climates. In cold climates, they are able to provide some portion of the required hot water, or preheat cold water as warm as 40 (°C) prior to feeding the conventional water heating systems, notwithstanding that the ambient temperature in such climate could drop to -20 (°C). Furthermore, the solar water heating systems require less maintenance compared to the other conventional systems, since they have fewer number of moving or fuel burning parts. Nowadays, advanced technology, optimized design methods and advanced materials have made solar water heating more efficient. In addition, due to the soaring fuel price, it is also considered as the most cost-effective approach throughout the year and in any geographical locations. Utilization of antifreeze fluids or two-phase flows has made solar water heating feasible in harsh cold climates as well.

Solar energy for water heating is trapped through a device called *Solar Collector*. A solar collector is a particular kind of heat exchanger that traps direct and diffuse solar radiant energy and converts it into thermal energy of useful form. It absorbs the incident solar thermal radiation in the short wavelength band and precludes the escape of the thermal radiation by means of the greenhouse effect. The transformed heat warms either the domestic water directly or through an interface media. Solar collectors are of different types, shapes, and configurations such as, flat-plate, evacuated-tube, concentrating parabolic-through and unglazed collectors. The heat transfer fluid could be water, air, mixture of water and antifreeze fluid, refrigerants or hydrocarbon oils. Any collector has its own characteristics, advantages and disadvantages; alternating its performance and efficiency based on numerous parameters. Solar collectors must be faced south and

installed with a tilt angle from horizontal equal to the latitude of the site plus 10° for winter and minus 10° for summer in order to maximize the collection of the solar irradiance.

Solar water heaters can be categorized as: thermosyphon systems, integrated collector storage systems (ICS), direct and indirect pumped systems. In the thermosyphon solar water heating (TSWH) systems both the collector and the storage tank are installed on the roof. The storage tank is well insulated and located at an elevation higher than that of the collector (see Figure 1-1b). As the fluid inside the collector absorbs heat from the sun, it expands and becomes less dense. This causes the induction of the convective currents which causes the dense cold water from the tank to descend into the collector and the warm water in the collector ascends into the tank. In this system, no pump is needed to circulate water and the auxiliary tank acts like a thermally operated valve to protect the system from freezing. As other option, to protect the system from freezing, a manually operated valve can be used to drain the entire system, or antifreeze such as ethylene glycol or propylene glycol can be used in collector. Configuration of collector and tank in the thermosyphon systems could be a flat-plate, an evacuated-tube, or concentrating parabolic-through collector which is directly connected to the potable water tank or through an interface heat exchanger (when antifreeze is used). Thermosyphon systems are so far the most widely installed water heating systems worldwide.

In the integrated collector storage (ICS) systems (batch system) collector is combined with the storage tank where the cold water enters from the bottom and passes through the black painted storage tank, absorbs heat and exits the storage tank from the top (see Figure 1-1a). In this system, the individual storage tank and pump are eliminated

and the flow rate is the function of demand. The heat loss from these systems at night is very significant thus, in regions where freezing is an issue, a flush-type valve is used to protect water from freezing. In direct (open) and indirect (closed) pumped system (see Figures 1-1c and 1-1d), the solar collector is installed on the roof and the storage tank is located somewhere else. For the direct system, water is circulated between the tank and the collector by a pump and for the indirect system, antifreeze is circulated between the collector and the hot side of a heat exchanger and potable water is circulated between the cold side of the heat exchanger and storage tank. In the pumped systems, a differential controller senses the temperature difference between the water leaving the solar collector and the water in the storage tank. The pump starts when the fluid in the collector is about 11°C warmer than the water in the bottom of the tank, and turns off when this difference is less than some preset value, which typically is 3-5°C. When 100% water is used in the collector, a recirculation type differential controller can be used to run the pump when the collector inlet water temperature drops below about 4°C. Thus, whenever the temperature approaches the freezing point, the valve opens to allow warm water from the storage tank to flow through the collector. Alternatively, a DC pump powered by a PV panel (which converts solar radiation to electricity) could be used to circulate water through the collector plate. In this case, however, the water circulates through the collector only when there is sufficient solar radiation.

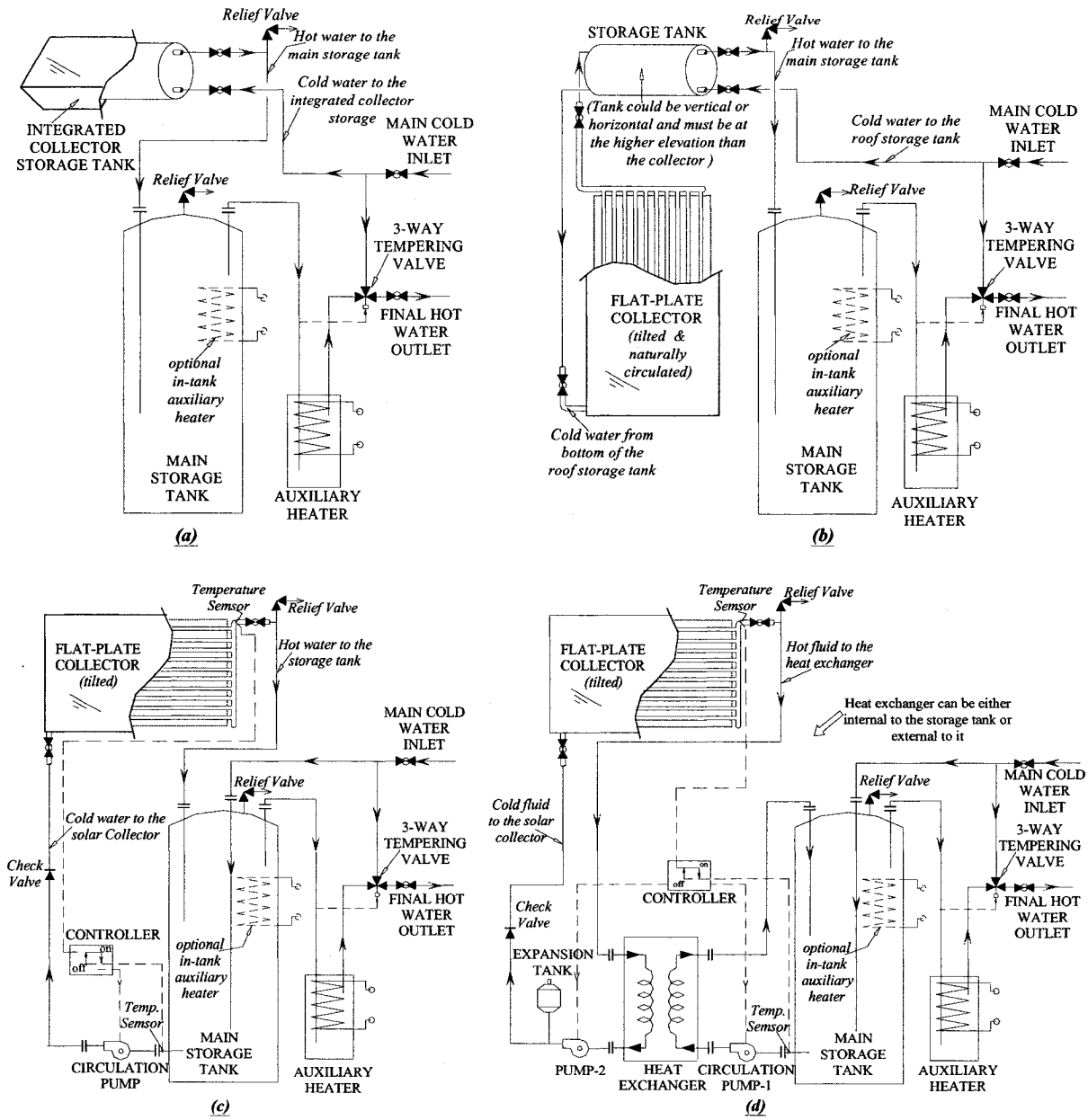

Figure1-1: (a) Natural Circulation Integrated Collector Storage System, (b) Thermosyphon (Natural Circulation) System, (c) Direct Forced Circulation System, (d) Indirect (close loop) Forced Circulation System with Antifreeze.

The drain back systems are almost similar to the pumped systems in which a pump that functions by a differential controller circulates water between reservoir tank and collector in a close loop. In this system the collector must be installed higher than all other components of the system, so that when the water temperature is low or there is not

enough solar radiation, entire fluid drains down into the small reservoir tank which is normally is installed a little bit higher than main storage tank (see Figure 1-2). For extra protection, an antifreeze solution can be used in the drain back systems. The thermal energy is transferred to the potable water through a heat exchanger which is installed inside the reservoir tank. The drain-back systems are reliable and work well, however, they require larger pump compared to other systems.

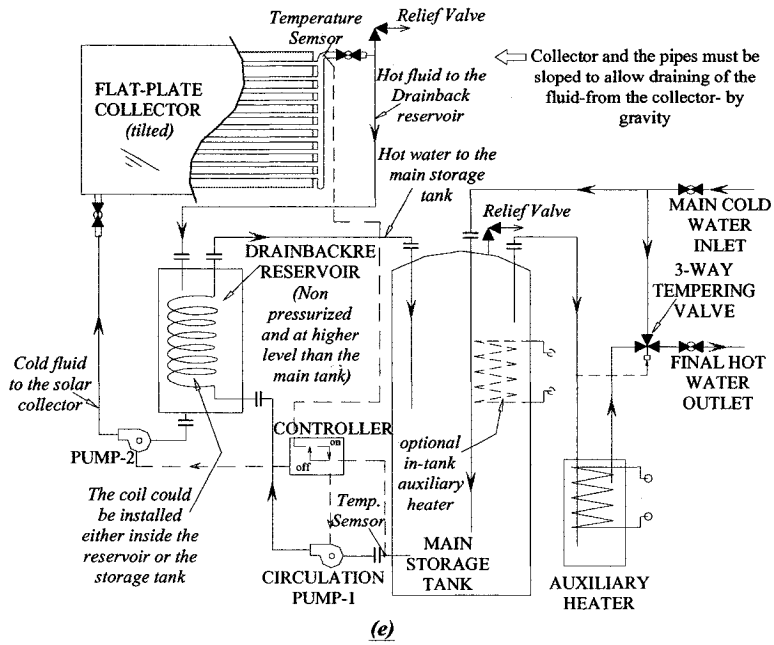

Figure 1-2: A Pumped Close Loop Drain-Back System

The integrated collector storage and thermosyphon system in which the potable water is naturally circulated are categorized as passive solar water heating systems. The indirect and direct systems in which the water or antifreeze is circulated by pumps are categorized as active solar water heating system. Active systems are more efficient and easy to retrofit than passive systems; however, they are more costly.

The solar energy for water heating can be trapped by either flat-plate, evacuated tube or concentrating collectors. Concentrating collectors use curved and reflective surfaces to focus sunlight on black-colored absorber pipe (receiver tube) through which

water or antifreeze is pumped. These collectors are capable of rendering fluids with very high temperatures; however, the concentrating collectors are more expensive and less effective for small applications. They require high level of direct radiation and also needs tracking system to face the sun continuously. Furthermore these collectors have climate and geographical limitations and are very sensitive to cloudy condition, due to their dependency on direct radiations. In evacuated-tube collectors, parallel rows of evacuated-tubes in which the absorbing plate and its attached *single* tube are placed inside a vacuumed glass tube. Evacuated tubes have the advantage of utilizing both direct and diffuse solar radiation, as the evacuated glass prevents the heat loss from the collector plates to the environment. The present evacuated tubes are using heat pipe (see section 1.4.5) to remove heat from the absorber plate and transfer it to the water inside the reservoir tank. These collectors are also able to warm water from medium to high temperatures (60-80°C). These systems prevent water from freezing and have efficiency in the range of 50 to 80%. The evacuated-tubes are, however, expensive, fragile and have high initial and maintenance cost. Contrarily, flat-plate solar collectors are simplest, less expensive, and easy to fabricate and operate ones. The flat plate collectors can utilize both direct and diffuse radiation with no need for tracking devices. The flat-plate collectors however, can only warm water to moderate temperatures (~70°C), and have significant heat loss from glazing side. Their efficiency is typically less than 50%. Nevertheless, these collectors are more architectural adaptive and are suitable for residential sector. The flat plate collectors can be either open loop system where heated potable water is directly sent to the services, or close loop system (indirect) where heated water or transfer fluid exchanges the thermal energy with the service water through a

secondary heat exchanger. For freezing climate like Canada, closed systems are more appropriate when anti-freeze solution flows through the collector. Solar water heating systems with flat-plate collectors, whether thermosyphon or pumped, are the most broadly installed systems to date.

In the present study, flat-plate collectors are considered for solar water heating, which are more appropriate systems for a one family dwelling unit. In the following review, the elements of the systems are discussed in detail. The review, along with the important factors that affect the performance and applicability of these collectors, summarizes the significant experimental and theoretical works to date.

1.3. LITERATURE REVIEW

1.3.1. Flat-Plate Collector

The flat plate collector is typically a rectangular box in which a black-color coated metallic or plastic plate is placed behind a glaze such as tempered glass or a fiberglass reinforced polyester (FRP) sheet. The black-coated plate, called the absorber plate, absorbs direct and diffuse solar irradiance and transfers it in the form of heat to the water, or any other fluid, directly or through connected tubes that carry the fluid (see Figure 1-3). Glaze, which is transparent to solar radiation, allows solar radiation to enter and strike the absorber black plate but suppresses or reduce convection and radiation losses to the outside environment. Glaze establishes greenhouse effect inside the collector box and by reducing convective and radiative losses, improves the performance of the collector. The flat-plate collectors are insulated from the bottom and sides to prevent conduction losses from back and sides of collector.

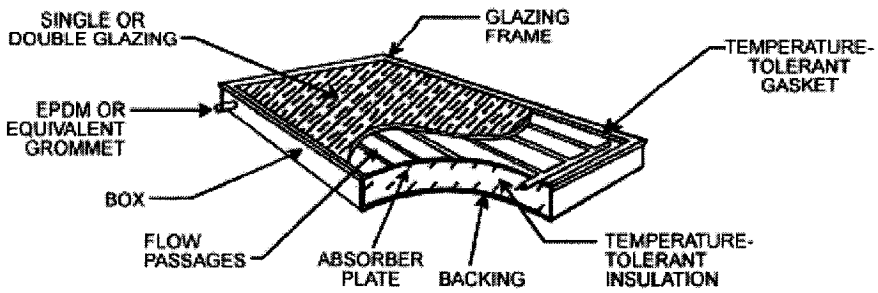

Figure 1-3: Schematic of a Flat-Plate Solar Collector, *Adopted from ASHRAE(2003)*

Several parameters influence the performance of a flat plate solar collector such as material, shape, thickness and coating of the absorber plate; type, thickness and number of glazes; size, shape and number of the tubes; distance between tubes, geometrical characteristic of the plate, type of antireflection coating on the glaze, space between absorber plate and glaze, collector's insulation material. Operating condition, such as flow rate, ambient and inlet water temperatures, wind velocity, solar irradiance, and climate condition can also drastically affect the collector performance. A significant portion of the research on flat plate collectors is focused to these critical parameters.

The early work on the utilization of solar energy for heating purpose goes back to late nineteenth century. Mouchot (1879), Mangon (1880) and Ericsson (1884) substantiated economic possibility of transforming solar energy to heat and utilizing it in many applications. Hottel and Woertz (1942) pioneered serious efforts in the quantitative analysis of flat-plate collectors. Their experimental and theoretical work established the fundamental quantitative relations among those parameters that contribute in the performance of a flat plate collector. Their study also discussed the importance of economic balance in comparison with the performance of the collector.

Bliss (1959) derived the mathematical models for efficiency factors that are applicable to a variety of solar collectors and other types of panel heat exchangers. He

argued that the appropriate use of these factors could lead to an accurate design, and eliminate the empiricism in the design of the solar collectors. He derived relations for the collector efficiency factor, F', which is the ratio of the actual useful heat collection rate to the useful heat collection rate attainable with entire collector surface at average fluid temperature; and collector heat removal factor F_R, which is the ratio of the actual useful heat collection rate to the useful heat collection rate attainable with entire collector surface at entering fluid temperature. He emphasized the importance of these factors from the fact that they are design constants of a particular collector construction and rarely depend on the operating condition of the collector. Bliss (1959) asserted that his derived efficiency factors were not only in agreement with previous models, but they also incorporate the effects of atmospheric radiation.

Kettleborough (1959) experimentally compared the performance of thermosyphon SWH systems with the thermostatically controlled SWH system. In the latter an expansion type temperature controlling valve, controls the ejection of hot water from top of the collector based on the set temperature. From this experimental study he discovered that contrary to thermosyphon systems, in thermostatically controlled system: (a) the final outlet water temperature can be controlled; (b) the hot water delivery is available even some hours before solar noon; (c) the storage tank can be placed below the collector; and (d) the efficiency of this system is generally higher than that of the thermosyphon system.

Liu and Jordan (1963) argued that it is important to consider the "average long-term performance" instead of "instantaneous rate of energy collection" prior to design a plate solar collector. They reported a simple procedure using a set of curves to predict the long-term performance of a collector at any tilt angle and at any location without

undergoing a detailed analysis. They presented the collector performance data that were calculated by their proposed method and concluded that the proposed method can reduce the necessity for such a meteorological data. They stated that the performance of a collector is basically a function of two parameters: $\overline{K}_T$ or monthly average clearness index which is the ratio of monthly-averaged total daily radiation to that of extraterrestrial daily insolation, and the difference between inlet water temperature to the collector and the ambient air temperature. They future stated that latitude of the region has less effect on the collector's performance. To validate the accuracy of the correction factor, they compared the hourly total radiation on a tilted surface estimated using the correction factor, with the experimental data and found a good agreement.

Rao and Suri (1969) introduced a simplified method to estimate the collector area for thermosyphon type solar collectors. They presented a set of performance curves to predict the collector area, absorbed heat, and collector efficiency for a given average maximum water temperature inside the storage tank. Their experimental model consisted of a black-coated corrugated plate on the top, and a plain plate at the bottom, both of which were welded together all way around forming water channels (i.e. a sandwich construction). This study, however, was limited to a certain flow rate and a certain temperature difference for one particular construction. Nevertheless it introduced a method that can be used for other design parameters.

Kern and Harris (1975) performed analytical investigation to identify the optimum tilt angle of the solar collectors not only as a function of latitude but also as a function of weather data and energy demand, which in turn provides the minimum collector area. They concluded that for inexpensive collectors, the rule of tilt equal to the

latitude for a south facing collector offers acceptable output; however, for large scale collectors or PV systems, meticulous determination of the tilt is necessary. They also concluded that the common practice of choosing tilt angle equal to the latitude plus 10^{o} for winter and the latitude minus 10^{o} for summer is sufficiently accurate for solar water heating applications. However, they underscored the importance of energy demand for the estimation of the tilt angle. They further observed that if the optimum value of the tilt angle has been carefully determined, a deviation of the tilt angle by 10^{o} from the optimum value does not have any significant effect on the collector efficiency.

San Martin and Fjeld (1975) experimentally compared the performance of three different configurations of the flat-plate collector which include a double glaze ordinary tube-in-sheet flat-plate collector, a water trickle (i.e. sandwich construction with a corrugated aluminum sheet on top), and a thermal trap flat-plate collector in which a transparent solid material such as methyl methacrylate with low thermal conductivity was adjoining the absorber plate. A flat-plate collector with thermal trap material can be exposed directly to the ambient air or can be covered with another glaze as the regular collectors. They pointed out that the thermal trap materials must be highly transparent to the short wavelength radiation but poorly transparent to the long wavelength radiation. They found that by using thermal traps, higher temperatures are achievable. The comparison showed that the thermal trap collector was twice more efficient than the sandwich-construction collector and was less sensitive to the overcast condition. The comparison further indicated that the thermal trap collector operates longer with higher solar energy collection rate compared to the other two collector configurations. Later, through an analytical study Kena (1983) showed that a 30 (mm) thick acrylic as the

thermal trap could have similar performance as a single-glaze collector. In his modified efficiency formula, he considered the effect of solar absorption in the trap material, which influences the collector performance. He discussed the cost and temperature limitations of the acrylic and clarified that it is preferred to add a cover to the system and use reduced trap thickness.

Abdel-Khalik (1976) analytically investigated the performance of a tube-in-sheet flat-plate collector with N bend segments of serpentine tube arrangement. His mathematical formulation described the temperature variations in each segment, and the collector heat removal factor, F_R. He found that the heat removal factor is a function of three dimensionless factors: F_1, F_2, and ($\dot{m}\, C_p/U_L A_c$) that are described in the literature. These relations and factors are also re-presented in Duffie and Beckman (2006).

Siebers and Viskanta (1977) theoretically compared the performance of flat-plate collectors operating under constant outlet temperature with variable mass flow rate, and compared the results with typical collectors working under constant flow rate. They argued that a collector operating at constant outlet temperature is economically beneficial as it facilitates the operation of the associated heating or cooling system at a uniform inlet temperature. They further argued that the cost of the collector's control system could be compensated by the design and operating advantages related to the easy operation of the heating or cooling system. They found that the efficiency of the constant outlet temperature collector is higher at noon and lower at early morning and late afternoon compared to that of the constant mass flow rate collector. However, there is no significant difference in the overall efficiency of both collectors. They concluded that the constant

outlet temperature collectors are as efficient as constant mass flow rate collectors and that both have similar respond to the environmental and design changes.

Iqbal (1979*b*) investigated the optimum slop of the flat-plate collectors in four Canadian cities with different climate conditions. He studied optimum tilt angle as functions of the collector area, yearly total heating load, and the ratio of space heating load to service hot water load. He used *f*-chart method for the sizing of the residential heating system and assumed a uniform hot water load throughout the year. He considered a flat-plate double glazed collector, for his study, and stated that the variation of F_R could be very small. He found that the optimum tilt angle increases as the collector area enlarges, by up to latitude plus 15° for the large collectors. He also observed that the load fraction supplied by collector varies linearly with the optimum slope angle, and that the ratio of the heating load to hot water load has no effect on the collector tilt angle. He concluded that a variation of $\pm 5^{\circ}$ in tilt angle has no significant influence on the load fraction. He also suggested that a flat roof for low heating fractions, and a vertical south facing wall for large fractions could be advantageous in the system design.

Cooper (1979) theoretically studied the relation between the inclination angle of a flat-plate collector and the heat loss due to natural convection between the absorber plate and cover, between multiple covers, and between the cover and surrounding. He expressed the top loss coefficient as function of wind speed, plate and ambient temperatures, plate emittance, inclination angle, and the sky temperature (which assumed to be 12 °C less than the ambient). He found that for inclination angles between 0-60°, the top heat loss coefficient was insensitive to the plate and ambient temperatures, and the external convection coefficient. For inclination angles greater than 60°, and especially for

the collectors with selective coat, he observed a reduction in the value of top loss coefficient. Furthermore, as the inclination angle approached 90°, some under-prediction of the collector performance was also observed. He also found that the top loss coefficient was a close function of the gap between the plate and cover. He also estimated the critical minimum spacing of 25 (mm) between the plat and cover, and argued that this spacing should be avoided as the top-loss coefficient is largest for this spacing.

Chiou (1982) numerically studied the effect of non-uniform flow distribution among the tubes of a flat-plate collector. He argued that non-uniform distribution of the flow is a realistic assumption that can be caused by inaccurate design and construction of the inlet or outlet manifolds. He further argued that it could also be occurred from the fouling and plugging of the tubes. He developed a numerical method to determine the variation of the performance of a collector influenced by non-uniformity, and found that the deterioration of efficiency could be from 2% to more than 20%. He suggested that the non-uniformity of the flow should not be overlooked when a collector is to be designed or analyzed.

Garg and Datta (1984) compared five different proposed relations for top loss coefficient, $U_{top.}$ In this study the heat balance equations were solved iteratively and the definite iterative results are compared with those of the proposed single equation. The comparison conducted over a variety of absorber plate temperatures ($T_{p,m}$) and plate emittances' (ε_p), collector tilt angles (β), ambient temperatures (T_{amb}), and wind velocities (V). Results showed that the values obtained from Malhorta et al.'s (1981) correlation is more accurate than those of Hottel and Woertz (1942), Klein (1975), and Agarwal and Larsen (1981). They determined that modification of Malhorta et al.'s (1981) correlation

not only includes all of the important factors of equations derived by other models, but at the same time improves this shortcomings since it considers the effect of tilt angle (as cosβ) and air spacing or spacing between covers (L). Moreover, it includes the effect of wind heat transfer in the wind factor (f) as a function of ($1/h_w$) so that as h_w increases the wind factor f approaches zero, which is physically more realistic than being a function of (h_w) as in Klein's (1975) model.

Francken (1984) proposed a new definition for the effectiveness of the solar collectors, ε_c, and argued that the consideration of the solar collector effectiveness as equivalent to the heat removal factor, F_R, is inconsistent with the fundamental concepts of effectiveness in conventional heat exchangers. He concluded that the effectiveness of a solar collector (ε_c) is an additional performance indicator, particularly when extensive temperature rises happens, and can be described by equivalence with that of a single-pass counter-flow heat exchanger. He found that both collector effectiveness and heat removal factor increases with the collector's efficiency factor (F'), however, ε_c is more sensitive to changes thereof. Furthermore, he observed that ε_c increases rapidly with an increase in the flow rate, whereas F_R decreases gradually. He concluded that the value of ε_c can be calculated by measuring the plate temperature at the fluid outlet.

Hahne (1985) numerically investigated the effect of various parameters on the efficiency and warm-up time of flat-plate collectors, under steady and transient conditions. He concluded that for suitable weather conditions (i.e. high values of ambient temperature and solar irradiance), any simple method provides reasonable design of the collector, however, for unfavorable weather conditions, more sophisticated designing methods are required that should account for inclination and pipe spacing effects.

Uhlemann and Bansal (1985) experimentally studied the effect of system pressurization of the system on the heat loss coefficient, U_L, collector efficiency factor, F', and overall performance of a thermosyphon system. The un-pressurized system consisted of two flat-plate collectors with parallel pipe-in sheet, and the pressurized system consisted of a flat-plate collector with serpentine pipe-in-sheet construction. The pressurized system was maintained at the city water pressure. Both systems were tested under identical outdoor condition. The results showed that the performance of non-pressurized system was better than the pressurized one because of higher temperatures in the pressurized system, which resulted in higher heat losses. They also observed that the tank and collector outlet temperatures were always 5(°C) and 1-2 (°C) higher than the average tank temperature for pressurized and non-pressurized systems, respectively. Furthermore, the water temperature distribution inside the tank was considerably different for both cases. The top to bottom temperature difference in the tank was as large as 35 (°C) for the pressurized system, and 3-4 (°C) for not pressurized systems. However, it was observed that in the pressurized system, night time reverse flow occurs for very short period of time, whereas for the non-pressurized system, the period of reverse flow was prolonged and associated with significant temperature drop in the tank. The mass flow rate in the pressurized system was also found to be 5 to7 times larger than that of the non-pressurized system. For identical solar radiation, they found that the average efficiency of non-pressurized and pressurized systems is 47% and 41%, respectively.

Fanney and Klein (1988) experimentally investigated the influence of flow rate on the thermal performance of the solar collector as well as the combination of the collector and an auxiliary heat exchanger. The result showed that a reduction in flow rate

significantly improves the collector efficiency and thermal stratification in the storage tank. A further increase in the stratification and collector efficiency was observed when the inlet water temperature was reduced. For both direct and indirect systems, they employed a simple differential temperature sensor to control the flow rate at the pumps. In addition, they used two different configurations for the flow entry (retun) from the collector into the tank. The first one was a 12.7 (mm) tube that introduced heated water from its open-end as an axial flow (standard return tube), and the second type was a tube with closed-end but equally spaced holes around its perimeter that introduced collector hot water radially into the tank (Stratification enhancing return tube). They concluded that the performance of the direct system can be enhanced with regular return for reduced flow rates yielding to a better stratification and mixing effects. However, the enhanced return tube has small benefit over reduced flow rates. They argued that the first approach of reduced flow rate is advantageous due to the reduced size and cost of the equipment but it shall be carried out cautiously to prevent any flow imbalances. The second approach is more costly but has advantages of operating the system at the typical flow rates. That is, the reduction of the entering flow momentum causes less internal mixing, enhances stratification in the tank, and avoids any flow imbalances.

Hollands and Lightstone (1989) performed study similar to that of Fanney and Klein (1988) to investigate the effect of low collector flow rates (as small as one seventh of the usual values) on the stratification in the tank. In their experimental setup the exit of the collector return pipe was located 60 (cm) below the top of the high tank. Comparison of the collector performance at low flow rate (0.0025 kg/sec.m^2) and high flow rate (0.02 kg/sec.m^2) showed 17% improvement of the solar delivered energy at low flow rates.

They pointed out the cost effectiveness of the low flow rate systems and also indicated that the performance of the low flow rates collector incorporated with a stratified tank, can be improved by 38% compared to a high flow rate collector and fully mixed tank.

Wang and Wu (1990) proposed a numerical model to study and predict flow and temperature distribution in the manifold-riser system of the solar collectors with parallel (Z pattern) and reverse (U pattern) circuits. In their model, all mixing effects, buoyancy, longitudinal heat conduction and flow non-uniformity effect were taken into account. From both experiments and simulations, they concluded that the mal-distribution of the flow has profound effect on the performance of a solar collector. They argued that in Z-pattern the end risers have more flow rate whereas less flow passes through the central rises where the temperature is higher. On the contrary in the U-pattern most of the flow passes through the first risers. They recommended utilizing Z-pattern in the big collectors due to its higher efficiency, even though U-pattern has less pressure drop.

Jones and Lior (1994) numerically studied the effect of different design parameters on the flow distribution in solar collectors with inlet and outlet manifolds connected to parallel tubes (risers) in the absence of buoyancy effect. They developed hydrodynamic model to predict the pressure and flow distribution, and validated their simulation model by the published data. They found that the efficiency of the collector drops when the uniformity of the distribution diminishes. They argued that the three main parameters that influence the flow distribution are the ratio of risers to manifold diameters, the number of risers, and the length of risers, and found that the non-uniformity of flow distribution increases with the increase of the first and second factor and decrease of the third one. Results of their simulation revealed that: (a) the riser flow

rate increases from each risers to next in the manifold direction for the Z-parallel construction (e.g. farthest risers from inlet of manifold has the largest flow rate) and decreases for the U-reverse one; (b) the non-uniformity increases with $(d_{riser}/d_{manifold})^4$ and with square of the number of the tubes (n^2); (c) for the ratio of the length to inside diameter of the risers, and the influence of distance between risers in insignificant. However, as the ratio decreases, particularly if the ratio goes below 75, the mal-distribution increases since it weakens the effect of frictional pressure change in the riser; (d) the flow distribution is likely to be uniform as the pressure drop in the risers become larger than that of the manifold due to frictional and inertial pressure changes.

Kikas (1995) analytically studied laminar flow distribution of water inside a typical solar collector with two equal sized manifolds and their connected parallel risers. He pointed out the importance of flow uniformity through parallel tubes to improve the efficiency of the collector and design parameters that affect the flow distribution in the riser tubes. He considered two types of circuits. One is direct circuit, where flow enters to the inlet manifolds and exits from outlet manifold in the same side of the collector, and the other is the reverse circuit where flow enters from one side of the collector and exits from the opposite side. He found that the flow is more uniform in reverse return circuit.

Khlifa (1999) experimentally examined the thermal performance of locally made thermosyphon SDWH collectors. He measured the temperature distribution along the plate length at several locations with respect to the pipe, and the natural circulation flow rates for two nonselective absorber plates installed at 45° and coupled to a storage tank. He found that, as anticipated, the natural circulation mass flow rate increases with the incident solar radiation, I_o. He also observed that the collector efficiency and heat

removal factors are poorly influenced by time, and can be assumed constant for a certain collector design, as was expected. He found that the mean plate temperature is always higher than the mean fluid temperature because of the heat transfer resistance of the material, although there was a good agreement between the temperature distributions thereof.

Weitbrecht et al. (2002) conducted an experimental study, similar to the theoretical study of Kikas (1995) and measurements of Wang and Wu (1990) to explore laminar flow distribution in solar collector. They also performed sensitivity analysis using theoretical approach to elucidate different possible flow distributions in the collector. They investigated the effects of various collector design parameters, in particular the effect of pressure drop and energy loss caused by friction on the flow distribution. Velocity and pressure drop measurement were performed for an inverse circuit or Z-configuration to determine the flow distribution and pressure lost coefficient in the junctions. They concluded that the flow distribution in the risers is a function of the ratio between energy loss in the rises and in the manifold. They argued that for uniform flow distribution, it is necessary for the system to be controlled only by energy losses in the risers and that the overall energy losses in the manifold must be much less than that in the risers.

Groenhout et al. (2002) proposed a novel design for SWH system with flat-plate collector and experimentally studied the heat loss characteristics of the system by indoor tests. Their design consisted of a double-side flat absorber plate, coated with low-emissivity surface, which was mounted on two fixed concentrating reflectors made of sheets covered with aluminum reflective foils. From top side it was covered by a low-iron

antireflective glaze. Heat loss measurement showed a considerable reduction of conductive and radiative heat losses from back and top due to this setup. It was found that an overall heat loss is about 30-70% less that of usual model.

Mills and Morrison (2003) considered a new design approach for a combination of flat-plate collector and tanks, to maximize the peak-time solar fraction while minimizing the material requirement of the system. They addressed the shortcomings of the existing collectors that overproduces hot water in summer and has reduced performance in winter. The main factor in their new design approach was the minimization of the supplied backup energy to meet the annual load rather than the maximization of the efficiency. Contrary to the conventional solar collectors which only uses upper surface of the absorber plat to harvest solar energy, they endeavored to use both sides of the plate by non-imaging reflectors which in returns consumes half material for equally exposed surface of a conventional flat-plate collector. However this technique has several problems such as extra cost and space of the reflectors, and the necessity to use thicker plate material. They also redesigned the tank to be placed under the collector and operated the system at higher temperatures through improved size and better insulation. They found that this system demands only half of the backup energy of an ordinary flat-plate and tank system. They determined that any improvement in the selective coating or mirror reflectance will reduce collector dimensions without affecting the solar fraction.

Lu et al. (2003) studied and tested the performance of a thermosyphon solar water heating system and optimized the actual data of the commercial collectors. They addressed all parameters that determines a natural circulation SDWH system and

mentioned the complexity of testing such a system, compared to what ASHRAE 93 or 95 has suggested for forced circulation systems. Result of their actual outdoor tests showed that the most crucial parameter that determined the system efficiency is absorber's coating. They concluded that in order to maximize the heat absorption and heat preservation of the system, first, the absorber must be black-chrome plated instead of black painted. Second, the storage tank must be insulated with PU foams (preferably of low density), and third underneath of the collector must be insulated with fiberglass.

Yeh et al. (2003) theoretically studied the effect of collector aspect ratio on the efficiency of sheet-and-tube SWH systems. They concluded that the efficiency of the collector increases as the inlet water temperature decreases, since low temperature water has higher capacity to absorb heat. They also found that for the higher inlet water temperatures the efficiency increases as solar incident radiation ascends. They defined the collector aspect ratio ($R= l/w= l/nW$) as the ratio of the one tube length (l) to the numbers of tubes (n) times tube spacing (W). They established that for a constant collector area and constant tube spacing, the collector efficiency (η) increases as the collector aspect ratio (R) increases or. Thai is, either the tube length increases or the tube number decreases. They, furthermore, concluded that when R increases, fluid velocity also increases resulting in an enhanced heat transfer rate from the pipe to the fluid, but on the other hand, it causes more energy loss due to additional frictional losses. They argued that for a constant collector area and tube spacing, decreasing the aspect ratio would be more economical approach to design solar water heating system with improved overall performance.

1.3.2. The Absorber Plate

Absorber plate is an essential component of a flat-plate collector from which enhancement of absorbed solar energy as well as improvement of the heat transfer from plate to the working fluid will tremendously increases the overall thermal performance of the collector. Absorber plate can be made of metals such as copper, aluminum, or steel; or plastics such as polypropylene or PVC. The plate-tube combination could be in diverse arrangements such as parallel or serpentine, and variety of shapes such as circular, rectangular or elliptical. Connection of the riser tubes to the plate can be made in a variety of ways such as tube above plates, profiled plate, or tube-and-extruded fins. Different techniques are used to join pipe to plate such as clamping, soldering, high-frequency welding, or laser welding which greatly affect the value of bond conductance. Different kinds of tube-in-plate and rolled plate collectors that are common in flat plate collectors are illustrated in Figure 1-4.

Black coat or absorbing coat is applied on the plate to transform the shiny surface to a black body that absorbs large fraction of the incident solar radiation (wavelength between 0.3 to 2.5 μm) but minimizes the emission of infrared radiation from the plate. Black coat is an important parameter in the performance of a collector. It can be selective, which is high in absorptance but low in emittance (ε = 0.08 to 0.12) or non-selective which is high in both absorptance (α = 0.9-0.98) and emittance (ε = 0.85-0.9) (Plante, 1983). Non-selective coats such as matt-black and carbon-black are suitable for low temperature applications such as swimming pool heating. Whereas, selective coatings such as black-chrome, black-zinc, black-copper, black-nickel, aluminum-oxides, iron-oxides, and stainless steel-oxides are suitable for moderate to high temperatures and

needs to be applied by electroplating or vacuum evaporation methods (Lenel and Mudd, 1984).

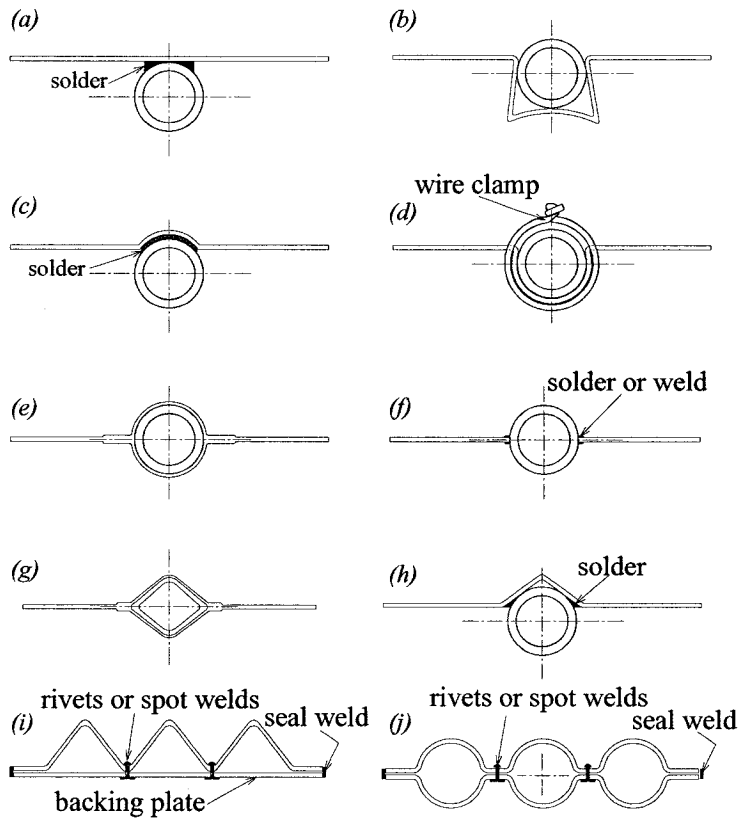

Figure 1-4: Different Designs of the Absorber Plate: (a) plate above tube with soldered bond; (b) self-clamping plate; (c) round profiled plate with soldered bond; (d) metallic wire clamped plate; (e) mechanically bonded plate around round tube; (f) soldered or HF welded fins to the pipe; (g) mechanically bonded fins around diamond shaped tube; (h) triangular profiled plate with soldered bond; (i) sandwich design with corrugated plate; (j) round rolled plates.

Hottel and Unger (1959) experimentally studied the properties of a selective coating made by spraying an aqueous solution of cupric nitrate onto a heated aluminum plate and then heating it to up to 170 (°C) to obtain a black cupric oxide. They found that an increase in plate operating temperature yields an increase in convective and radiative losses. They further observed that the radiative losses were predominant when the plate operating temperature was greater than 40(°C). At a plate temperature of 80(°C), they found that almost 99% of the re-radiation were of the wavelengths greater than 4μm while

more than 98% of the radiation reaching the absorber plate were of the wavelengths less than 3μm. Based on these results they concluded that the application of selective black coating on the plate surface that has low emissivity for long wavelength radiations could significantly increase the absorber plate performance. They further argued that the efficiency of a single glaze collector with a selective-black-coated absorber would be comparable to a double or triple glaze configuration with a nonselective-black coated absorber. Various variables such as concentration of nitrate in spray, particle size and rate of spray, drying plate and baking temperatures, amount of deposit per unit area, and interval between sprays and bakes, and time of baking; determines the characteristics of the coat.

Kokoropoulos et al. (1959) prepared selective coating by electroplating copper and cobalt on the polished surfaces and then oxidizing them through heating in air. Experiment over different film thicknesses and base metals revealed that for good selective coat with high absorptivity in the solar radiation range of 0.3-2.5 μm and low emissivity in infrared range of 5-10 μm, the thickness of the coating must be equal or greater than the wavelength of the radiation that is to be absorbed (10^{-5} to 10^{-4} cm) and about 10% or less than the longer wavelength (infrared) radiation that is emitted. Furthermore, the coat must be black semiconductor so that the conductance increases as the plate temperature raises, resulting in the reduction of emittance.

Whillier (1964) conducted theoretical and experimental investigation of the thermal resistance of the metallic joints in solar collectors. He found that tube-in-strip construction form has the best thermal characteristic due to integration of the tubes with the absorber plate. This construction, however, squanders copper plate material He also

mentioned that the sandwich construction in which a thin layer of water passes through the entire absorber plate (either plane or corrugated), is also a thermally acceptable construction. However, the shortcoming of the sandwich construction is the high water pressure drop within the plates and the difficulty of sealing the joints adequately. He also argued that the most common construction in which the tubes are bonded to the flat plate by soft-soldering has two disadvantages: first it is expensive due to the challenges in soldering tubes to long thin copper sheets, and second is the cracking of the solder due to the thermal stress arises from cooling and heating. He further determined that the cracks can diminish the bond performance as the efficiency loss due to unsoldered bond is about 17%. In addition, an air gap between the plate and tube (as thin as 0.5 mm) created by inadequate soldering, could significantly increase thermal resistance which in turn, reduces the collector efficiency factor, F'. Whiller (1964) showed that a copper shim wrapped three-quarters of the way around a tube and then pulled tight around the tube with thin steel wires displays very favorable bound conductance.

Whillier and Saluja (1965) theoretically and experimentally studied the effect of the design details on the performance of a flat-plate collector solar water heating system. In this study they tested two identical commercially existing collectors, one with selective and other with non-selective coating. They implement three different tests: Laboratory test to determine radiative characteristics of glass and absorber plate, indoor calorimetric tests to measure the heat loss coefficient at zero irradiance, outdoor tests to determine collector performance at two different mass flow rates with inlet temperature about ambient and exit set temperature of 60 (^{o}C) above ambient. They concluded that in order to enhance efficiency of these commercial collectors, (a) the existing galvanized plate

must be replaced with a copper plate so that fin efficiency would increase from measure value of 83.3% to 95.3%; (b) bond conductance must be improved by wiring and tightening the plate around tubes that reduces negative effect of cracks, and (c) galvanized steel must be coated with a shiny durable low emissivity surface before application of selective coat. They argued that the combination of indoor tests and theoretical calculations are sufficient to determine collector's limitation and expensive outdoor test are not necessary.

Khan (1967) experimentally investigated the bond conductance of three different contact methods between the flat-plate and tube, namely, soldering, duPont adhesive bonding, and wire clamping in every 150 (mm) intervals. The result of outdoor and indoor calorimetric test showed that bond conductance is equal to 37.22, 6, and 5 (W/m.^{o}C), respectively. He concluded that the solder bond is the adequate joining method.

Shing-An (1979) analyzed the heat transfer process in a corrugated steel collector and experimentally derived an equation to predict the efficiency of the corrugated plate solar water heater, which was the function of U_L, $(\tau\alpha)$, ambient and collector temperatures, through a simplified test method. The collector efficiency factor (F') also was found to be 0.94.

Hollands and Stedman (1992) introduced the concept of "step-change" of the fin in the tube-in-sheet absorber plates where the fin becomes thinner distant from the tube yielding a material saving of 17.65%. They derived an equation for the fin efficiency with step-change in the thickness and estimated the optimum location for the step change. They found that the optimum ratio of the thick part-to-thin part thicknesses is 3. This

optimum ratio is located at 43% of the total fin length form the base. They determined that for step-change located at $0.5L$, material saving could be 25% yet fin efficiency would only drop by 0.5% (from 95.65% to 95.15%).

Ghamari and Worth (1992) experimentally studied the effect of tube spacing on the performance and cost-effectiveness of the flat-plate collectors. They argued that the cost-effectiveness of a solar system is more desirable than its performance unless other factors require sacrificing cost for better efficiency. They mentioned that an increase in the number of tubes in a collector improves the fin efficiency factor, F, and the cost. Therefore an optimum tube spacing that maximizes the cost-effectiveness of a collector (rate of useful energy to collector cost) must be considered. They conducted measurements for a single tube with a semi-circular profiled absorber plate for 12 different plate widths. They also derived an equation relating the tube spacing (W) to the tube cost per unit length (c_t) sheet cost per unit area (c_s), and two other factors, a and μ_o, that were obtained from the plot of collector efficiency versus tube spacing. The solution of this equation provides the optimum cost-effective tube spacing for the specific site location and material unit price.

Tiris et al. (1995) theoretically investigated the effects of fin shape on the efficiency and cost of an aluminum flat-plate collector. Four types of fins were considered in this study, that were straight rectangular fin, straight rectangular fin with reduction in local thickness, straight triangular fin, and straight fin with inverse parabolic shape. The results showed that an inverse parabolic fin performs the best with 16% saving in material cost, even though this fin reduces the efficiency by only 3.11%. They also

found that in cases where the ratio of the material cost reduction to the efficiency reduction is concerned, a fin with step change in the thickness is preferable.

Rommel and Moock (1997) studied a narrow rectangular construction shape as the absorber plate of the solar collector where fluid is in contact with the entire inner surface of the plate. They developed temperature distribution relations for a fully developed laminar flow yielding an expression for the collector efficiency factor, F'. These relations showed that for a laminar flow F' is independent of the flow rate, increases as duct gets narrower, and has dependency on the fluid thermal conductivity, λ, and irradiance. They compared F' values obtained from their design with that of a typical flat-plate tube-in-sheet construction, and found that the narrow-duct absorber has higher collector efficiency factor. They also derived a relation for the optimal duct height with respect to the solar irradiance, dissipated energy due to friction and required pumping energy. They found that for duct height smaller than that of the optimum height, the gained energy inclines but for heights larger than the optimum height, the energy gain is not a function of height. They found that for duct heights in 3-6 (mm) range, the values of F' as large as 0.98 can be achieved.

Tripanagnostopoulos et al. (2000) theoretically and experimentally studied the performance of glazed and unglazed flat-plate solar collectors with colored absorbers. They considered black, red brown and blue colored absorbers. They also utilized booster reflectors to increase solar radiation input to compensate extra heat losses of unglazed plate and less absorptance of solar spectrum of the colored collector. The experimental and theoretical result showed that the efficiency of colored absorbers, whether glazed or unglazed, is close to that of back colored if dark tone of colors is used. They also

concluded that absorbers with selective color coatings are more efficient, and selective coatings for unglazed absorbers must be weather resistance. They found that the use of booster reflectors is promising and cost effective to increase the output thermal energy. They, moreover, pointed out that the colored unglazed collectors are less efficient but economical and useful for low temperature purposes.

Eisenmann et al. (2004) developed correlations between the material content of an absorber plate and tubes, with F', W, and δ in order that save material and reduce collector's cost. They found that it is feasible to save 25% in material only with reducing W and δ, without deteriorating F'. They presented a simple design tool and associated nomographs that for a certain value of F' gives the optimum value of W and δ. They found that the width of the contact zone between the tube and plate affects the fin efficiency and collector efficiency factors slightly. On the contrary, reduction of U_L considerably increases F and F'. They also observed that the effect of pipe wall thickness was negligible on F', but significant from the material aspect.

1.3.3. Suppression of Convection and Radiation Losses

Usually a single glaze is incorporated as the top cover to impede thermal and radiative losses of flat-plate collectors. Glaze can be glass, or any other plastics with high transmittance of solar radiation (wavelengths less than 2 μm), but with low transmission of thermal energy (wavelengths greater than 2 μm). Glass, polycarbonate, polyester, Teflon FEP, Tedlar PVF, acrylic, and GRP (glass reinforced polyester) are some examples of the material that can be used individually or in conjunction with other glaze to perform solar transmittance while suppressing thermal radiation. Among these, low-iron tempered glass (4-6 mm thick) has sufficient strength against atmospheric condition

and is the most commonly used glaze as the top cover of flat-plate collectors. The top cover is an essential and crucial component that influences the performance of a solar collector. Numerous studies have been focused on minimizing thermal and radiative losses while maximizing the solar transmittance to enhance overall efficiency of the collector. It includes the etching of glass by fluoride based acids or applying antireflection coats in order to reduce the reflections of incident solar radiation form outer surface, which is the major part of the solar transmission losses, or applying IR reflective coating on the inner surface of the glass that reflects thermal radiation from absorber plate to minimize radiative heat losses. The use of double or triple covers significantly reduces the convective losses but at the cost of decreased solar energy due to absoption and reflection by additional covers. Another approach is to use vacuum glazing which is the evacuation of the narrow space between double glazing systems. Evacuation of the gap between absorber plate and cover plate or filling the gap with inert gases to suppress the thermal and radiation losses has been strived; however, it is an expensive and practically difficult approach. Installing selective arrays of solar transparent insulation material (TIM), known as "convection suppressing devices," with a honeycomb structure of different cross sections is considered an inexpensive technique and has been on the spotlight of the researchers for very long time. Honeycomb array of TIM's, as schematically shown in Figure 1-5, is made of transparent plastic or glass using evacuated spaces and air gaps to perform thermal insulation.

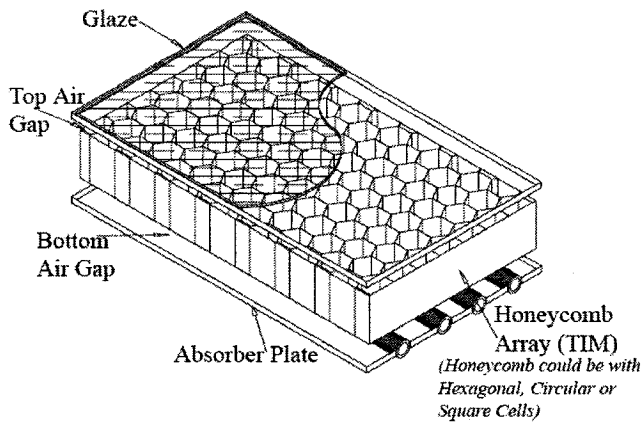

Figure1-5: Honeycomb Array of TIM's Over Absorber Plate

Edlin (1958) experimentally studied the effect of different types of transparent plastic material (films) in lieu of glass glazing to be utilized in the flat plate collectors. He measured the percentage of transmittance of the solar irradiance over broad range of solar incident angles and solar altitudes. He compared three plastic glazes: Teflon FEP fluorocarbon (100-X), Weatherable Mylar Polyester, and Polyethylene with regular window glass. He found that Teflon-FEP film (2mm) has higher transmittance to glass than the others. On clear and overcast days the Teflon-FEP transmittance was found to be 96.6% and 88%, respectively. After one year of exposure to outdoor environment, he observed that both Teflon and Mylar manifested same transmittance as that of a new film.

Hollands (1965) conducted a theoretical study on the performance of the flat plate collectors when a selective honeycomb shaped panel of transmitting material is placed between absorber plate and glazing. The result showed that the panel can suppress convection losses and reduce radiation losses under definite conditions. He concluded that if honeycomb layers are thin enough, conduction losses through the panel walls can be ignored and good transmittance can be achieved. He also presented the efficiency curves for this type of collectors and predicted efficiencies higher than that of the conventional collectors, particularly at higher plate temperatures.

Eaton and Blum (1975) theoretically and experimentally studied the effect of evacuating a flat-plate collector housing under medium pressure of 1-25 Torr. For this setup they found that the convection losses can be suppressed and higher absorber plate temperatures and collector efficiencies can be attained. When selective coating with high absorptance and low emittance was applied on the absorber plate, higher steady-state temperatures for the absorber plate were obtained. They investigated the problem of collector case sealing and suggested that this issue can be resolved by using high temperature silicon sealants.

Gani and Symons (1979) simulated the effect of cover design in the thermal performance of flat-plate collectors for a high absorber plate temperature (150 °C). They conducted simulation for a variety of cover arrangements, cover materials with different surface treatments, and absorber surface treatments. They reached at several conclusions that are: (a) the change of absorber plate emittance has a major effect on the collector performance; (b) for multiple covers, the thickness of air gap has no significant effect on the variation in overall heat loss; however, for single cover system with honeycomb devices, the effect is significant; (c) An array of honeycomb with 60-90 (mm) thickness is advantageous however, when it is combined with a single glaze cover, emittance of the absorber plate is an essential parameter; (d) FEP Teflon or Polycarbonate covers should only be use along with a low emittance inner cover or selective absorber; (e) FEP Teflon and anti-reflection etched low glass iron, which had the highest solar transmittance, have equal values of $(\tau\alpha)_e$; however, the latter is the most desirable selection when using glass covers; (f) Application of antireflection coatings such as indium oxide or tin oxide reduces the cover transmittance, but when it is combined with a non-selective (black)

absorber plate, it could reduce the overall heat loss significantly, and improves the collector's performance. On the other hand when a selective absorber plate is used, the effect of reflective coatings is not important. They further concluded that a single high transmittance cover along with convection suppressing devices and a selective-coated absorber plate is the best possible design for high temperature purposes, which can thermally compete with an evacuated tube collector.

Cathro at al. (1984) addressed several difficulties that exist with antireflection coating application methods and proposed a new procedure through dip coating of glass in an "ethanol based colloidal silica sol". They concluded that the application of this antireflection film increased transmittance of the glass by 0.05, eliminated 60% of reflectance losses and resulted in 4% and 7% performance increase for a single and double glaze flat-plate collector, respectively. They observed that such an increase of efficiency was independent of the operating temperatures. The outdoor test also exhibited satisfactory stability against weather.

Chow and Harding (1985) experimentally and theoretically studied the effect of antireflection coatings on two different covers: flat double glaze and evacuated tubular glasses. They studied the solar transmittance of a pack of glass tubes as a function of incident angle and orientation, and the impact of antireflection coating (silica film in this study) on inner and outer surfaces of the tube. Their results showed that the pack of north-south aligned tubes is preferred as the cover than an east-west aligned one. Moreover, the transmittance of north-south aligned tubular glass cover is generally better than double-glaze cover, and also more improved than that of east-west coated at higher

incident angles. The application of antireflection coat has shown to enhance the transmittance of both plane and tubular covers by 8%.

Wijeysundera and Iqbal (1991) investigated the effect of inner plastic film thickness on the top loss coefficient. They studied a cover system consisted of an exterior glass and interior Teflon glazes (from 12.5 to 100 μm). They computed the top loss coefficient (U_{top}) over a variety of design and operating conditions and compared their results with those of a glass cover alone. They found that for either single or multiple covers, U_{top} is a weak function of the film thickness when ε_p is small (i.e. selective coating). The dependency of U_{top} on the film thickness decreases as the emissivity descents, and become independent of it when absorber plate emissivity reaches 0.1. Moreover, for any film thickness, U_{top} increases as either the wind heat transfer coefficient or the absorber plate temperature increases. They concluded that these dependencies are considerable only if ε_p is large.

Abou-Ziyan and Richards (1997) experimentally studied the effect of air gap between the honeycomb array and the absorber plate or top cover, on the heat transfer rate across a rectangular-cell honeycomb. They emphasized the importance of the air gaps in cutting conduction pass from absorber to the honeycomb and from honeycomb to the glaze which causes significant reduction in the conductive-radiative losses. Contrarily, the increase of top and bottom air gaps deteriorates, more or less, convection suppressing ability of the honeycomb and reduces the critical Rayleigh number. Nonetheless, with even slight drop of critical Rayleigh numbers for larger air gaps, Rayleigh number was 45-50 times larger than that of air gap alone, indicating the effectiveness of honeycomb cells in reducing the convection losses. They also found that

the reduction of critical Rayleigh is higher at larger tilt angles (i.e. 30° and 60°). It was noticed that an arrangement of honeycomb cells with both top and bottom air gaps is more effective than that of bottom air gap alone. They also optimized the ratio of top or bottom air gap thickness to honeycomb thickness, δ/L, in order to maximize U_{top}, and found that the minimum U_{top} is attainable at $\delta/L = 0.6$ for horizontal collector, and at $\delta/L = 0.4$ for collector with 30° and 60° tilt angles.

Reddy and Kaushika (1999) conducted a theoretical study on transparently insulated ICS solar water heaters and an experimental study on the cover systems with TIM installed between the top cover and absorber plate. The experiment included absorber-parallel and absorber-perpendicular honeycomb structures. They found that the absorber-perpendicular configuration showed greater solar collection-storage efficiencies compared to absorber-parallel arrays. However, they indicated that with taking total cost of the solar water heater into account, a double wall structured polycarbonate material (10mm thickness) with absorber-parallel configuration of TIM is cost-effective with comparable reduction in the heat loss coefficient (3.8 W/m^2K), as other perpendicular arrangement.

Gombert et al. (2000) studied transmittance of porous sol-gel antireflection coating on the solar collectors. This coating was applied on the glass by same method used by Cathro et al. (1984). They found that the solar transmittance of the glass by using this antireflection coating improved 6% at normal incident angles, and could do better at larger incident angles. They argued that the advantage of this coating is its inorganic composition which exhibits excellent temperature and UV strengths.

Abdullah et al. (2002) experimentally investigated the performance of flat plate solar collector with several arrangements of honeycomb arrays made of polycarbonate sheets. Arrays of 16 (mm) thickness were placed within 60 (mm) gap between absorber and cover glass. They found that for a single honeycomb cells fitted in the gap, the bottom gap (i.e. the gap between the absorber plate and bottom of honeycomb) is critical and that the optimum distance to obtain highest efficiency of the unit and lowest heat loss coefficient, is 3 (mm). Double honeycomb units showed less variation of heat loss with change in the top or middle gaps. It was concluded that a distance of about 25% of the air gap above and below a single honeycomb units can improve the collector performance significantly. This study demonstrated a reduction of 49% and 56% in $F_R U_L$ for collectors with single and double honeycomb units, respectively, compared to that of the air gap alone. The tests also exhibited 15% and 32% reduction in $F_R(\tau\alpha)_n$ for single and double honeycomb units, respectively. They concluded that the effect of optical efficiency, ($\tau\alpha$), is prevailing at low temperature ranges whereas the effect of U_L is dominant for high temperatures. They recommended using compound honeycomb in solar collectors when the temperatures are high and whenever an adequate design determining the honeycomb thickness as well as top and bottom distances has been performed.

Furbo and Jivan Shah (2003) studied the effect of antireflective (AR) coatings on the performance of a flat-plate collector, used in solar water heating systems, for different incident angles. They found that with AR coating, the transmittance increased with an increase in the incident angles up to 70° where the maximum increase in the transmittance is by 9%. A further increase in incident angles caused a decrease in the transmittance. They also observed 4-6% increases in the collector efficiency due to AR

coating. They concluded that for a solar heating system, the annual energy production could be increased by 12% to 20% if the mean collector fluid temperature is 60 (°C) and 100 (°C), respectively.

1.3.4. Heat Transfer Fluids

Heat transfer fluid is responsible to carry the thermal energy from the absorber plate to the storage tank. The heat transfer fluid must posses high thermal conductivity, high heat capacity and low viscosity; however, freezing point, boiling point, erosion, corrosion, toxicity, and cost confine the deployment of most of the fluids. Water has very good thermo-fluid properties; it is nontoxic and inexpensive. However, its high freezing and low boiling temperature as well as scaling and corrosion problems has been the major issue. Alternatively, the use of antifreeze solutions such as 30-50% ethylene glycol or propylene glycol in water has been successfully incorporated. However, the glycol-water mixtures deteriorate in case of overheating; therefore, it requires periodic monitoring of PH, inhibitor concentration and freezing point to ensure the solution's effectiveness and stability. Furthermore, in order to prevent intoxication of consumed domestic hot water by glycols additional heat exchanger or double wall pipe is necessary. Silicon fluids, synthetic and paraffin hydrocarbons, refined mineral oils, and refrigerants have also been used as another option. Silicon fluids have very high boiling and very low freezing points, they don not degrade, and they are also non-corrosive and nontoxic. On the contrary, silicon fluids are expensive and due to high viscosity and low heat capacity, require large diameter pipes and pumping capacity. Although initial cost of solar collectors with silicon fluids are higher then those of other fluids, their low maintenance cost may minimize the life cycle cost of the system. Hydrocarbon oils have lower

freezing point and lower specific heat but higher viscosity than water. Furthermore, the synthetic hydrocarbons are almost nontoxic. Phase change fluids such as refrigerants, on the other hand, have very good thermal properties, low boiling and freezing point and high heat capacity. They quickly respond to small temperature changes and can be circulated naturally from condenser to evaporator (in relatively short distances) and transfer very high amount of thermal energy per unit mass of refrigerant. HFC refrigerants like R134a, R407C, and R410A with GWP around 1300 (known as the green refrigerants) are environmentally safer and would be an appropriate option, accordingly.

Bickle (1975) introduced a passive approach to protect solar collectors from freezing damages. He pointed out the troubles and penalties that are involved with the active methods to avoid or protect systems from freezing. In this approach as water freezes it expands against an amenable area so that water expansion does not damage the system. In this technique a gas or air filled flexible pipe with smaller diameter compared to that of water pipe is inserted inside the water pipe. This air tube can be connected to a reservoir or be sealed. When the flexible tube is connected to a reservoir, the air pressure does not increase when water expands; however, the reservoir must be as close as possible to the freezing fluid to avoid creation of ice blockage. Contrarily, for the sealed one, the expansion of water increases the pressure inside the air tube that, in return, causes an increase of water pressure, and thus, the sealed tube must be large enough to bear that pressure rise within a safe limit.

Wilcox and Barnaby (1977) suggested heating of the collector either by means of electric heaters or recirculation of hot water from the tank to protect the water from freezing. They mentioned that the annual required energy to protect water from freezing

is equal to the product of the collector overall heat loss coefficient and the annual degree-hours that ambient temperature is below a base freeze protection temperature. Result of their calculations for several cities showed that the cost of heating the collector is negligible in the regions where winter is mild and suggested that for cold climates, sophisticated evaluation of the cost effectiveness is required.

Xinian et al. (1994) theoretically and experimentally studied the sequential freezing techniques to protect the collector from freezing. In the sequential freezing techniques, the water is pushed out of the collector instead of being trapped by ice blockage at both ends of tube, by maintaining a temperature gradient across the collector, and controlling the freezing sequences inside the tube. They showed that a collector designed based on the sequencing principle can operate in winter with no need for heat exchanger system, electrical heaters, or drain down. Their experimental model consisted of metallic riser tubes and the rubber manifold, so that the rubber manifold can neither be destroyed by the expansion of ice nor loss heat as fast as metallic pipe (resulting in sequential freezing). Furthermore, their results indicated that the temperature of the heat source (i.e. storage tank through the connected pipes in this case) could affect the sequence of freezing.

Phase-changing fluids are widely studied as a suitable heat transfer medium for heat pipes in the solar collectors or solar cooling cycles because of their excellent thermal and physical properties. Thus far, heat pipes operating with phase changing fluids exhibited very good performance. A heat pipe, as shown schematically in Figure 1-6(a), is a sealed and adequately evacuated metallic pipe that contains a small quantity of water or refrigerant. When this pipe is placed vertically (or slightly sloped) and the lower end is

heated, the fluid in the lower part of the tube absorbs thermal energy and starts boiling. The vapors ascend through the core of the pipe, towards cooler regions (i.e. the upper end) where they get condensed by transferring the latent heat to other fluid, substances or the environment, through the top. The condensed fluid then descends back through the inner surface of the pipe to the hot region by gravity and re-evaporates.

With the fluids of large latent heat of vaporization and condensation, a large amount of heat is transferred with small amount of fluid resulting in high efficiency. The maximum temperature up to which the heat pipe can operate is the critical temperature of the working fluid. Advanced heat pipes, as depicted in Figure 1-6(b), contain a capillary wick to facilitate return of condensate, by means of surface tension, towards the warmer end, particularly in absence of gravity.

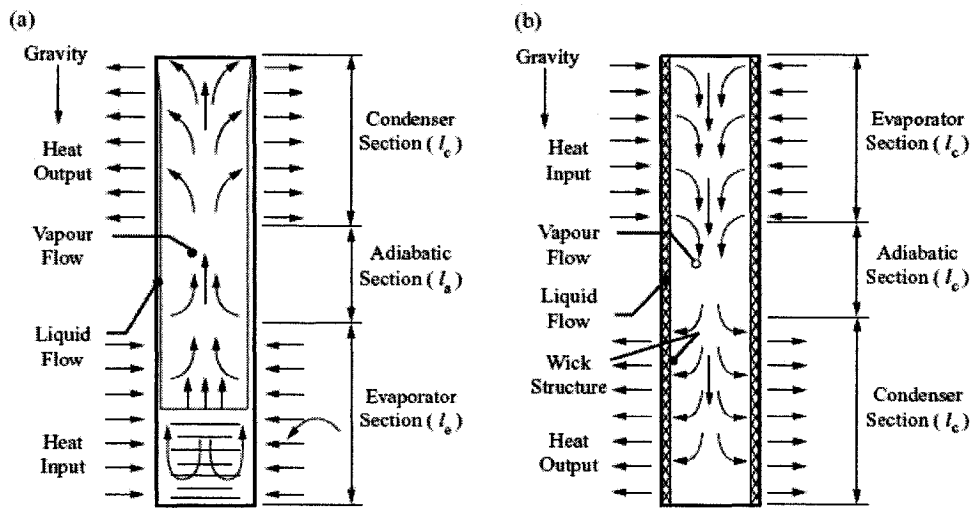

Figure 1-6: Schematic of (a) Conventional Gravity Assisted Heat Pipe. (b) Capillary Induced Heat Pipes, *Adopted from Joudi and Witwit, (2000)*

Utilization of heat pipes and phase change materials (PCM) have been studied considerably by researchers for thermosyphon solar water heaters with flat-plate or evacuated tube collectors.

Soin et al. (1979) were apparently the first who experimentally studied the effect of various design parameters on the performance of a flat-plate collector, operating under phase-change of fluid. They argued that such a system has numerous advantages that includes, high heat transfer coefficients (due to boiling and condensing process), no pumping of fluid is required, and freezing, fouling, and corrosion problems are eliminated. They observed that the system efficiency varies with the liquid level in the collector. As the liquid level increases in the collector, efficiency increases continuously until superheat region disappears and liquid begins to re-circulate. After re-circulating, the efficiency keeps increasing but very slightly. It was seen that efficiency increased as insolation amplified but further increase of insolation, after a certain value, dropped off efficiency due to increase of saturation temperature. They argued that influence of liquid level must be accounted in the Hottel-Whillier equation and presented a modified relation to predict the efficiency of a collector undergoing phase-change.

Akyurt (1984) designed and manufactured several heat pipes for solar water heating systems. He monitored these models for more than a year, and observed good performance. He also mentioned that this system did not show any start-up or gas generation difficulties.

Soin et al. (1987) modified his previous model in order to include condensing heat transfer coefficient. This new model predicts the performance of two-phase water heating system satisfactorily. They argued that to avoid superheating of the vapor, liquid level in the collector loop must be kept above 80%. Comparative long term experimental study of two-phase water heating system with a thermosyphon one indicated that the performance of the system with 75% liquid level is 4-8% and 10-12% less than that of thermosyphon

for clear sky and cloudy days, respectively. However, for liquid level above 80% the performance was found to be 5% improved.

Hammad (1995) experimentally studied the performance of a flat plate collector utilizing the wicked heat pipes and working at low temperature conditions. He concluded that the system possess high heat transfer capacity, it is corrosion and freeze free, no need for pumping, and requires less collector area than a collector that uses water whether naturally circulated or forced. He observed that the inclination of the pipes provides a "diode property" which transfers heat unidirectional. As a result, the cooling of storage tank during night time, due to reverse heat flow will be eliminated, which is a shortcoming in the water operated collectors. He found that the efficiency of his experimental model was about 60% which is better than the conventional water cooled collectors.

Pluta and Pomierny (1995) fabricated and studied combination of two-phase heat pipe with the traditional thermosyphon solar water heating systems. They used Freon R-22 as the phase-change fluid, with the fluid fill level of up to one-third of the pipe's height. Their results confirmed the advantages of heat pipe systems; however, they pointed out that appropriate selection of phase-change fluid, and proper design and construction of the collector plays an important rule in achieving good performance.

Chun et al. (1999) investigated the performance of SDWH systems using heat pipes to develop a suitable configuration for commercial purpose. The study carried out with wicked and wickless heat pipes filled with different fluid that was chemically stable and nonfreezing over the testing range. They suggested using heat pipe with wick when solar irradiance is low (since it distributes fluid uniformly along the surface of the pips),

however, for high irradiance they did not observe noticeable difference between performance of wickless and wicked pipes. They also observed that the operation of the system is not sensitive to the type of fluid and that sufficient application of black-chrome coating on the surfaces drastically improves the performance.

Hussein et al. (1999) mathematically analyzed the thermal performance of wickless heat pipes as a function of different parameters such as solar radiation, inlet water temperature, thickness and material of absorber plate, ratio of pitch distance to heat pipe's diameter and the ratio of heat pipe condenser section length to its total length. They concluded that (a) the efficiency of the wickless heat pipe increases with a decrease of inlet temperature; (b) the efficiency increases with a decrease in tube spacing; (c) for a constant value of the tube spacing, the efficiency was almost insensitive to the higher values of $k_p\delta_p$ (i.e. greater than 0.2), thus the material of the absorber plate can be limited by the pitch; (d) efficiency increases as the ratio W/D_o decreases, but the effect of W/D_o ratio on the efficiency weakens as the diameter decreases or inlet water temperature increases; (e) for a broad range of tube diameters, the variation in efficiency diminishes with a decrease in pipe diameter or a "limited" increase of heat pipe condenser section length to its total length.

Mathioulakis and Belessiotis (2002) theoretically and experimentally investigated the performance of a TSWH system with an integrated wickless gravity assisted heat pipes. In this study, a tank was placed behind the absorber plate but connected to the upper part of the loop (condenser) so that condenses would naturally return to the lower part of the loop (evaporator). The evaporator part of the system was a flat plate collector and the condenser part a multi-tube heat exchanger with welded fins inserted inside the

tank. Results showed up to 60% instantaneous efficiency and a successful operation even under freezing and overheating condition. They also proposed a theoretical model to optimize the system design.

Esen and Esen (2005) designed, fabricated and examined a thermosyphon solar collectors using wickless heat pipes with different "environmental friendly" refrigerants as the working fluid. They found that R410A acquired highest performance and collection efficiency (50.84%), followed by R407C and R-134a and concluded that high enthalpy of vaporization results in large amount of heat transfer by small amount of vapor, low viscosity and high surface tension enhances capillary effect, and high liquid conductivity decreases the temperature drop in the condenser and evaporator sections of the heat pipes. They also observed that all absorber plates manifested very uniform temperature throughout the test minimizing the heat losses. For the similar solar irradiance, they found that the temperature of the absorber plate charged with R410A refrigerant was lower than those of charged with R407C and R134a, resulting in higher efficiency and lower heat losses from the system.

Hussein et al. (2006) experimentally studied the effect of pipe cross section and fluid filling ratio on the performance of wickless heat pipes incorporated into flat-plate collectors. This study was performed over three different cross sections of wickless heat pipes: circular, elliptical, and semi-circular; and also over three different fill ratios for each cross section. They found that wickless heat pipe flat plate collector with elliptical cross section has higher performance at low fill ratios and it improves efficiency of the collector, accordingly. The optimum fill ratio to receive "higher instantaneous rate of thermal energy gain" was found to be 10% for elliptical cross section and around 20% for

the circular one. At 20% fill ratio for semi-circular section shows very weak performance compared to those of the other two cross sections. They concluded that due to higher surface area to volume ratio of elliptical cross section, compared to the other cases, the pressure and consequently the temperature is higher for same fill ratio and the heat flux leads to higher solar energy gain. When fill ratio was increased from 10% to 20%, the instantaneous rate of thermal energy gain dropped due to increase of the heat capacity of the heat pipes (i.e. collector) which led to temperature and pressure drop inside the pipe. They also observed that a further increase in the fill ratio significantly reduces the performance of the heat pipe.

1.3.5. Computer Simulation

Researches have been widely employing different computer simulation programs to predict the characteristics of the solar water heating system and to adequately size its pertinent components to ensure the satisfactory performance of the system. Among these software, the transient simulation program (TRNSYS) developed by Solar Energy Laboratory, University of Wisconsin-Madison (Klein S.A. et al., 2004) has been recognized as the most complete and accurate among the existing software.

Gutierrez et al. (1974) simulated a pumped circulation system to investigate the effect of three different schemes of auxiliary heating systems: inside the tank, in parallel with tank and in series with tank. The result showed that: (a) heater in series (in the tank's exit line to the load) consumed the lowest and in parallel consumed the highest amount of auxiliary heating energy. However, when the set temperature is low, the effect of heater position is not a significant variable, but for high temperature applications locating of the auxiliary heater must be well analyzed; (b) as the load increases, the average operating

temperature of the collector decreases resulting in the reduction of collector heat losses which in turn increases the amount of auxiliary energy and also the utilized solar energy; (c) the storage tank capacity influences the average water inlet temperature into the collector; (d) water withdrawal time (i.e. load pattern) is very important. The difference in amount of auxiliary energy, between the least and the most favorable withdraw time is 17% regardless of heater location; however, the influence of load pattern decreases as the tank size increases; (e) it was seen that the "least favorable" time to withdraw water is morning, when the collector starts to operate. Early morning withdraw causes higher average temperature in both tank and collector resulting in higher heat losses; however, if the tank is very well designed and its losses are minimized, the effect of load time is insignificant within the period when the collector its stops operation in afternoon; (f) the "most favorable" time to withdraw water is in early afternoon (3 hours period centered at the noon) when the collector inlet temperature is high; (g) a 20(^{o}C) decrease in the ambient temperature have predominant effect in the performance than 20(^{o}C) increase in the minimum set temperature. They concluded that any method that reduces inlet water temperature to the collector will increase the performance.

Baughn and Young (1984) calculated the optimum flow rate of flat-plate collectors incorporated in a two-tank direct forced circulation system with on-off pump operation. Determination of the annual optimum flow rate is carried out using a transient simulation program called SHOW, which was subjected to an early mornings and evenings water withdraw patterns. In this study, they underscored the strong influence of flow rate on the overall performance of the system, collector efficiency, storage tank stratification, and required pumping power. They pointed out that the optimum flow rate

is also a function of water distribution profile and location of the system. Their results indicated that the solar fraction increases as flow rate ascends up to about 5.1 (mL/sec.m^2) and then stays almost unchanged until 13.44 (mL/sec.m^2), then it decreases slowly as flow rate goes up. They mentioned that this drop in solar fraction, for flow rates above 13.44 is due to the degradation of the tank stratification. They found that this calculated range is in good agreement with other published data. They concluded that since performance (and consequently solar fraction) drops quickly for flow rates below 5.1 (mL/sec.m^2) and slightly for larger values, it is recommended to use the values closed to the higher values of the calculated limit (0.0051 – 0.0134 kg/sec.m^2). They, moreover, used these data to estimate the required pumping power which found to be much lower than practically used values.

Buckles and Klein (1980) compared performance of different combinations of the forced circulation solar water heating systems using TRNSYS simulation. This study included combinations of either single or double (auxiliary) tank, intermediate heat exchange inside or outside the tanks, auxiliary heater inside either of the tanks, and also considered direct or indirect forced circuits. They also modified ***f***-chart method in order to include the effect of tank insulation thickness in the evaluation. They found that: (a) the annual solar fraction decreases slightly with this order: single tank with external heat exchanger, double tank with external heat exchanger, single tank with internal heat exchanger, and double tank with internal heat exchanger. They suggested using the single tank due to reduced storage losses and external heat exchanger because of its higher effectiveness compared to that of internal one; (b) for different collector areas, system with small storage capacity has higher annual solar fraction since smaller storage tank has

less energy losses. However, the difference between the solar fraction of small and large storage systems decreases as the collector area increases. When the system is sized to provide large fraction of load, a tank with bigger capacity could work at lower average temperatures; (c) for a system with reasonable storage capacity, hourly distribution pattern of consumed hot water has insignificant effect on the annual performance; (d) for an identical hourly distribution pattern, variation of day-to-day water withdrawals in weekdays will greatly reduce the annual performance particularly when daily withdraw goes above the storage capacity. Comparing simulation and calculation (f-chart) results with the reported experimental data, they concluded that the discrepancies between the methods can be eradicated if the effect of heat losses from auxiliary tank is considered in the system load.

Morrison and Braun (1985) developed a simulation model for TRNSYS to study characteristics of horizontal and vertical tanks in thermosyphon SWH systems, and found good agreement between obtained results and existing experimental data for the collector inlet and outlet, and tank temperatures throughout the day except for that at the beginning of the day. Their results showed that: (a) for tanks with different height to diameter ratios, the conduction between water layers inside the tank has small effect on the performance of tall vertical tank but major effect on that of horizontal tank; (b) due to the short conduction path in the horizontal tank, adequate stratification cannot be preserved. By using a separate auxiliary tank, conduction from top auxiliary zone into the bottom preheat zone can be eliminated and annual solar fraction can be improved from 0.49 to 0.55; (c) low collector flow rates enhance tank stratification resulting in lower inlet temperatures into the collector which in turn reduces heat losses from the collector.

However, fully stratified tank has higher heat loss, from the very hot layer at the top than a partially stratified fixed inlet; (d) for tall vertical tank, the ratio of optimum collector volume to load volume (the volume of delivered hot water to the load) varies from 1.0–1.2 and 0.8–1.0 in summer and winter, respectively; (e) comparison of a thermosyphon system with a forced circulation system when both were subjected to Rand load profile, showed very slight difference in the performance when the flow rate is low; however, at the optimum flow rate, forced system exhibited slightly better performance; (f) thermosyphon system is more sensitive to load pattern than forced system with fully mixed tank, unless pumped system operates with lower flow rates where the variation with load profile will be similar to that of thermosyphon system. Their major conclusion was that the thermosyphon system has highest performance when the daily load flow is almost equal to the collector volume flow. Whenever, the daily collector volume flow rate is more than the daily load flow, the performance will be mostly depend on the collector flow rate since it dictates conduction inside the tank and convection.

Shariah and Ecevit (1995) simulated thermosyphon solar water heating (TSWH) system with internal auxiliary electric heater using TRNSYS, to study the effect of different load temperatures on the long-term performance of the system. They observed that the efficiency and annual solar fraction is greatly depend on the load water temperature, in particular, when the system is operating with higher solar fractions. Moreover, when the ratio of daily load volume to the collector area is large, the effect of load temperature on the annual solar fraction is large. The collector efficiency is also highly influenced by the ratio of the tank volume to the collector area (V_c/A_c) whenever this ratio is less than or equal to 40 (lit/m^2), for any collector area and load temperatures.

They also found that the average tank temperature is closely influenced by the tank volume, collector area and in particular the load temperature. They concluded that the performance of a system operating with solar fractions less than 70% is highly affected by collector area.

Shariah and Löf (1996) investigated the effect of tank height on the performance and annual solar fraction of a thermosyphon SWH system for different hot water load (set) temperatures and tank capacities using TRNSYS. The result illustrated that: (a) for all tank heights and set temperatures, an increase in tank volume from 60 liters to approximately 150-200 (lit) resulted in an increase in solar fraction. Further increase in the tank volume from 150 to 400 (lit) causes some dependency on set temperature and tank height; (b) increase of tank height from 0.4 to 1.6 (m) resulted in an increase in annual solar fraction for all set temperatures. A shorter tank with higher set temperatures, results in very poor stratification and high inlet temperature into the collector which in turn yields low performance and lower solar faction; (c) when the tank height is equal to 1.0 (m), the solar fraction reaches the maximum value for any set temperature. For tank height more than 1.0 (m), no major improvement in solar fraction was observed; (d) solar fraction is highly affected by tank height when tank volume is large, in particular when the set temperature is also high; (e) solar fraction for large collector areas increases as V_c/A_c ratio increases and reaches a maximum value as the ratio reaches 50-60 at load temperatures in the range 70-80 (^{o}C). Contrarily, for the small collectors area (2m^2), the effect of this ratio on the solar fraction is insignificant for set temperatures of 60-80 (^{o}C). For volume to area ratio of about 100 and set temperature less than 70 (^{o}C), variation of solar fraction is insignificant; (f) solar fraction decreases from 0.85-0.95 to 0.5-0.6 when

the set temperature increases from 50 to 80 (°C) for a 4m^2 collector; likewise a decrease in solar fraction from 0.65 to 0.35 was observed for a 2 (m^2) collector.

Michaelides and Wilson (1996) optimized the design criteria of an active SWH system for hotel application using TRNSYS simulation. Three different daily hot water load profiles correspond to 40, 50, and 60 liters per day per consumer were considered. It was found that the optimum collector area, which maximizes the lifecycle saving per hotel consumer, is respectively 1.2, 1.0, and 0.8 (m^2) for high, medium, and low hotel hot water load profiles. They also found that the collector size is affected by the load profile and annual thermal load. The optimum collector area was found to be 0.4, 0.35, and 0.3 m^2 per annual GJ of load for low, medium and high load profiles, respectively. Solar fraction varied as 0.80, 0.75 and 0.65, respectively, for low, medium and high load profile.

Shariah and Löf (1997) used TRNSYS to simulate a thermosyphon SWH system and studied the effect of using an auxiliary heater and its location on the system performance. The simulations were conducted for two different auxiliary heater locations (inside the tank and in series with tank towards services), two water load temperatures, two different daily hot water consumption volumes, and four different types of daily load profiles. They also considered the effect of storage tank volume and thermal and optical properties of the collector. They proclaimed that designing a solar water heating system that delivers 100% of hot water consumption of a household without any backup auxiliary heater is not cost-effective and that, 50-80% of hot water demand can be supplied by solar system and the rest by an auxiliary heater which has the capacity of heating 100% of the demand when there is not enough solar energy. Their simulation results showed that (a)

the scheme of applying auxiliary heat to the delivered water affects the performance of the system, and it is also a function of collector size and quality, load profile, and load volume and temperature; (b) solar fraction varies for each water withdraw (load) profile even under identical operating condition. Solar fraction is highest for the system operated with Rand profile, followed by evening profile, then continuous profile and finally it is the lowest (as half as Rand profile) for the morning water withdrawal; (c) enlarging the size of the tank (i.e. doubling it) has insignificant effect on the system performance, and thus the suggested value of 40-50 (lit/m^2) when Rand profile is used is still valid; (e) increasing the set temperature of supplied water from 60 to 80 (°C) reduces solar fraction by 30-40%; (f) for efficient collectors, location of auxiliary heater is unimportant when continuous profile is used, but for inefficient collectors, the external heater is superior; (g) internal heater maintains the higher temperatures at the upper parts of the tank causing extreme heat losses throughout the day and during the time when water is not in use. However, for external heater in series scheme, the high tank temperatures occur only in the afternoon. Systems with external heater has higher solar fraction than that of internal heater in particular with morning or evening withdrawal.

Michaelides and Wilson (1997) studied the effect of auxiliary heater location on the performance of TSWH systems, using TRNSYS. They considered in-tank auxiliary heater and external heater for the system subjected to Rand load profile. The results indicated that the system with external heater has higher solar fraction and collector efficiency than that with internal heater. The annual solar fraction of the system with external heater was 86%, whereas that of the in-tank heater located at the top and bottom of tank was 77% and 59%, respectively. They also studied the effect of collector

return pipe and auxiliary heater height on the annual solar fraction and average efficiency. They concluded that the system performance increases with the heater elevation from the bottom of the tank. Solar fraction of about 80% at the height of 940 mm, from the bottom of the tank, and 55% at the height 305 mm, was observed.

Shariah and Shalabi (1997) used TRNSYS to optimize design parameters of a thermosyphon solar water heating system. Solar fraction was used as the optimization parameter. Their results showed that (a) the solar fraction is highly dependent on the number of riser tubes with a maximum value for 8 tubes; (b) tube spacing affects solar fraction. The solar fraction is observed to be highest with small tube spacing; however, an increase of tube spacing from 8 to 15 (cm), has no significant effect on the solar fraction. Further increase of tube spacing (from 15 cm) decreases the fraction; (c) the influence of tube diameter on solar fraction is evident when tube diameter is small; (d) size of the pipes connecting collector to the tank affects the solar fraction; (e) increasing tank height from 0.4 (m) to 0.8 (m) increased fraction satisfactorily; however, the optimum height depends on both ambient temperature and solar insolation. The recommended tank height, for their case, was about 0.8-1.0 (m); (f) height of return pipe is a critical parameter. Solar fraction improved by approximately 10% when the return pipe height increased from 0.2 (m) to 1.0 (m); (g) solar fraction improved by about 20-25% when the auxiliary heater and thermostat is located close to the top of the tank rather than close to the bottom of the tank.

Shariah et al. (1999) studied the effect of thermal conductivity of the absorber plate on the performance of the thermosyphon SWH systems using TRNSYS. They studied effect of the thermal conductance of steel, aluminum, and copper plates on the

solar fraction, fin efficiency factor, collector efficiency factor, and heat removal factor. They found that the thermal conductivity of absorber plate has a very strong effect on characteristic factors: F, F', and F_R. Solar fraction is affected by thermal conductivity when it is in the range 10-50 (W/m °C). They also observed that the annual solar fraction and characteristic factors increase by 4-7%and 12-19%, respectively, when aluminum plate was used instead of steel plate; whereas no appreciable difference was observed by switching aluminum to copper plate. They concluded that use of use of copper plate instead of aluminum plate is not advantageous unless corrosion or health issues are taken into account.

Kalogirou and Papamaracou (2000) used TRNSYS to model a TSWH system consisted of two flat-plate collectors and a storage tank. They also validated their simulation model with simple experiments. The validation of TRNSYS model with experiments exhibited good agreement with an average erroe of 4.68%. Their result showed that (a) the natural circulation flow (thermosyphon) during the day is affected by incident solar radiation. The flow starts to increase from morning and reaches the maxima at solar noon, and then starts to decrease during the afternoon; (b) variation of the system efficiency is not in accordance with flow rate variation during the day. The highest efficiency (i.e. 50%) was observed around 11 am but it decreased throughout the afternoon when after 4 pm became 15%; (c) annual solar fraction of the system is about 0.79, which reaches 1.0 in summer with no need for any auxiliary heating; (d) pay-back time of the system was estimated to be 8 years; (e) collector efficiency and outlet temperature varied with solar radiation. They concluded that TRNSYS can be used

confidently as a tool to optimize all design parameters of the system that influences the performance.

Jordan and Vajen (2000) studied the effect of hot water load profile on the fractional energy saving factor of the solar water heating system [The Fractional energy saving factor is the ratio of the consumed auxiliary energy for SWH system to demanded energy for conventional WH systems]. In this study, a more realistic hot water load profile based on statistical methods was derived for the period of one year with one minute time steps. TRNSYS was used to study the effect of this realistic model, flow rate, and water withdraw time; on the fractional saving, and to compare it with conventional simple load profiles. The result of simulation showed that less solar energy in summer was delivered using realistic profile compared to that of conventional one since the realistic model counts for reduced hot water consumption in summer, holidays, and uses sine-function for distribution.

Shariah et al. (2002) used TRNSYS to optimize tilt angle of solar collectors for TSWH systems operating in accordance with Rand load profile. Using solar fraction as the optimization parameter, they found that the optimum tilt angle is 5-8^{o} larger than a tilt angle that maximizes solar radiation at the top of the collector. They also found that operating conditions affect the value of the optimum angle. Moreover, optimum tilt angle for the systems with adequately high solar fraction was found to be between latitude and latitude + 20^{o}. It was also observed that in summer, the collected useful energy is significantly higher than the load energy, particularly for collector with 3 m^2 or greater area.

Wongsuwan and Kumar (2005) studied the performance of a forced circulation SWH system and compared TRNSYS simulation results with the data obtained from their experiments and another simulation model based on artificial neural network (ANN). Based on the comparison they found that (a) TRNSYS predicted hourly values of collector outlet temperature slightly higher before noon and lower in the afternoon, except on overcast days when the deviation was large; (b) hourly mean temperature inside the tank was predicted more accurately in the cloudy periods but with deviation in clear days probably because TRNSYS assumes U_L a constant value and does not counts for larger changes in U_L at the end of the day; (c) hourly delivered useful energy was predicted to be 6.6% higher for clear day condition but in good agreement for all other climate conditions; (d) difference in daily useful energy was about 8.1%, thus, hourly predications provide better data than daily predictions for all weather condition. They concluded that both TRNSYS and ANN predict hourly and daily estimates of the system sufficiently well.

1.4. MOTIVATION AND OBJECTIVES OF THE THESIS

Reduction of the greenhouse gas emissions has recently gained significant attention in Canada at both governmental and public levels. Moreover, cold weather and life style make the residential sector a large energy consumer, or in other word, a big contributor in the production of greenhouse gases in Canada. Therefore, utilization of renewable energies, particularly solar energy, for residential sector seems to be necessary step towards the reduction of CO_2 gas emissions in Canada. However, the solar systems in cold climate like Canada may not be as efficient as those in warm or moderate climates. In cold climates, freezing of the working fluids and its related damages to the system is a

burden. Furthermore, heat losses from the systems are relatively high, and available solar irradiance is relatively low. Many types of solar systems (such as space heating, water heating and PV system) which are suitable for the cold climate have been studied and used in Canada for long time. However, contrary to the natural circulation water heating systems, there have been relatively few published studies in the literature that are focused on the detailed parametric study of the forced circulation solar water heating systems, in particular for the cold climate . There is, moreover, scarcity of the published data concerning the heat transfer phenomena and thermo-fluid behavior of the solar collectors. Therefore, present study is aimed to:

- Conduct a theoretical study to optimize the design of a forced-convection solar water heating system for a residential unit in Montreal
- Develop an indoor experimental facility to study the thermal performance of solar collectors, and to study the heat transfer phenomena inside the tubes
- Conduct an experimental study to investigate the effect of heat transfer enhancement devices in solar collectors

The work presented in this thesis can be extended to an extensive future works on solar thermal systems for cold climate, in particular, the investigation of thermo-fluid behavior in such a complicated geometry which is still poorly understood.

1.5. OVERVIEW OF THE THESIS

This thesis is organized in five chapters. In Chapter-1, literature review, motivation and objective of this thesis is presented. In addition, different methods used for solar water heating systems have been described. Main part of the first chapter includes an extensive literature review covering most of the previous theoretical, experimental, and computer simulation investigations that have been conducted on the field of solar water heating by flat-plate collectors. This literature review is divided into the subsections based on main components of a flat-plate collector. In Chapter-2, an analytical investigation of the solar water heating system for a residential unit in Montreal is conducted using *f*-chart method and all of the governing equations for the solar water heating system with flat-plate collectors are presented along with meteorological and other required design data for Montreal. In Chapter-3, an extensive computer simulation of the same residential unit is performed using TRNSYS software. A detailed parametric study is conducted for different design parameters of the given solar water heating system. The main design parameters are also optimized. Chapter-4 is focused on a detailed experimental study of the thermal performance of flat-plate collectors. The effect of several heat transfer enhancement devices inside a tube of a flat-plate solar collector is analyzed with main emphasis on the investigation of heat transfer phenomena when free and forced convections are combined together in a laminar flow regime inside the tubes of the collector. The details of the test facility developed during this research are also described in Chapter-4. The overall conclusion of the thesis based on the conclusions presented in Chapters 2, 3, and 4 along with the contributions to research, and future recommendations are presented in Chapter 5.

CHAPTER 2

ANALYTICAL EVALUATION OF THE PERFORMANCE OF A FLAT-PLATE SOLAR COLLECTOR

2.1. PROLOGUE

Evaluation of the actual performance of a solar collector can be performed only by exposing it to on-site solar radiation and measuring the actual data such as fluid temperatures and flow rate, irradiance on the collector surface, outdoor temperature, wind velocity, and collector surface temperature, over a specified period of time. Geometry of the collector and site condition can also influence the performance of a solar collector. The methodology for such experimental measurements and tests are standardized by ASHRAE93-2003, ASHRAE95-1987, and ASHRAE109-1986 procedures. However, in the design stage, most of the required data are unknown for the designer. There are several analytical and numerical methods available to size and estimate the short-term (instantaneous) and long-term (monthly and annual) performance of a solar collector. Some of these methods require collector operating temperature to calculate the critical radiation level, collector characteristics, or the correlation factors which are the results of the large amount of computer simulations. One of the widely used methods to estimate the solar water heating characteristics is the simplified *f*-chart method developed by Klein et al. (1976). This method correlates the hourly output of various dimensionless variables from simulation, that are used to estimate the long-term thermal performance of the liquid-or air-based collectors by using monthly average meteorological data. For our proposed system, i.e. solar water heater in Montreal, *f*-chart method that presented by Beckman et al. (1977) has been used to approximate the size of the system and monthly performance prior to any computer simulation—by TRNSYS—to be done.

2.2. METEOROLOGICAL DATA

2.2.1. Solar Angles

In the following, different solar angles that are important from the design aspect are discussed.

Latitude **(φ)**: It is the angular location north or south of the equator. For instance, Montreal is located at latitude $\varphi = 45.5^{o}$N.

Solar declination angle **(δ)**: It is the angle between the earth-sun line and the earth equatorial plane. It varies daily because of tilted axis of earth. It can be calculated using the following equation from Duffie and Beckman (1991):

$$\delta = 23.45 \sin[360^{\circ}(284 + n)/365] \tag{2.1}$$

where n is the day number in a year.

Tilt angle **(β)** or slope: It is the angle between the horizontal and the plane of collector. The optimum tilt angle to obtain the largest heating load fraction from sun for any solar heating system facing south is $\varphi \pm 10^{\circ}$ (Plante, 1983). For solar water heating systems, the optimum tilt angle is equal to the latitude (φ) (Beckman et al., 1977). For solar water heating since the water heating load is almost identical all year around, a deviation by up to $\pm 15^{o}$ from the optimum tilt angle has no significant effect on the performance according to Beckman et al. (1977).

Hour angle **(ω)**: It is the angular displacement of the sun from solar noon (local meridian) caused by earth's rotation on its axis. It is equal to 15^{o} per hour from the solar noon, counted positive for afternoons and negative for mornings. The solar sunset hour angle (ω_s) is given by following relation according to Duffie and Beckman (1991):

$$\omega_s = -\tan\varphi \cdot \tan\delta \tag{2.2}$$

Incident angle **(θ)**: It is the angle between the direct (beam) radiation on a surface and normal to that surface. If the tilt is set equal to the latitude, the incident angle will be zero. The recommended average values for n and δ from Duffie and Beckman (1991), as well as calculated values of ω_s, for 45.5° latitude, are presented in Table 2-1.

Table 2-1: Average Solar Declination and Sunset Hour angles (in Degrees) for Montreal at 45.5° of Latitude

Month	Jan	Feb	Mar	Apr	May	Jun	Jul	Aug	Sep	Oct	Nov	Dec
n	17	47	75	105	135	162	198	228	258	288	318	344
δ	-20.9	-13.0	-2.4	9.4	18.8	23.1	21.2	13.5	2.2	-9.6	-18.9	-23.0
ω_s	67.1	76.4	87.6	99.7	110.3	115.7	113.2	104.1	92.2	80.1	69.6	64.4

2.2.2. Monthly Average Ambient Temperature and Wind Speed

The average monthly outdoor temperature, $\overline{T}_{amb}$, for Montreal from Duffie and Beckman(1991), and also average normalized temperature data over a period of 1971 to 2000 issued by the Environment Canada (2006) from Montreal Mirabel International Airport (45.67°N), Montreal P.E. Trudeau International Airport (45.47°N) and McGill (45.5°N) stations are presented in Table 2-2.

Table 2-2: Monthly Average Ambient Temperature (°C) for Montreal

	Jan	Feb	Mar	Apr	May	Jun	Jul	Aug	Sep	Oct	Nov	Dec
Duffie & Beckman (1991)	-9.0	-7.0	-2.0	5.0	12.0	17.0	18.0	17.0	15.0	8.0	1.0	-6.0
Mirabel Inter'l Airport	-12.1	-9.8	-3.4	3.5	12.5	17.0	19.5	18.3	13.2	6.9	1.0	-5.0
P. E. Trudeau Int'l A	-10.4	-8.9	-2.4	5.7	13.3	17.9	20.9	19.5	14.4	7.9	1.6	-6.6
McGill Station	-8.9	-7.2	-1.2	7.0	14.5	19.3	22.3	20.8	15.7	9.2	2.5	-5.6

The values in Table 2-2 varied at each station over different months. For the calculation purpose, in the present study the data from Duffie and Beckman (1991) is used. The normalized wind speed in (km/hr) from the same three stations is shown in Table 2-3. The most frequent wind direction in Montreal is SW.

Table 2-3: Monthly Normalized Average Wind Speed (km/h) for Montreal

	Jan	Feb	Mar	Apr	May	Jun	Jul	Aug	Sep	Oct	Nov	Dec
Mirabel Inter'l Airport	13	12	12.7	12.7	10.9	9.3	8	7.5	8.2	9.9	11.3	11.7
P. E. Trudeau Int'l A.	16.6	15.4	15.9	15.8	14.2	13.2	12.2	11.3	12.2	13.8	15.3	15.4
McGill Station	12.4	12.4	12.3	12.3	11.5	11.5	10.9	10.2	10.2	10.8	11.2	11.6

2.2.3. Monthly Average Radiation

Monthly average total daily radiation, $\overline{H}$ (kJ/m^{2}day), on a horizontal surface is obtained for most of the North American cities using *Pyranometer* which measures the shortwave radiation from sun and sky, and *Pyrheliometer* which measures the direct normal incident radiation. Monthly averaged radiation on the horizontal surface can be obtained from Duffie and Beckman (1991), and also metrological data measured by the local station. Monthly average radiation on a tilted surface, $\overline{H_T}$, can also be calculated by this equation from Duffie and Beckman (1991):

$$\overline{H_T} = \overline{R} \times \overline{H} \tag{2.3}$$

where, $\overline{R}$ is the ratio of the monthly average daily radiation on the tilted surface to that on the horizontal one. This ratio can be calculated from the following equation:

$$\overline{R} = \left(1 - \overline{H_d}/\overline{H}\right)\overline{R_b} + \overline{H_d}/\overline{H}\left(\frac{1+\cos\beta}{2}\right) + \rho\left(\frac{1-\cos\beta}{2}\right) \tag{2.4}$$

(Duffie and Beckman, 1991) where, $\overline{H_d}$ is the monthly average diffuse radiation, $\overline{R_b}$ is the ratio of the monthly average direct (beam) radiation on a tilted surface to that on the horizontal one. Ground reflectance, ρ, is depends on angle of incident and varying from 0.2 to 0.7. When the ground is bare or covered with less than 25.4 (mm) snow, ρ is assumed to be 0.2. ρ is calculated to be 0.7 when the ground is covered with more than 25.4 (mm) of snow. Maure and Galanis (1979) have used 0.2 and 0.4 for bare and snow covered ground, respectively. The ratio $\overline{H_d}/\overline{H}$ can be calculated from either of the following equations:

$$\overline{H_d}/\overline{H} = 1.39 - 4.03\ \overline{K_T} + 5.53\ \overline{K_T}^2 - 3.11\ \overline{K_T}^3 \tag{2.5}$$

Liu-Jordan (*from* Beckman et al, 1977), or:

$$\overline{H_d}/\overline{H} = 0.775+0.00653\,(\omega_s\text{-}90) - [0.505+0.00455\,(\omega_s\text{-}90)] \times \cos[115\,\overline{K_T}\text{-}103] \quad (2.6)$$

Collares-Pereira (*from* Duffie and Beckman, 1991)

In equations (2.5) and (2.6) $\overline{K_T}$ is the monthly average clearness index, which is the ratio of the monthly average total daily radiation to that of the extraterrestrial daily insolation ($\overline{H_0}$) or:

$$\overline{K_T} = \overline{H}/\overline{H_0} \quad (2.7)$$

The extraterrestrial daily insolation, $\overline{H_0}$, is the amount of solar radiation outside the atmosphere, and function of the day number, latitude, declination, the sunset hour angles and the solar constant G_{sc}. The values of $\overline{H_0}$ for different latitudes are tabulated in Duffie and Beckman (1991). The ratio $\overline{R_b}$, finally, can be calculated using the following formula from Duffie and Beckman (1991) as:

$$\overline{R_b} = \frac{\cos(\varphi-\beta)\cos\delta\sin\omega_s'+(\pi/180)\omega_s'\sin(\varphi-\beta)\sin\delta}{\cos\varphi\cos\delta\cos\omega_s+(\pi/180)\omega_s\sin\varphi\sin\delta} \quad (2.8)$$

where, ω_s' is sunset hour angle on the tilted surface and is equal to:

$$\omega_s' = \min[\omega_s, \cos^{-1}(-\tan(\varphi+\beta)\tan\delta] \quad (2.9)$$

(Duffie and Beckman, 1991)

Different parameters related to the monthly average daily radiation on the collector surface are calculated using the equations (2.3) to (2.9) for Montreal. The values of $\overline{H_0}$ and $\overline{H}$ are taken from Duffie and Beckman (1991). These quantities are summarized in the Table 2-4.

Table 2-4: Monthly Average Daily Radiation on the Collector Surface Tilted at 45.5 Degrees

	$\overline{H_0}$	$\overline{H}$	K_T	$\overline{H_d}/\overline{H}$	$\overline{R_b}$	ρ	$\overline{R}$	$\overline{H_T}$
	MJ/m^2	MJ/m^2						MJ/m^2
Jan	12.10	4.60	0.38	0.45	2.80	0.70	2.02	9.29
Feb	17.20	8.37	0.49	0.38	2.10	0.70	1.73	14.46
Mar	24.80	13.39	0.54	0.36	1.50	0.40	1.33	17.74
Apr	32.90	16.74	0.51	0.40	1.10	0.20	1.03	17.23
May	38.80	19.68	0.51	0.42	0.90	0.20	0.91	17.89
Jun	41.30	20.52	0.50	0.44	0.80	0.20	0.85	17.48
Jul	40.00	21.35	0.53	0.41	0.80	0.20	0.85	18.15
Aug	35.10	18.42	0.52	0.40	1.00	0.20	0.97	17.87
Sep	27.50	12.97	0.47	0.42	1.30	0.20	1.14	14.79
Oct	19.60	8.37	0.43	0.44	1.90	0.20	1.47	12.31
Nov	13.30	4.19	0.32	0.53	2.60	0.20	1.71	7.17
Dec	10.50	3.35	0.32	0.51	3.10	0.40	2.01	6.75

Maure and Galanis (1979) reported the maximum (in summer), minimum (in winter) and average values of $\overline{H}$ based on the measured data at Montreal stations. Iqbal (1979a) also presented the average daily total and diffuse solar radiation on horizontal surface for few Canadian cities as well. These values are slightly different from that of Duffie and Beckman (1991) that were shown in Table 2-4. These values are presented in Table 2-5 for comparison purpose.

Table 2-5: Monthly Average Daily Total and Diffuse Radiation (MJ/m^2.day) on Horizontal Surface for Montreal: *1-Maure and Galanis (1979), 2- Iqbal(1979)*

	Month	Jan	Feb	Mar	Apr	May	Jun	Jul	Aug	Sep	Oct	Nov	Dec
1	$\overline{H}$	5.33	8.46	12.99	16.07	19.37	22.68	20.59	16.86	12.40	8.28	4.48	3.24
2	$\overline{H}$	5.26	8.73	12.47	15.79	18.48	20.94	21.17	17.18	13.17	8.26	4.55	3.79
	$\overline{H}_d$	2.89	4.38	5.85	6.61	8.18	9.18	9.24	8.01	5.88	3.96	2.55	2.27

2.3. WATER HEATING LOAD

In solar heating system design, it is necessary to estimate the long-term (monthly or annual) average heating loads. The water heating load or the amount of the energy required to warm water from the inlet cold water temperature to a desired temperature is

dependent on several factors that include hot water consumption, cold water inlet temperature, geographic location and orientation of the building, system characteristic and quality of construction. This load also includes any heat loss from the storage tank, piping system, and the amount of the energy that is required to reheat the water that was already heated but not used. The hot water also being wasted from sink, shower, dishwasher and laundry machine which is drained without being used. The amount of this wasted hot water is estimated to be about 20% of total hot water consumption in a residential building that consumes 199 lit per day, according to Lutz (2005).

2.3.1. Household Hot Water Consumption

The hot water consumption is depends on the lifestyle of people, season of the year, time of the day, and geographical parameters. It usually accounts for almost 20% of the total energy consumption of any residential unit in North America. For a one family dwelling unit in North America, Babbitt (1960) has suggested 227-378.5 (lit) of hot water per day for a one bath and 378.5-757 (lit/day) for two bath houses. Becker and Stogsdill (1990) indicated average household consumption of 236 (lit/day) with peak hourly use of 19 liters per hour at 8:00 am. Gilbert, et al. (1985) estimated 250.6 (lit/day) with maximum hourly use of 15.5-33.7 (lit) based on a study over 110 single dwelling units in North America. Perlman and Mills (1985) studied 59 homes in Canada and found an average value of 236 (lit/day), varying from 171 in July to 249 (lit/day) in January, with an average hourly use of 37 (lit). They also found that the average hot water consumption per person per day varies from 46.5 to 85.5 liters. The monitoring of hot water consumption by Hiller (1998) over 14 homes performed indicated 224 (lit/day). Kempton (1987) studied the hot water consumption of eight single-family dwelling units and found

that the hot water usage varies from 44.3 to 126 (lit/day) per person. Usibelli (1984) estimated the average hot water consumption of 67 (lit/day) per person. US Department of Energy-DOE (1993) gives a national average of 171.5 (lit/day) per household or 28.4 (lit/day) per person. Finally, a study by NAHB (2002) in Ohio recorded average household consumption from a high range of 227 to 321 to a low range of 75.7 to 151.4 (lit/day). Based on these studies an average hot water consumption of 246 (lit) per day (65 USGPD) per dwelling unit is considered in the present study.

2.3.2. Inlet Cold Water Temperature

Monthly average inlet water temperature, $\overline{T}_{main}$, is a function of outdoor ambient air and main supply water intake temperatures. NAHB (2002) has issued average monthly inlet water temperature over a year. These values for Montreal varies from 4-5(°C) in winters to 11-12(°C) in summers. The cold water inlet temperature can also be calculated from the equation developed by Christensen and Burch of National Renewable Energy Laboratory (NREL, 2005). However, this equation overestimates the main temperatures, particularly for winter. Actual data based on the measurements by Marcoux and Dumas (2004) for several days of each month from 1994 to 2004 are available. These data are depicted in Figure 2-1. These data are averaged over a month and presented in Table 2-6 that used in the present study.

Table 2-6: Monthly Average Inlet Cold Water Temperature in Montreal

Month	Jan	Feb	Mar	Apr	May	Jun	Jul	Aug	Sep	Oct	Nov	Dec
Temperature (°C)	3.3	2.9	2.9	5.5	11.2	15.8	20.8	22.3	20.1	15.4	10.4	5.6

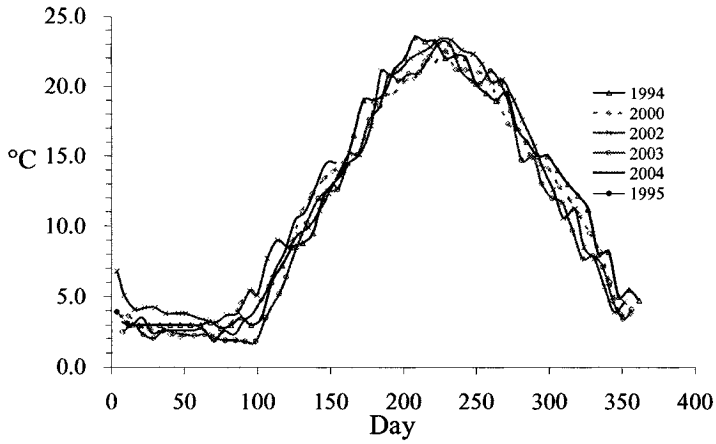

Figure 2-1: Inlet Cold Water Temperature in Montreal, *Marcoux and Dumas (2004)*

2.3.3. Hot Water Load

The hot water load is the required amount of energy to heat the demanded water from inlet cold water temperature to a desired or set value (typically T_{hot} = 60 °C) plus losses. Water heating load can be expressed by the following equation:

$$L_W = N_{day} \times GPD \times (T_{hot} - \overline{T}_{main}) \times \rho \times C_P + Losses \qquad (2.10)$$

(Beckman et al. 1977) where N_{day} is the number of days in a month, ρ is the water density (1 kg/lit), and C_p is the specific heat of water (4190 J/kg°C). The losses from the auxiliary hot water storage tank or an auxiliary section of a single tank need to be considered in the load (Buckles and Klein, 1980). A recommended value is between 9 – 11 (MJ/day) for a single family house that is calculated using reference data according to AMETEK Inc. (1984). Using equation (2.10) and data from Table 2-6, daily and monthly water heating loads for a one family house in Montreal are calculated and presented in Table 2-7.

Table 2-7: Monthly Domestic Water Heating Load for a one Family House with 246 lit/day of Consumption

Month	Jan	Feb	Mar	Apr	May	Jun	Jul	Aug	Sep	Oct	Nov	Dec
Number of days	31	28	31	30	31	30	31	31	30	31	30	31
Daily Load (MJ/day)	67.5	67.9	67.9	65.2	59.3	54.6	49.4	47.8	50.1	55	60.1	65.1
Monthly Load (MJ)	2091	1901	2105	1956	1838	1638	1532	1483	1503	1705	1803	2017

2.3.4. Hot Water Load Profile

The hourly distribution of the hot water consumption in a day can be affected by several factors. It can vary from day to day, from season to season and from family to family. For instance, the hot water consumption in winter is lower than summer yet temperature requirements is higher. However, daily (or monthly) total consumption and consequently hot water load is almost constant. Different cyclic load profiles such as Rand (Mutch 1974), constant, early morning, early afternoon, late morning, or late afternoon has been considered and studied. For this study hot water consumption of 246 lit/day (65 USGPD) is distributed during a day according to the Rand profile as shown in Figure 2-2.

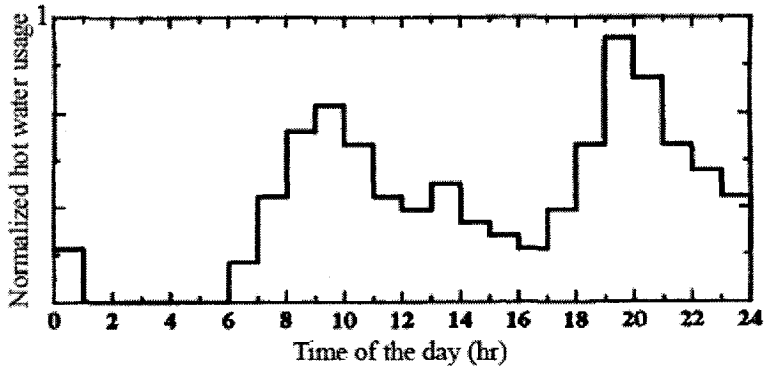

Figure 2-2: Normalized Daily Hot Water Consumption, *Adopted from Mutch (1974)*

2.4. THE COLLECTOR PERFORMANCE

2.4.1. Energy Balance Equation

The performance of a flat-plate collector can be determined from the energy balance equation that describes the relation between useful energy, Q_u, at a given time,

absorbed solar energy by the collector, S, and thermal and optical losses. The absorbed solar energy, S, is equal to the incident solar radiation on the collector's surface minus the optical losses. Thermal losses to the surrounding are due to the infrared radiations, convection and conduction. The thermal losses depends on the overall heat loss coefficient, U_L, to the surrounding; ambient temperature, T_{amb}, and the mean absorber plate temperature, $T_{p,m}$. The steady-state energy balance equation from (Duffie and Beckman, 1991) can be written as:

$$Q_u = A_c [S - U_L (T_{p,m} - T_{amb})] \tag{2.11}$$

This equation can also be written as:

$$Q_u = A_c \times F_R [I_T (\tau\alpha)_{avg} - U_L (T_{f,in} - T_{amb})] \tag{2.12}$$

(Duffie and Beckman, 1991), where Q_u is the useful energy collection rate, A_c is the collector area (m^2), $T_{f,in}$ is the inlet fluid temperature (°C), F_R is the collector heat removal factor, I_T is the solar radiation incident rate on the collector surface per unit area (W/m^2) and $(\tau\alpha)_{avg}$ is the average solar-transmittance product. The second term in the bracket represents the thermal losses.

2.4.1.1. Transmittance-Absorptance Product

The solar transmittance through the collector's transparent cover, τ, is the fraction of the total incident solar radiation that is transmitted through the collector's transparent cover. It is equal to 0.88 for a single-glaze low iron tempered or sheet glass and is about 0.91 for a low-iron white crystal glass. The solar absorptance of the collector's absorber plate, α, is the fraction of the total solar incident radiation absorbed by the absorber plate. For a plate with a selective coating (high absobtivity-low emissivity) such as Black-Chrome or Black-Copper, α is about 0.93-0.97 (Plante, 1983). Both α and τ are functions

of material and the incident radiation angle. With a good accuracy, product of $(\tau\alpha)$ is equal to:

$$(\tau\alpha) \approx 1.01\tau \times \alpha \tag{2.13}$$

(Duffie and Beckman, 1991). The amount of thermal losses from the top cover is being reduced since glass absorbs part of the solar radiation. To count for the reduction of heat losses from the cover an effective transmittance-absorptance that is slightly greater than (τα) and approximately can be calculated by following equation given in (Duffie and Beckman, 1991).

$$(\tau\alpha)_e \approx 1.02(\tau \times \alpha) \tag{2.14}$$

According to Duffie and Beckman (1991), for a single cover collector, $(\tau\alpha)_e$ is about 0.86 and 0.81 for selective and nonselective collectors, respectively. ASHRAE (2003) suggests a value of 0.84 for $(\tau\alpha)_e$.

For long-term performance calculations, monthly average values of $(\tau\alpha)$ can be used. Generally, in a collector test, the transmittance-absorptance values are obtained at normal incident and the monthly average values, which are lower than that of the normal. Beckman et al.(1977) suggested that for a collector installed with a tilt equal to latitude $\pm 15^{\circ}$ and facing south, the ratio of monthly average transmittance-absorptance product to that of normal incident, $\overline{(\tau\alpha)}/(\tau\alpha)_n$, called incident angle modifier, is almost constant and equal to 0.96 for a single cover collector.

2.4.1.2. Absorbed Solar Energy

The solar incident radiation, I_T, is composed of the beam (direct) and diffuse radiations, and reflected radiations from surrounding or ground. The rate at which this incident radiation is being absorbed by the collector's absorber plate is depends on the

incident radiation, the fraction (τ) of the incident radiation that is transmitted through transparent cover, and the fraction (α) of incident radiation absorbed by the flat-plate. The hourly or monthly absorbed solar energy, S (MJ/m^2), can be defined as:

$$S = I_T \times (\overline{\tau\alpha}) \tag{2.15}$$

(Duffie and Beckman, 1991), so the monthly or hourly average absorbed radiation will be given by:

$$\overline{S} = \overline{H} \cdot \overline{R} \cdot (\overline{\tau\alpha}) \tag{2.16}$$

(Duffie and Beckman, 1991) where $\overline{R}$ and $\overline{H}$ can be obtained from Table 2-4.

2.4.1.3. Overall Thermal Loss Coefficient

The thermal losses from the collector to surrounding are due to the radiation and convection through the top cover, and also conduction through insulated bottom and sides. An empirical relation for the heat loss coefficient from the top, U_{top}, was developed by Klein (1975) for the plate temperature between ambient and 200°C is given as:

$$U_{top} = \left\{ \frac{N}{\frac{C}{T_{p,m}}\left[\frac{(T_{p.m} - T_{amb})}{N+f}\right]^e} + \frac{1}{h_w} \right\}^{-1} + \frac{\sigma(T_{p.m} + T_{amb})(T_{p,m}^2 + T_{amb}^2)}{(\varepsilon_p + 0.00591N \cdot h_w)^{-1} + \frac{2N + f - 1 + 0.133\varepsilon_p}{\varepsilon_g} - N} \tag{2.17}$$

(Duffie and Beckman, 1991) where N is the number of the glass covers, $\sigma = 5.6996 \times 10^{-8}$ (W/m^{2}K^4), ε_g is glass cover emittance (0.88), and ε_p is the plate emittance (0.08-0.12 for the selective coating and 0.95 for non-selective coating (Plante, 1983 and Duffie & Beckman, 1991). The plate mean temperature ($T_{p,m}$) is unknown and is typically higher than mean fluid temperature. However, for efficient plates, it can be approximated as $\frac{1}{2}(T_{f,out}+T_{f,in})$. Both T_{amb} and $T_{p,m}$ are in Kelvin. The other parameters in the above equation can be computed as:

$$f = (1 + 0.089h_w - 0.1166h_w\varepsilon_P)(1 + 0.07866N) \quad (2.18)$$

$$C = 520(1 - 0.000051\beta^2) \text{ for } 0^\circ < \beta < 70^\circ \quad (2.19)$$

$$e = 0.43(1 - 100/T_{P,m}) \quad (2.20)$$

(Duffie and Beckman, 1991), where, h_w is the wind heat transfer coefficient in (W/m^2 $^\circ$C) and can be estimated from the following equations for different range of wind speeds (V) in (m/sec).

$$h_w = 5.7 + 3.8V \quad \text{if } 0 \le V < 10 \text{ (m/sec)} \quad (2.21)$$

(AMETEK, 1984)

$$h_w = 7.14 + V^{0.78} \quad \text{if } V > 5 \text{ (m/sec)} \quad (2.22)$$

$$h_w = 5.8 + 3.9V \quad \text{if } V < 5 \text{ (m/sec)} \quad (2.23)$$

Ito Model (Kautsch et al., 2002).

Malhorta et al. (1981) derived a modified expression for the top heat loss coefficient. This equation improved the shortcoming of the equations derived by Klien (1975), while retaining all important factors. It includes the effect of tilt angle, spacing between the covers (λ), and also incorporated the effect of wind heat transfer in the loss coefficient as a function of $1/h_w$, which physically is more realistic than being a function of h_w in Klien (1975) model. This model provides the most accurate results than those of other former models (Garg and Datta, 1984). The improved equation of Malhorta et al. (1981) is given as:

$$U_{top} = \left\{ \frac{N}{\frac{C}{T_{p,m}}\left[\frac{(T_{p.m} - T_{amb})}{N + f}\right]^{0.252}} + \frac{1}{h_w} \right\}^{-1} + \frac{\sigma(T_{p.m} + T_{amb})(T_{p,m}^2 + T_{amb}^2)}{[\varepsilon_P + 0.0425N(1 - \varepsilon_p)]^{-1} + \frac{2N + f - 1}{\varepsilon_g} - N} \quad (2.24)$$

where:

$$C = 204.429(\cos\beta)^{0.252} / \lambda^{0.24} \tag{2.25}$$

$$f = (9/h_w - 30/h_w^2)(T_a/316.9)(1+0.091N) \tag{2.26}$$

The thermal loss from the back side of the collector (i.e. through insulation) can be expressed as:

$$U_b = k/t \tag{2.27}$$

where k and t are the insulation thermal conductivity in (W/m^2 °C) and thickness in (m), respectively. Similarly, the thermal losses from sides can be estimated as:

$$U_{side} = \frac{(k/t)_{side} A_{side}}{A_c} \tag{2.28}$$

(Duffie and Beckman, 1991); and finally the overall heat transfer coefficient, U_L, is equal to:

$$U_L = U_{top} + U_b + U_{side} \tag{2.29}$$

For a 5 (cm) thickness Rock wool insulation with k = 0.04 (W/mk), amount of U_b + U_{side} is almost 1 (W/m^2 °C). It is suggested to separate the insulation from the absorber plate by 12-20 (mm) distances and have a reflective foil on the insulation facing of the plate.

2.4.1.4. Fin and Collector Efficiency Factors

The typical geometry of a flat-plate sheet-and-tube solar collector is depicted in Figure 2-3. The absorber plate, in this setup, acts as a fin.

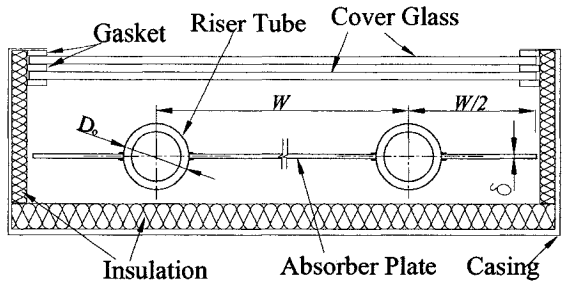

Figure 2-3: Typical cross section of a Sheet-and-Tube Solar Collector

Considering negligible temperature gradient in the flow direction (inside the tubes) and through the plate, the solar energy collected by the absorber plate per unit length on the both sides of the pipe is given as:

$$q'_{fin} = (W\text{-}D)\,F\,[S\text{-}U_L(T_b - T_{amb})] \tag{2.30}$$

(Duffie and Beckman, 1991), where D is outside diameter of the pipe, T_b is the temperature at the base of fin and F is the straight fin's efficiency and defined as:

$$F = \frac{[\tanh m(W-D)/2]}{m(W-D)/2} \tag{2.31}$$

(Duffie and Beckman, 1991), where $m = \sqrt{U_L/k\delta}$, and k is the plate thermal conductivity. The solar energy collected from the pipe surface is:

$$q'_{tube} = D\,[S\text{-}U_L(T_b - T_{amb})] \tag{2.32}$$

(Duffie and Beckman, 1991). Therefore, useful energy gain per unit length is:

$$q'_u = q'_{fin} + q'_{tube} \tag{2.33}$$

This useful energy is then transferred to the fluid, thus:

$$q'_u = W\,F'\,[S\text{-}U_L(T_f - T_{amb})] \tag{2.34}$$

(Duffie and Beckman, 1991) where F' is the collector efficiency factor and it is constant for any collector geometry and flow rate, that is:

$$F' = \frac{1/U_L}{W\left[\frac{1}{U_L[D+(W-D)F} + \frac{1}{C_B} + \frac{1}{\pi D_i h_{f,i}}\right]} \tag{2.35}$$

(Duffie and Beckman, 1991) where C_B is the bond conductance. The value of bond resistance ($1/C_B$) is negligible for a very good bond such as ultrasound soldered bond or Laser welding. D_i is inside diameter of the pipe, and $h_{f,i}$ is the heat transfer coefficient between the pipe wall and the circulating fluid with no phase change. The collector efficiency factor decreases as either W or U_L increase, and increases as either $k\delta$ or $h_{f,i}$ increase. Duffie and Beckman (1991) have shown that both the heat removal and collector efficiency factors are invariable for a specified design and are very weak function of the local time. Furthermore, the collector efficiency factor, F', for a constant value of W increases as $k\delta$ increase; however, for the small quantities of W (less than 5 cm) the variation of F' is not significantly affected by $k\delta$. In addition, for $k\delta$ >0.2 the variation of F' is very small. The Practical values of $k\delta$ ranged from 0.005 to 0.4 (for 1 mm copper plate $k\delta$ =0.4).

The collector tube spacing (W) for straight tubes based on the 95% efficiency in transferring heat from the absorber is shown in Table 2-8. The data shows that for a given plate thickness the tube spacing for aluminum is smaller than copper.

Table 2-8: Collector Tube Spacing (cm) for 95% Plate Efficiency.
Adopted from AMETEK (1984)

Plate Thickness (mm)	0.1	0.2	0.3	0.5	1.0
Copper	9.0	11.5	12.5	14.5	16.0
Aluminum	7.5	9.5	10.5	13.0	15.0

2.4.1.5. Collector Efficiency and Heat Removal Factor

The collector heat removal factor, F_R, relates the actual useful energy gain to the useful energy gain if the entire plate temperature was at the inlet fluid temperature. This factor is expressed in Duffie and Beckman (1991) as:

$$F_R = \frac{\dot{m}C_p(T_{f,out} - T_{f,in})}{A_c[S - U_L(T_{f,in} - T_{amb})]} \tag{2.36}$$

In other word, F_R is measure of the reduction in the useful energy gain due to the deviation of the collector temperature from the inlet fluid temperature. Consequently, it is favorable to optimize the absorber plate characteristic in such as way that shifts the surface temperature toward that of inlet fluid. F_R is basically a function of flow rate; however, the fluid temperatures, collector material and geometry (i.e. plate thickness, tubes spacing and length, tube diameter, etc.) can significantly affect F_R. Therefore it is reasonable to relate F_R to the collector efficiency factor F', that is:

$$F_R = \frac{\dot{m}C_P}{A_c U_L}\left[1 - \exp\left(\frac{-A_c U_L F'}{\dot{m}C_P}\right)\right] \tag{2.37}$$

(Duffie and Beckman, 1991). $\dot{m}$ is the collector flow rate. Beckman et al. (1977) suggested a reference mass flow rate equal to 0.015 (lit/sec.m^2 of the collector area) or 0.0139 (kg/sec.m^2) for a 50-50 ethylene glycol-water solution. Other studies have also indicated mass flow rate of the collector fluid in the range of 0.001—0.014 (kg/sec.m^2). An increase in mass flow rate can increase heat transfer rate from plate to the fluid which, in turn, yields an increase in F_R. However, it reduces the overall performance by decreasing the degree of the thermal stratification in the storage tank. Combining heat balance equations, 2-11 and 2-12, the mean absorber plate temperature can be obtained as:

$$T_{p,m} = T_{f,in} + \frac{Q_u / A_c}{U_L F_R}(1 - F_R) \tag{2.38}$$

(Duffie and Beckman, 1991)

Finally, collector efficiency can be defined as:

$$\eta = \frac{Q_u}{A_c I_T} = \frac{\dot{m} C_p (T_{f,out} - T_{f,in})}{A_c I_T} = F_R (\tau\alpha)_n - F_R U_L (T_{f,in} - T_{amb}) \tag{2.39}$$

(Duffie and Beckman, 1991)

The above equation shows that for a constant U_L, η varies linearly with $(T_{f,in} - T_{amb})/I_T$ with a slope equal to $(-F_R U_L)$ and y-axis intercept equal to $F_R(\tau\alpha)_n$. The collector efficiency is an essential parameter to determine the collector area. Both $F_R(\tau\alpha)_n$ and $F_R U_L$ are very critical parameters that control the performance of a solar collector. The value of $F_R(\tau\alpha)_n$ and $F_R U_L$ can be obtained from the standard collector test results and the equations given by Duffie and Beckman (1991) or ASHRAE 95 for different collector geometries. Based on the standard test result for a single-glaze cover with non-selective black coat are $F_R(\tau\alpha)_n = 0.78$ and $F_R U_L = 7$ (W/m^2 °C), and with selective black coat are $F_R(\tau\alpha)_n = 0.84$ and $F_R U_L = 4.67$ (W/m^2 °C). Tiwari et al. (1991), found that lower value of $F_R(\tau\alpha)_n = 0.6$ and higher $F_R U_L = 8.9$ (W/m^2°C) representing a poorly designed collector. Analytical calculation of F_R for the serpentine tube geometry with N segments was developed by Abdel-Khalil (1976) and is described in Duffie and Beckman (1991).

2.4.2. Collector-Heat Exchanger Efficiency Factor

In order to prevent fluid from freezing in winter, an antifreeze solution can be used on the collector side. Consequently, an auxiliary heat exchanger and pumping systems will be required to transfer heat from the working fluid to the domestic water. As a result, another efficiency factor, F'_R, needs to be introduced to account for the combined

efficiencies of the collector and auxiliary heat exchanger. F'_R is to be replaced with F_R in the main heat balance equation. According to the analytical equation driven by deWinter (1975):

$$(F'_R / F_R) = \left[1 + \left(\frac{A_c F_R U_L}{(\dot{m}C_p)_c}\right)\left(\frac{(\dot{m}C_p)_c}{\varepsilon_{HX}(\dot{m}C_p)_{\min}} - 1\right)\right]^{-1} \quad (2.40)$$

where, $(\dot{m}C_P)_{\min}$ is the smaller of the fluid capacitance rates in the heat exchanger, $(\dot{m}C_P)_c$ is the fluid capacitance in the collector side, and ε_{HX} is the heat exchanger effectiveness. The Ratio (F'_R/F_R) is a value between 0-1 and indicates the penalty in Q_u due to the incorporation of the additional heat exchanger and double-flow circuit.

2.4.2.1. Selecting Collector Side Fluid

Conventionally, water is the best heat transfer fluid in the collector for solar domestic water heater. However, a solution of 30 to 50 percent ethylene glycol or propylene glycol in water will satisfy the requirements of the system while preventing the fluid from freezing. Ethylene glycol has better physical properties but propylene glycol is less toxic and is preferred to use in domestic applications according to ASHRAE (2005). Freezing point and specific heat of 30, 40, and 50 percent mixture–by volume–of these substances in water is taken from ASHRAE (2005) and presented in Table 2-9 for medium temperature water heating ranges. Considering the average daily (-9°C), minimum daily (-17°C) and extreme minimum (-37°C) temperatures in January for Montreal (Environment Canada, 2006) a 40% solution of propylene glycol in water with an average specific heat of C_p = 3800 (J/kg °C) is selected for the present study. Obviously system performance in summer will be higher water alone is used as the working fluid. Assuming an identical flow rate of 0.012 (kg/sec.m^2) on both sides of the

heat exchanger, $\varepsilon_{HX} = 0.7$, and $F_R U_L = 4.67$ (W/m^2 °C) which are within the recommended range, the ratio (F'_R/F_R) is estimated to be 0.96 for a 40% solution of propylene glycol in water.

Table 2-9: Freezing Point and Specific Heat of Ethylene glycol and Propylene glycol, *Adopted from ASHRAE Fundamentals (2005)*

	Freezing Point [°C]			Specific Heat [kJ/kg °C] at different solution percentages											
				5°C			25°C			50°C			70°C		
	30%	40%	50%	30%	40%	50%	30%	40%	50%	30%	40%	50%	30%	40%	50%
Ethylene glycol	-15.7	-25.3	-37.0	3.60	3.42	3.22	3.66	3.49	3.30	4.81	4.38	3.99	3.79	3.64	3.47
Propylene glycol	-13.2	-21.4	-33.7	3.81	3.65	3.47	3.86	3.72	3.55	3.93	3.80	3.65	3.99	3.87	3.73

2.5. *f*-CHART

2.5.1. *f*-Chart Parameters

The *f*-Chart method, developed by Klein et al. (1976), estimates the fraction of monthly or annual total heating load that is supplied by the solar system. In other word *f* indicates the fraction of the hot water energy requirements that is supplied by the solar system or (Buckles and Klein, 1980), that is,

$$f = \frac{Q_{Load} - Q_{Auxiliary}}{Q_{Load}} \tag{2.41}$$

where Q_{Load} is the total monthly (or annual) energy removed from the system to support requirements of the water heating and $Q_{Auxiliary}$ is the total monthly (or annual) auxiliary energy, whether electrical or fuel, that is supplied to the system to support the portion of the total load that is not supplied by the solar energy. In addition, Q_{Load} should account the thermal losses from the storage tank and auxiliary heating system, to the surrounding. The solar fraction, *f*, is a superior indicator of the system performance compared to the other parameters such as collector efficiency or heat removal factor, since it manifests the

overall performance of the entire system not a component (i.e. collector) alone, over specific period of time or operating conditions. Maximizing the solar fraction, therefore, is more realistic and understandable approach when performance of the system in whole is concerned. For instance, increasing flow rate in the collector increase the heat removal factor and consequently improves the collector efficiency factor but in turn deteriorates stratification inside the storage tank thus, reduces the overall performance of the system. The range of parameters used in the development of the correlations for *f*-chart method, for liquid based systems from Duffie and Beckman (1991) are as follow:

$$0.6 \le (\tau\alpha)_n \le 0.9$$
$$5 \le F'_R A \le 120 \qquad (\mathrm{m}^2)$$
$$2.1 \le U_L \le 8.3 \qquad (\mathrm{W/m^{2o}C})$$
$$30^\circ \le \beta \le 90^\circ$$
$$83 \le (UA) \le 667 \qquad (\mathrm{W/^oC})$$

In this method the primary variable is the collector area, and *f* is the ratio of total useful delivered energy to the heating load during a month or year and it is function of two dimensionless parameters that defined as follow:

$$X = \frac{\text{Collector Losses}}{\text{Heating Load}} = A_c \times F'_R \times U_L (T_{ref} - \overline{T}_{amb}) \times \Delta t / L_W \qquad (2.42)$$

$$Y = \frac{\text{Absorbed Solar Radiation}}{\text{Heating Load}} = A_c \times F'_R (\overline{\tau\alpha}) \times \overline{H_T} \times N / L_W \qquad (2.43)$$

(Duffie and Beckman, 1991), where T_{ref} = 100 (°C), and Δt is number of seconds in a month. These equations can be rearranged as:

$$X / A_c = F_R U_L \times (F'_R / F_R) \times (T_{ref} - \overline{T}_{amb}) \times \Delta t / L_W \qquad (2.44)$$

$$Y / A_c = F_R (\tau\alpha)_n \times (F'_R / F_R) \times [(\overline{\tau\alpha})/(\tau\alpha)_n] \times \overline{H_T} \times N / L_W \qquad (2.45)$$

For a specified collector area, f for liquid-based system can be calculated from the following equation for $0<X<3$ and $0<Y<18$:

$$f = 1.029Y - 0.065X - 0.245Y^2 + 0.0018X^2 + 0.0215Y^3 \quad (2.46)$$

(Duffie and Beckman, 1991)

The equation of f for air system can found in Duffie and Beckman (1991).

2.5.2. Storage Capacity Factor

For storage capacity over 50 liters of water per square meter of the collector area, long-term performance is not very sensitive to the capacity. However, since f-Chart is developed based on 75 liters of water per m^2 of the collector area, for storage capacities in range 37.5 to 300 (lit/m^2), the following correction factor has to be introduced into values of X / A_c.

$$X_C / X = (\text{Actual Capacity} / 75)^{-0.25} \quad (2.47)$$

(Duffie and Beckman, 1991)

2.5.3. Service Water Heating Factor

The performance of the system when heating load in entirely due to the service water heating system has to be modified by the following correction factor Duffie and Beckman (1991). This correction factor counts for the main cold water, ambient air and desired hot water temperatures. This method is also based on 75 (lit/m^2) storage capacity and Mutch's (1974) profile (Rand) for hourly hot water usage distribution.

$$X_C / X = (11.6 + 1.18T_{hot} + 3.86T_{main} - 2.32\overline{T}_{amb}) / (T_{ref} - \overline{T}_{amb}) \quad (2.48)$$

2.5.4. f-Chart Results and Discussion

Assuming a value for the collector area in such a way that the collector is able to supply 90% of the hot water heating load in hot season, i.e. from May to Aug, all f-Chart

parameters are calculated using equations (2.42) to (2.48) and all other data from previous sections. The results are summarized in Table 2-10 for a solution of 40% propylene glycol in water. The required collector area is estimated to be around 8–6 (m^2) for Montreal.

Table 2-10: Monthly Solar Water Heating Load Fraction for Different Collector Areas (*f*-Chart Method) with a 40% propylene glycol-water solution in Montreal

Month	N	X/A	Y/A	X_C/X (SHW)	X/A corrected	$A = 8\ m^2$			$A = 6m^2$			$A = 3m^2$		
						X	Y	f	X	Y	f	X	Y	f
Jan	31	0.628	0.102	1.06	0.67	5.3	0.8	0.4	4	0.6	0.3	2	0.3	0.2
Feb	28	0.613	0.157	1.02	0.63	5	1.3	0.7	3.8	0.9	0.6	1.9	0.5	0.3
Mar	31	0.584	0.193	0.96	0.56	4.5	1.5	0.8	3.4	1.2	0.7	1.7	0.6	0.4
Apr	30	0.566	0.195	0.97	0.55	4.4	1.6	0.8	3.3	1.2	0.7	1.6	0.6	0.4
May	31	0.577	0.223	1.11	0.64	5.1	1.8	0.9	3.9	1.3	0.8	1.9	0.7	0.5
Jun	30	0.591	0.237	1.25	0.74	5.9	1.9	0.9	4.4	1.4	0.8	2.2	0.7	0.5
Jul	31	0.645	0.272	1.47	0.95	7.6	2.2	0.9	5.7	1.6	0.8	2.9	0.8	0.5
Aug	31	0.675	0.276	1.56	1.05	8.4	2.2	0.9	6.3	1.7	0.8	3.1	0.8	0.5
Sep	30	0.660	0.218	1.47	0.97	7.8	1.7	0.8	5.8	1.3	0.7	2.9	0.7	0.4
Oct	31	0.650	0.165	1.34	0.87	7	1.3	0.6	5.2	1	0.5	2.6	0.5	0.3
Nov	30	0.640	0.088	1.22	0.78	6.2	0.7	0.3	4.7	0.5	0.2	2.3	0.3	0.1
Dec	31	0.634	0.077	1.11	0.71	5.6	0.6	0.2	4.2	0.5	0.2	2.1	0.2	0.1

These results show that a collector with 8 square meters of area can supply 90% of the household hot water consumption (at 60°C) in summer and between 20 to 70% of it in winter. The solar contribution has the lowest values in December and January; however, solar fraction of 70% in February is achievable with this collector. However, considering cost, heat losses and reliability of the system, collectors with large area that are designed to supply higher portion of the required hot water by only solar energy is not recommended. It is practical to consider an auxiliary heater that is able to supply 100% of the demand in overcast days and around 20% of it even in sunny days. For Montreal a collector with 6 square meters of area seem to be suitable. It can supply 80% of the hot

water demand in summer and between 20 to 60% in winter, and the remaining portion can be supplied by an auxiliary electric heater that placed inside storage tank or outside storage tank in parallel or series. The result determines that collector even with smaller areas around 3 m^2 can supply 50% of the consumed hot water in summer, and it is still capable of supplying some part of hot water load in cold months. For the system with only water as the collector fluid, the required area is smaller than that for the antifreeze solution, for instance, it is estimated that a collector with area of 6.5 m^2 that circulates only water as working fluid (direct system) can provide same fraction that an 8 m^2 collector with antifreeze solution (indirect system) does. In this study, hot water set temperature is assumed to be 60 ^oC; it is obvious that setting outlet hot water at lower temperatures will reduce the monthly load resulting smaller required collector areas or higher solar fractions for the fixed collector area. Particularly in summer, less hot water could be consumed at lower set temperature which yields to further increase of solar fractions for a chronic collector area. Accuracy of the *f*-chart method has been investigated and compared with measured data, TRNSYS hourly simulation data and other performance methods. Haberl (2004) has reported that *f*-chart predictions versus measurements vary from 2 to 15%, 1.1 to 4.7% versus TRNSYS simulation and 2.5 to 9% versus other developed methods. However, according to Duffie and Beckman (1991) concurrence of monthly solar fractions with other methods is not as good as the annual fraction and it is suggested to use *f*-chart method to only estimate annual performances. DOE-EERE has recommended a ***rule of thumb*** to size a solar water heating system that meets 90-100% of household water consumption in summer. It suggests 2 (m^2) of collector area for each of the first two members and additional 0.7 (m^2) for every other

members of a family living in the US Sun Belt area (i.e. Southern states). For Northern states the additional area is about 1.1-1.2 (m^2). It is, moreover, recommended to use 190 to 227 liters of storage tank for 1-3 people family, a 303-liters tank for 3-4 people, and larger tank for 4-6 people family. Another rule of thumb recommends 1.5 (m^2) of collector area per person that supplies 50 to 80% of the annual water heating load by solar energy (Duffie and Beckman, 1991). The required collector area obtained from these rule of thumbs is consistent with the values that were estimated hereinbefore using *f*-chart method. In the next chapter these results will be compared with TRNSYS program simulation results and all pertinent parameters will be investigated and optimized.

CHAPTER 3

OPTIMIZATION OF THE FORCED CIRCULATION SOLAR WATER HEATING SYSTEM PARAMETERS USING TRNSYS

3.1. PROLOGUE

Satisfactory performance and reliability of a solar water heating system requires adequate sizing of its components, as well as accurate prediction of the delivered useful energy, outlet water temperature and tank temperature. TRNSYS 16 (Klein S.A. et al., 2004) is an extensive software for transient simulation of solar systems (thermal or PV), low energy solar multi-zone buildings, renewable energy systems, fuel cells and their related equipments. This program is developed by Solar Energy Laboratory, University of Wisconsin-Madison and enriched by the contributions of TRANSSOLAR Energietechnik GmbH, Centre Scientifique et Technique du Bâtiment (CSTB), and Thermal Energy Systems Specialists (TESS). In TRNSYS, the components of a system (project) are set up by connecting them graphically in an environment called "Simulation Studio." Components in TRNSYS are defined by mathematical models in terms of their algebraic or differential forms and referred to as "Type." TRNSYS is broadly recognized and is currently the best available solar design tool which provides the most accurate and comprehensive predictions that have been validated repeatedly. TRNSYS allows users to analysis each component of a system in detail. TRNSYS deploys weather data that is provided by the Typical Meteorological Year (TMY) in the simulation process, and requires at least four known parameter from the system, such as A_c, $F_R U_L$, $F_R(\tau\alpha)_n$, and V_c to perform simulation.

As showed in Section 1.3.5, researchers have been widely using TRNSYS to study and optimize solar systems. Nevertheless, most of these published studies focused

on the natural circulation (thermosyphon) systems operating in hot or moderate climates. Fewer studies, to the best of the author's knowledge, have investigated the various design parameters of a forced circulation systems operating in the cold climate. Moreover, most of the studies considered inlet cold water temperature and collector flow rate constants which, in fact, can vary from month to month. This chapter is focused on the modeling and optimization of a solar water heating system for a one family residential unit in Montreal. All of the pertinent design parameters are studied and optimum (suggested) values are determined. The study is focused on maximizing the solar fraction of the entire system as well as maximizing the collector's performance.

3.2. TRNSYS MODELS

Two forced circulation systems are modeled in this study. The first is the ***indirect*** system that includes secondary flow—antifreeze and an external heat exchanger—and the second is the ***direct*** system—without secondary flow and heat exchanger. The secondary flow for the first system is assumed to be a solution of glycol in water with different percentages (in volume) of glycol. The indirect system is considered to be more practical for residential application in cold climates, like Montreal. This study, basically, focused on two different sets of simulations for the indirect system. The first set of simulations is conducted to optimize the whole system parameters for the given collector characteristic factors. This is followed by the second set of simulations, which is conducted to optimize the collector parameters to achieve the optimum values of the collector efficiency and characteristic factors. These models are consisted of:

- *A flat-plate collector with different areas*: To optimize the system, *first*, the characteristic factors from standard test data—that was also used in *f*-chart method in

chapter 2—have been selected here with $F_R(\tau\alpha)_n$ = 0.84 and $F_R U_L$ = 4.67 (W/m^2 °C). To optimize the collector itself, *second*, a theoretical collector is modeled, and the collector's monthly and annual efficiencies as well as the collector's characteristic factors are determined and studied over a wide range of design parameters. The collector is considered to be facing south with the tilt equal to Montréal's latitude (i.e. 45.5°).

- *A constant effectiveness counter flow heat exchanger*: The flow rate in the cold side of the heat exchanger is subjected to daily load distribution pattern (Rand profile) and the daily hot water consumption of 246 (lit/day). The flow rate in the hot side is variable and subjected to the collector's "suggested" optimum flow rates per square meters of the collector area.
- *A fully stratified storage tank (6 nodes)*: Different tank height and tank volumes–to–collector area ratios (V_c/A_c) are considered. Overall tank heat loss coefficient is assumed to be between 2.5 to 3 (kJ/hr.m^{2}K).
- *The forcing functions providing actual monthly average main cold water temperatures and hourly load profile corresponding to 246 liters per day of demand*: Cold water temperature is considered to vary every month according to the actual data that are given in section 2.3.2.
- *An auxiliary electric heater in series with storage tank and after tempering valve mixing point*: Both the tempering valve and auxiliary heater are set to desired hot water temperature, T_{set}= 60 (°C). As an option, an in-tank electric heater is considered in the model but is disabled for the first study.

- *Two constant flow circulation pumps*: These pumps function by an on/off differential controller which generates the on/off signals as a function of the collector and tank cold-side outlet temperatures and two dead band temperatures.
- *Connecting pipes (supply and return) between the collector and hot side of the heat exchanger*: Different pipe lengths and pipe internal diameters are considered for the first set of simulations. The overall heat loss coefficient is considered to be 3 ($kJ/hr.m^2K$) for both set of simulations.
- *Weather and Meteorological data*: It is taken from the Typical Meteorological Year (TMY) data bank for Montreal.
- Required equation, integration, and output components. Corresponding equations to calculate the solar fractions, collector efficiencies, and collector characteristic factors are illustrated in chapter 2.

The *indirect* model is depicted in Figure 3-1. For the *direct* model the heat exchanger and pump-2 are eliminated and the domestic (potable) water is circulated directly between the collector and the tank. The direct system is shown in Figure 3-2. The Primary design parameters used in this study are summarized in Table 3-1.

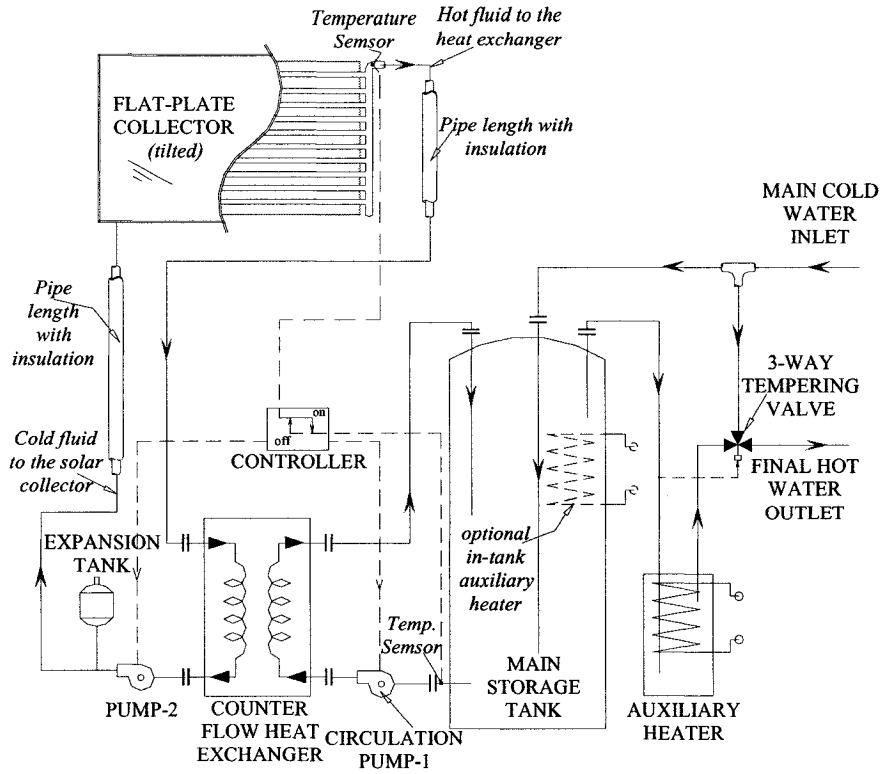

Figure 3-1: Schematic of the Indirect Forced Circulation System Model

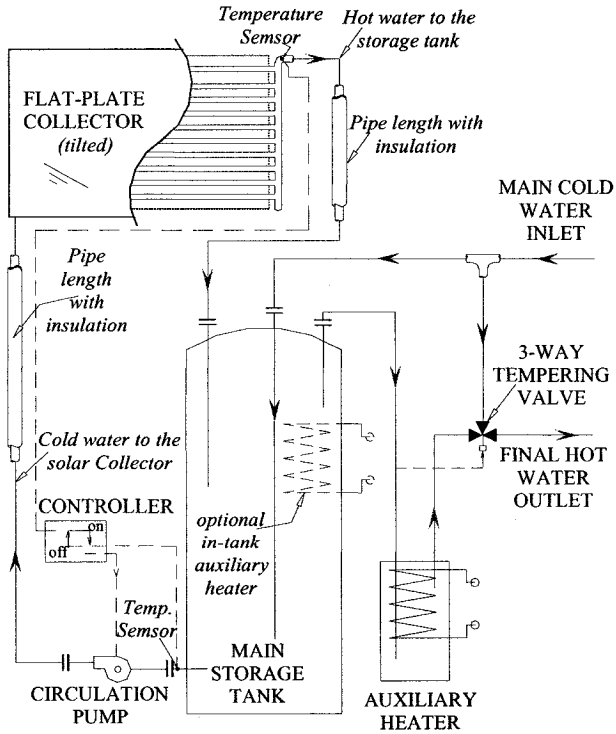

Figure 3-2: Schematic of the Direct Forced Circulation System Model

Table 3-1: Range of Studied Parameters for the First Set of Simulations: System optimization

Design Parameters	Values
A_c	8, 6, 4, 3 (m^2)
C_p (glycol-water)	3.2– 4.0 (kJ/kg°C)
Daily Consumption	246 (lit/day)
V_c/A_c	20–300 (lit/m^2)
φ	45.5°
T_{main}	2.9 – 22.3 °C
T_{set}	60°C
ε_{HX}	0.3 – 1
$F_R(\tau\alpha)_n$	0.84
$F_R U_L$	16.8 (kJ/hr.m^2 K)
$\dot{m}/A_c$	5–60 (kg/hr.m^2)
$D_{in/out}$ (Pipe ID)	19.94, 25.4, 38.3, 50.5 mm
$L_{in\text{-}out}$ (2L)	4–32 m
$U_{in\text{-}out}$	3 (kJ/hr.m^2K)
H_t	0.4 – 2.4 m
U_{tank}	2.5–3 (kJ/hr.m^2K)
ρ	1000 (kg/m^3)

3.3. SIMULATION RESULTS AND DISCUSSION

3.3.1. OPTIMIZATION OF THE SYSTEM PARAMETERS

3.3.1.1. Required Collector Area

Both direct and indirect models are studied for four different collector areas that are 8, 6, 4, and 3 (m^2); to estimate the monthly and annual solar fractions and terminate the adequate collector area. Obtained monthly solar fractions, from simulation, for both direct and indirect models over those four collector areas are depicted, respectively, in Figures 3-3 and 3-4. These simulation data as well as those of calculated data—for the same collector areas'—using f-chart method are summarized in Table 3-2. The results showed that an 8 (m^2) collector in the direct pumped system is able to supply 95-100% of the hot water demand from May to September. The same area can supply 90-99% of the hot water requirement from May to September with indirect pumped system using a 40% mixture of propylene glycol in water (i.e. C_p = 3.8 kJ/kg°C at 50°C). Results also

indicates that with a 6 (m^2) and 4 (m^2) collector, solar fraction is about 88–93% and 66–76%, respectively, during June to September months for an indirect system with the same glycol-water mixture. The 6 m^2 collector is also able to supply more than 30% of the demand during cold months. Comparing the monthly solar fractions of the collectors with different areas shows that replacing an 8 m^2 collector with 6 m^2 deteriorates the solar fractions by only 1.5—9.5% in the hot months and 12—23% in the cold months, whereas replacing an 8 (m^2) collector with 4 (m^2) one reduces the solar fractions by 20—29% and 34—50% in the hot and cold months, respectively. Moreover, considering the cost ineffectiveness of the large collectors (i.e. 8 m^2) which supplies 90-100% of the required hot water (Shariah and Löf, 1997), a collector with 6 (m^2) of area, that provides 75-95% of the demand, in summer, seems to be adequate size for this application in Montreal. The results also indicates that the reduction of the monthly solar fraction, for a 6 m^2 collector, due to incorporation of heat exchanger and secondary flow–indirect system–is only about 5–15% compared to the direct system. This degradation of solar fraction decreases as collector area reduces.

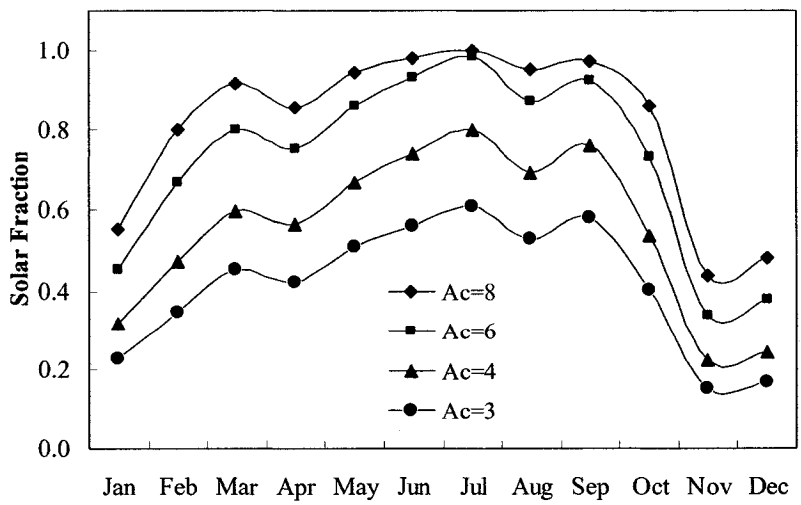

Figure 3-3: Variation of the Monthly Solar Fraction versus the Collector Area (m^2) –*Direct System*

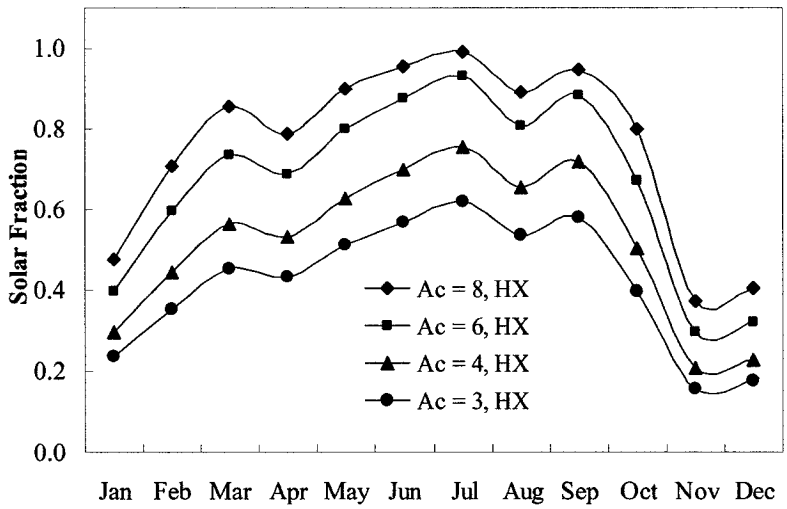

Figure 3-4: Variation of the Monthly Solar Fraction versus the Collector Area (m²) –*Indirect System*

All cases are studied with identical V_c/A_c = 75 (lit/m^2), and $\dot{m}/A_c$ = 40 (kg/hr.m^2). Comparison of the results from *f*-chart method and TRNSYS simulation results reveals that the *f*-chart method underestimated the monthly solar fractions by 2 to 43% in August and December, respectively. The difference between the two data sets increases as the collector area decreases, with the largest difference of 46% in December for a 3 (m^2) collector area. The comparison also indicates that in the absence of simulation software, *f*-chart method can be only used to estimate the collector area—since both of the methods estimated required collector area of six square meters. Agreement between monthly solar fractions—estimated by those two methods—is not as good as that of annual fractions, so it is suggested to use *f*-chart method to only estimate the annual solar fraction (Duffie and Beckman, 1991).

Table 3-2: The monthly Solar Fractions for Different Collector Areas (Direct and Indirect systems)

	TRNSYS: Indirect System *40% glycol-water mixture*				TRNSYS: Direct System *water*				*f*-Chart: Indirect System *40% glycol-water mixture*			
Area	**8 m²**	**6 m²**	**4 m²**	**3 m²**	**8 m²**	**6 m²**	**4 m²**	**3 m²**	**8 m²**	**6 m²**	**4 m²**	**3 m²**
Jan	0.47	0.39	0.30	0.23	0.55	0.45	0.32	0.23	0.39	0.31	0.21	0.17
Feb	0.71	0.60	0.45	0.35	0.80	0.67	0.48	0.34	0.67	0.55	0.39	0.32
Mar	0.85	0.73	0.56	0.45	0.92	0.80	0.60	0.45	0.83	0.70	0.51	0.41
Apr	0.79	0.69	0.53	0.43	0.86	0.75	0.57	0.42	0.84	0.71	0.52	0.42
May	0.90	0.80	0.63	0.51	0.95	0.86	0.67	0.51	0.89	0.77	0.57	0.47
Jun	0.96	0.88	0.70	0.57	0.98	0.93	0.74	0.56	0.89	0.78	0.58	0.48
Jul	0.99	0.93	0.76	0.62	1.00	0.98	0.80	0.61	0.91	0.81	0.62	0.52
Aug	0.89	0.81	0.66	0.54	0.95	0.87	0.69	0.53	0.89	0.79	0.61	0.51
Sep	0.95	0.88	0.72	0.58	0.97	0.93	0.76	0.58	0.77	0.66	0.49	0.40
Oct	0.80	0.67	0.50	0.40	0.86	0.73	0.54	0.40	0.62	0.51	0.36	0.30
Nov	0.37	0.30	0.21	0.16	0.44	0.34	0.22	0.15	0.28	0.21	0.14	0.11
Dec	0.40	0.32	0.23	0.18	0.48	0.38	0.24	0.17	0.23	0.18	0.12	0.09

3.3.1.2. The Effect of Glycol Percentage

The specific heat of glycol-water solution varies with temperature and volumetric percentage of glycol in water. Within the temperature range of 5–110°C (operating temperature range of the collector) the specific heat of 20%, 30%, 40%, and 50% ethylene glycol in water varies from 3780–4022, 3603–3901, 3418–3628, and 3223–3628 (J/kg K), respectively. These values for the same percentages of propylene glycol in water vary from 3940–4169, 3807–4109, 3652–3999, and 3474–3879 (J/kgK), respectively (ASHRAE 2005, Chapter 21). The solution densities for both ethylene and propylene glycol solutions at the mentioned temperature range, varies from about 963 to 1079 (kg/m^3). To study the effect of glycol percentage (i.e., the effect of specific heat variation) on the monthly solar fraction and collector efficiency of the indirect system, the simulations were conducted for different values of C_p varied from 3.2 to 4.0 (kJ/kg°C) for a 6 (m^2) collector with an identical ratio of V_d/A_c = 75 (lit/m^2), and $\dot{m}/A_c$ = 40 (kg/hr.m^2). The solution density is considered to have an average value of 1000 (kg/m^3)

in the concerned range. The variation of the monthly solar fractions (f) and the collector efficiencies (η) with the specific heat are depicted in Figures 3-5 and 3-6, respectively. In Figure 3-6, the monthly collector efficiency for the direct system with the identical collector area is also presented. The results show that the effect of C_p on the monthly and annual solar fractions and collector efficiency is almost insignificant. Therefore, selecting the percentage or type of glycol solution could be based on mixture's freezing point, cost, and corrosion parameters. Considering daily minimum temperature of -17°C for Montreal, a 40–50% solution of propylene glycol–which is also less toxic than ethylene glycol–would be appropriate for the winter. Therefore, the degradation of the solar fraction from the direct system is basically caused by the incorporation of the additional heat exchanger not by the addition of glycol to water. The difference between the efficiencies of the direct and the indirect systems is about 6–8.8% in the hot season and 8.5–15.8% in the cold season. For all values, the difference between the monthly collector efficiencies is very small since the collector efficiency is mainly a function of the collector construction and is a very weak function of local time.

Furthermore, for a 6 (m^2) collector, the result shows only 8.3% and 9.5% reduction of the *annual* solar fraction and the collector efficiency, respectively, due to the additional heat exchanger and using of the antifreeze (i.e. from f = 0.72 and η = 42 % for direct forced system with water alone to f = 0.66 and η = 38% for the indirect system with antifreeze and heat exchanger).

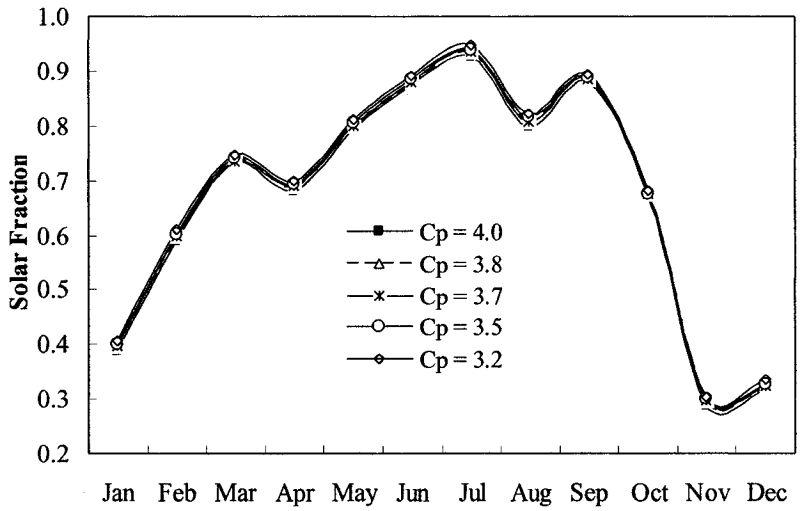

Figure 3-5: Variation of the Monthly Solar Fraction versus the Specific Heat (kJ/kg°C) –*Indirect System.*A_c*=6 m*^{2}

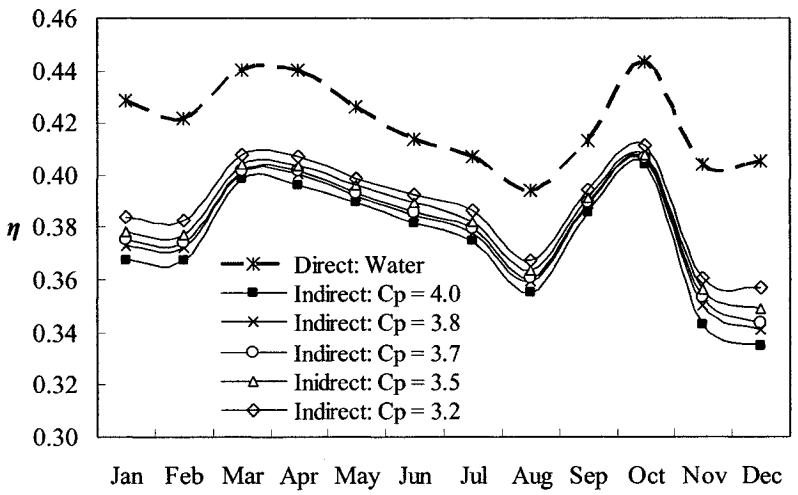

Figure 3-6: Variation of the Monthly Collector Efficiency versus the Specific Heat (kJ/kg°C) –*Direct and Indirect System,* A_c*=6 m*^{2}

3.3.1.3. The Effect of the Mass Flow Rate

The effect of collector mass flow rate on the annual and monthly solar fractions and collector efficiency was modeled for collector mass flow rate-to-collector area ratios from 5 to 60 (kg/hr.m^2). In this the case, the collector area and tank volume to collector area ratio (V_c/A_c) were kept constant at 6 (m^2) and 75 (lit/m^2), respectively. The C_p was set equal to 3.8 (kJ/kg°C). The variation of the monthly and annual solar fractions and collector efficiencies with the collector flow rate are presented in Table 3-3 and Table 3-

4, respectively. Variation of the annual solar fraction and collector efficiency are also depicted, respectively, in Figures 3-7 and 3-8. Results showed that the maximum values–as large as 0.95–of the monthly solar fraction, occurring in July, are about 42% greater than annual values and the minimum values, occurring in November, are 54-58% less than annual ones. Likewise, maximum values–as large as 0.41–of the monthly efficiency, occurring in April and October, are about 2–8 % greater than annual values and the minimum values, occurring in November and December, are 6–14 % less than annual ones. It was, also, found that both the collector efficiency and the solar fraction increases rapidly as the $\dot{m}/A_c$ ratio increases, and reach their maximum values when the ratio is around 30 (kg/hr.m^2) and then decrease slowly with an increase in the flow rate from 40 (kg/hr.m^2) and to above. The results in both figures indicate that the operation of the system at the optimal collector flow rate increases the collector's useful solar energy gain that in turn improves the solar fraction and the collector efficiency. The results also indicates that as long as the $\dot{m}/A_c$ ratio is around 25-40 (kg/hr.m^2), the flow rate can be kept constant throughout the year and the monthly variation of flow rate has no significant effect on the overall fraction and efficiency. The highest and the lowest monthly solar fractions is found to be 0.95 (in July) and 0.3 (in November); and those for the efficiency 41% (in October and April) and 36% (in November and December).The optimum values are found to be in good agreement with the previously published data, such as Beckman et al. (1977) and Baughn and Young (1984).

Table 3-3: Variation of the Monthly and Annual Solar Fraction with the Collector Flow Rate-to-Area Ratio (kg/hr.m²)

$\dot{m}/A_c$	5	10	20	30	40	50	60
Jan	0.28	0.36	0.40	0.40	0.39	0.37	0.35
Feb	0.43	0.53	0.60	0.61	0.60	0.57	0.55
Mar	0.52	0.65	0.72	0.74	0.73	0.72	0.69
Apr	0.51	0.62	0.69	0.70	0.69	0.66	0.64
May	0.60	0.73	0.80	0.81	0.80	0.78	0.74
Jun	0.66	0.81	0.88	0.89	0.88	0.86	0.82
Jul	0.72	0.87	0.94	0.95	0.93	0.91	0.87
Aug	0.65	0.78	0.83	0.82	0.81	0.79	0.76
Sep	0.67	0.82	0.88	0.89	0.88	0.87	0.84
Oct	0.48	0.60	0.67	0.68	0.67	0.66	0.64
Nov	0.22	0.28	0.30	0.30	0.30	0.28	0.26
Dec	0.24	0.30	0.34	0.34	0.32	0.31	0.29
Annual	0.49	0.60	0.66	0.67	0.66	0.64	0.61

Table 3-4: Variation of the Monthly and Annual Collector Efficiency with the Collector Flow Rate to Area Ratio (kg/hr.m²)

$\dot{m}/A_c$	5	10	20	30	40	50	60
Jan	0.27	0.34	0.38	0.38	0.37	0.35	0.33
Feb	0.26	0.33	0.38	0.38	0.37	0.35	0.34
Mar	0.28	0.35	0.40	0.40	0.40	0.39	0.38
Apr	0.29	0.36	0.40	0.41	0.40	0.38	0.37
May	0.29	0.36	0.39	0.40	0.39	0.38	0.36
Jun	0.28	0.35	0.39	0.39	0.38	0.37	0.35
Jul	0.28	0.35	0.38	0.39	0.38	0.36	0.34
Aug	0.28	0.34	0.37	0.37	0.36	0.35	0.34
Sep	0.28	0.35	0.39	0.39	0.39	0.38	0.36
Oct	0.29	0.36	0.40	0.41	0.41	0.40	0.38
Nov	0.26	0.33	0.36	0.36	0.35	0.33	0.31
Dec	0.26	0.33	0.36	0.36	0.34	0.32	0.30
Annual	0.28	0.35	0.39	0.39	0.38	0.37	0.35

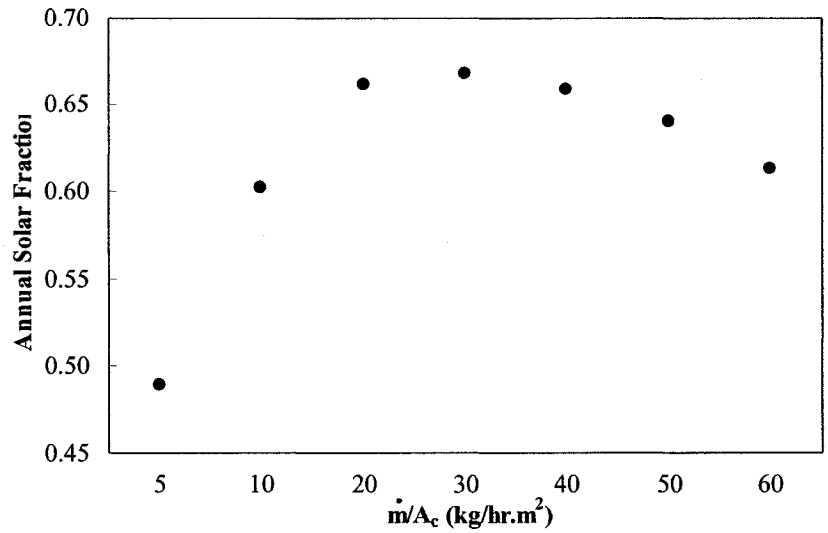

Figure 3-7: Variation of the Annual Solar Fractions versus the Collector Flow Rate-to-Area Ratio–*Indirect system with $A_c = 6\ m^2$*

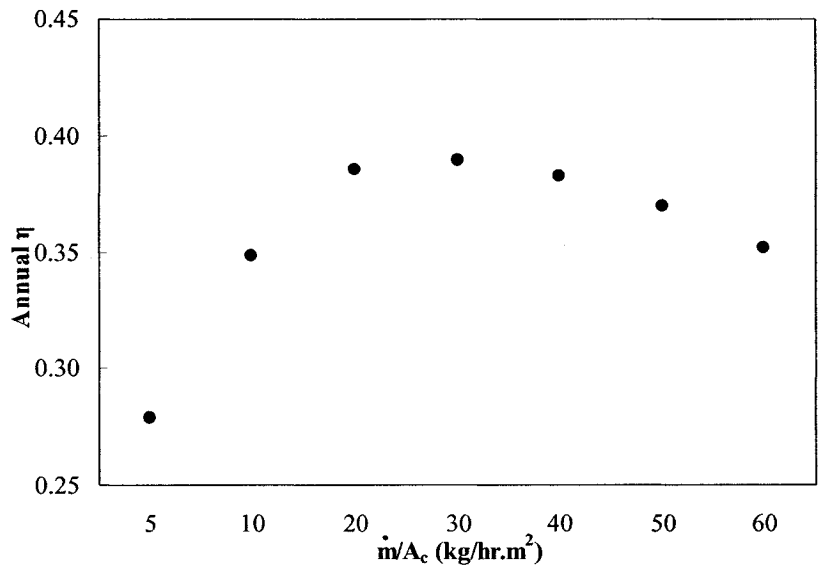

Figure 3-8: Variation of the Annual Collector Efficiency versus the Collector Flow Rate-to-Area Ratio–*Indirect system with $A_c = 6\ m^2$*

3.3.1.4. The Effect of the Tank Volume

The effect of the tank volume on the system performance is studied for various tank volume–to–collector area (V_c/A_c) ratios, for a 6 (m^2) collector with 30 ($kg/hr.m^2$) flow rate. The results showing the impact of the variation of V_c/A_c on the monthly and

annual solar fractions are presented in Table 3-5 and depicted in Figure 3-9. Results showed that the maximum values–as large as 0.95–of the monthly solar fraction, occurring in July, are about 43–46 % greater than annual values and the minimum values, occurring in November, are 56–58% less than annual ones. It was, also, found that the monthly and annual solar fractions increased as V_c/A_c increases from 20 to 45 (lit/m^2). For V_c/A_c values between 45 and 100, the change in solar fractions is small. For the ratios above 100 (lit/m^2) –as tank gets larger– the monthly solar fraction decreased slightly due to an increase in the heat losses form the storage tank to the environment. It can be observed that as the tank volume increases, the rate of the removed energy from the tank to supply the load, and the rate of energy transfer from the heat exchanger to the tank increases. In the meanwhile, the required auxiliary energy decreases as the tank volume increases. However, the rate of increase of the energy to the load is small for the greater tank volumes due to increased surface area and its corresponding amplified heat losses. The recommended values are determined to be around 55-65 (lit/m^2) for this study. For a tank with V_c/A_c = 65 (lit/m^2) the highest solar fraction is found to be 0.95 in July and 0.3 in November. The obtained optimum value of *Vc/Ac* ratio for this forced indirect system is found to be close to those of published data for a thermosyphon system such as Shariah and Löf (1996).

Table 3-5: Variation of the Monthly and Annual Solar Fraction with Tank Volume-To-Collector Area Ratio (lit/m²)

V_c/A_c	20	30	40	45	50	55	60	65	70	75	80
Jan	0.36	0.39	0.40	0.41	0.41	0.41	0.41	0.41	0.41	0.40	0.40
Feb	0.52	0.57	0.59	0.59	0.60	0.60	0.60	0.60	0.60	0.61	0.61
Mar	0.62	0.69	0.71	0.72	0.73	0.73	0.73	0.74	0.74	0.74	0.74
Apr	0.60	0.65	0.68	0.68	0.69	0.69	0.69	0.70	0.70	0.70	0.70
May	0.70	0.76	0.78	0.79	0.80	0.80	0.80	0.80	0.81	0.81	0.81
Jun	0.78	0.83	0.86	0.87	0.87	0.88	0.88	0.88	0.89	0.89	0.89
Jul	0.84	0.90	0.93	0.94	0.94	0.94	0.95	0.95	0.95	0.95	0.94
Aug	0.72	0.77	0.80	0.80	0.81	0.81	0.82	0.82	0.82	0.82	0.83
Sep	0.77	0.83	0.86	0.87	0.87	0.88	0.88	0.88	0.89	0.89	0.89
Oct	0.56	0.61	0.64	0.65	0.66	0.66	0.67	0.67	0.67	0.68	0.68
Nov	0.24	0.27	0.28	0.28	0.29	0.29	0.29	0.30	0.30	0.30	0.30
Dec	0.26	0.29	0.31	0.31	0.32	0.32	0.33	0.33	0.33	0.34	0.34
Annual	0.57	0.62	0.64	0.65	0.65	0.66	0.66	0.66	0.67	0.67	0.67

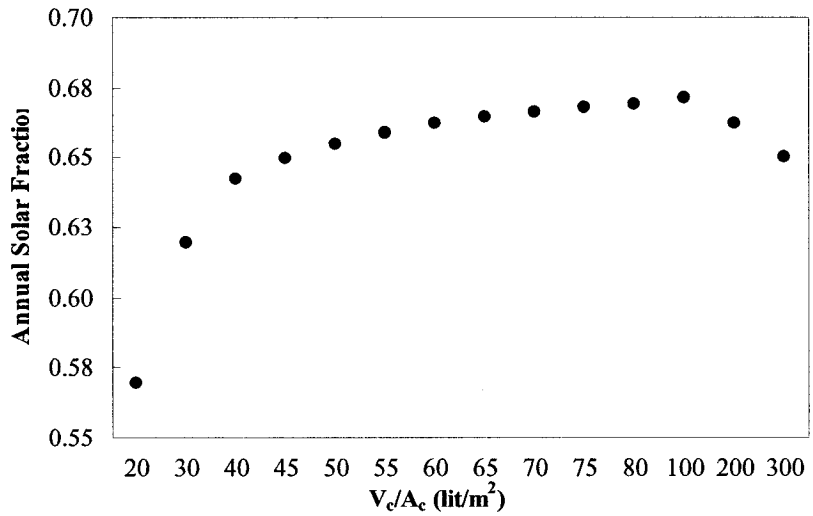

Figure 3-9: Variation of the Annual Solar Fraction versus the Tank volume–to–Collector area Ratio–*Indirect system with $A_c = 6\ m^2$*

3.3.1.5. The Effect of the Tank Height

The effect of the tank height on the system performance is studied for a 6 (m^2) collector with 30 ($kg/hr.m^2$) flow rate and a tank with V_c/A_c = 65 (lit/m^2). Figure 3-11 presents the variation of the annual solar fraction with the tank's height. It was found that the solar fraction increases with the tank height. However, the annual solar fraction is

almost constant for the H_t between 1.2 and 1.8 (m). Therefore, any tank height in this range is desirable and can be selected based on the space limitations and cost. These values are close to those of published data for thermosyphon systems; for instance, Shariah and Shalabi (1997). Results for the same tank height ranges also showed that the maximum values (i.e. 0.9–0.96) of the monthly solar fractions, occurring in July, are about 42–44% greater than annual values and the minimum values (i.e. 0.28–0.8) occurring in November, are 56–58% less than annual ones.

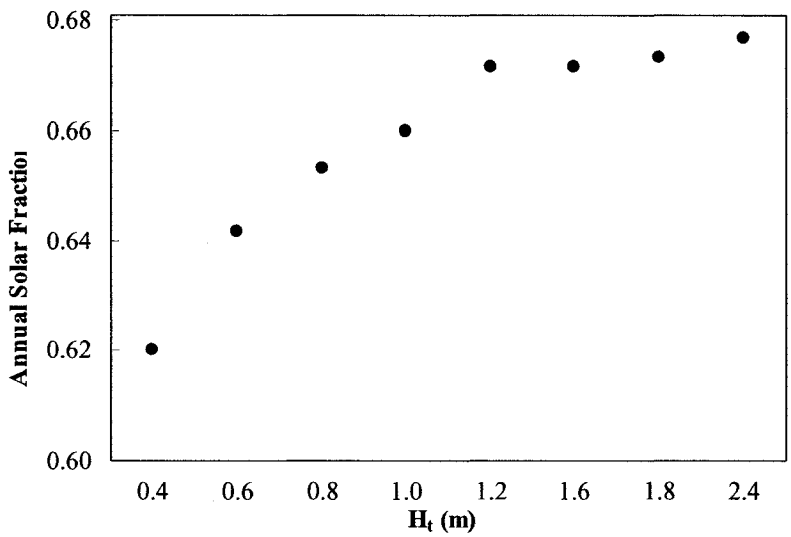

Figure 3-10: Variation of the Annual Solar Fraction versus the Tank Height –*Indirect system*

3.3.1.6. The Effect of the Heat Exchanger Effectiveness

The variation of the monthly and annual solar fractions is studied for different heat exchanger effectiveness (ε_{HX}) varying between 0.3 and 1.0 and for the specific configuration shown in Figure 3-1. The simulation first examined for both parallel and counter flow heat exchangers where it was terminated that a counter flow heat exchanger presents better solar fractions. Figure 3-10 shows the impact of the effectiveness of a counter flow heat exchanger on annul solar fraction. The results show that the solar fractions increased with ε_{HX} up to ε_{HX} in the range of 0.7–0.8. A further increase in ε_{HX}

resulted in a slight decrease in solar fraction. As the effectiveness increases (up to 0.8) the solar fractions increases as the result of improving the useful energy gain from the collector, the energy rate from the tank to the load, and the energy rate from the heat exchanger to the tank increases, and also decrease of the required auxiliary energy. Contrarily, as ε_{HX} increases further, from 0.8, the useful energy gain from the collector, energy rate from the tank to the load, and energy rate from heat exchanger to the tank slightly decreases, and required auxiliary energy increases; causes reduction of the solar fractions. Simulation results also showed that the maximum values (i.e. 0.87–0.95) of the monthly solar fraction, occurring in July, are about 42–46 % greater than the corresponding annual values and the minimum values (i.e. 0.28–0.3) occurring in November, are 55% less than annual ones. A counter flow heat exchanger with ε_{HX} around 0.7 –corresponding to the most of existing commercial HVAC heat exchangers– is considered to be suitable for our application.

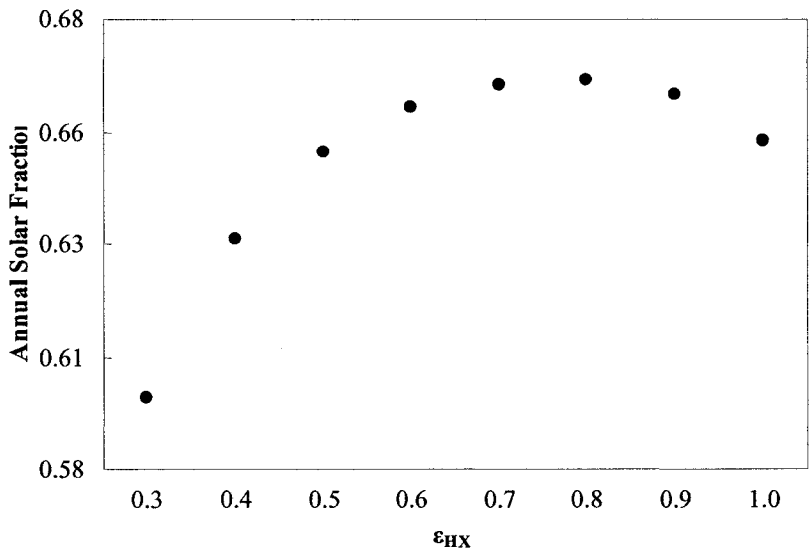

Figure 3-11: Variation of the Annual Solar Fractions versus Heat Exchanger Effectiveness

3.3.1.7. The Effect of the Supply and Return Pipes

The effect of the length and inside diameter of the connecting pipes –between the collector and heat exchanger– is studied for different supply plus return pipe length (*2L*) varying from 2 to 40 (m), and for four different pipe inside diameters: 19.94 mm, 25.4 mm, 38.3 mm, and 50.05 mm. Variation of the annual solar fraction with the pipe length and diameter is depicted in Figures 3-12. These monthly values of the solar fraction are also summarized in Tables 3-7 and 3-8. It is found that the monthly and annual solar fractions decrease as the pipe length increases, but the collector efficiency increases as the total length increases. This behavior is mainly caused by amplifying the heat loss, from the pipes to surrounding, as the length increases. On the other hand, higher heat losses from the inlet pipe to the collector yields to lower inlet temperature to the collector resulting improvement of the efficiencies. It is also seen that due to larger heat losses, the solar fractions decrease as the pipe diameter increases, whereas the collector efficiency increase as the diameter increases because of smaller pressure drop and lower inlet temperatures. The rate of the changes for shorter pipe length (around 4 to 8 meters) or smaller pipe size (less than 25.4 mm) is small, whereas it is larger for longer pipes and greater sizes. It is determined that a pipe with 19.94 or 25 (mm) ID and total length around 4–10 (m) results better performances. The difference between solar fractions of the system with 2 meters and 40 meters connecting pipe length with 25 mm ID is found to be as small as 3.7 to 5.3% only. Results, also, showed that for any pipe diameter the maximum values –as large as 0.96– of the monthly solar fractions, occurring in July, are 43% greater than annual values and the minimum values, occurring in November, are 55–

57% less than annual ones. It was, moreover, found that the impact of the supply and return pipe length and diameter on the collector efficiency is negligible.

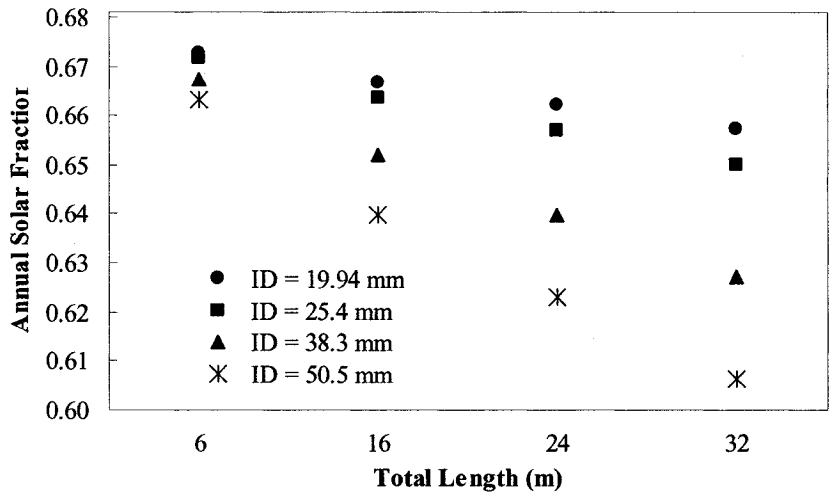

Figure 3-12: Variation of the Annual Solar Fraction versus the Supply and Return Pipe Length and Diameter

Our results are consistent with those of published data (for thermosyphon system) by Shariah and Shalabi (1997).

Table 3-6: Thee monthly and Annual Solar Fraction Variation with Total Supply and Return Pipes Length, ID = 25 (mm)

2L (m)	Jan	Feb	Mar	Apr	May	Jun	Jul	Aug	Sep	Oct	Nov	Dec	Annual
2	0.41	0.61	0.75	0.71	0.82	0.90	0.96	0.83	0.90	0.68	0.30	0.34	0.67
4	0.41	0.61	0.75	0.71	0.82	0.90	0.96	0.83	0.89	0.68	0.30	0.33	0.67
6	0.41	0.61	0.75	0.70	0.81	0.89	0.96	0.83	0.89	0.68	0.30	0.33	0.67
8	0.41	0.61	0.74	0.70	0.81	0.89	0.95	0.82	0.89	0.68	0.30	0.33	0.67
16	0.41	0.60	0.74	0.70	0.81	0.88	0.95	0.82	0.88	0.67	0.30	0.33	0.66
24	0.40	0.60	0.73	0.69	0.80	0.88	0.94	0.81	0.88	0.66	0.29	0.33	0.66
32	0.40	0.59	0.72	0.68	0.79	0.87	0.93	0.80	0.87	0.65	0.29	0.32	0.65
40	0.39	0.59	0.72	0.68	0.78	0.86	0.92	0.79	0.86	0.65	0.28	0.32	0.64

Table 3-7: Variation of the Monthly and Annual Solar Fraction with the Supply and Return Pipe Length and Size

	ID = 19.94 mm				ID = 25.4 mm				ID = 38.3 mm				ID = 50.5 mm			
2L (m)	6	16	24	32	6	16	24	32	6	16	24	32	6	16	24	32
Jan	0.41	0.41	0.41	0.40	0.41	0.41	0.40	0.40	0.41	0.40	0.39	0.38	0.41	0.39	0.38	0.37
Feb	0.61	0.61	0.60	0.60	0.61	0.60	0.60	0.59	0.61	0.59	0.58	0.57	0.60	0.58	0.57	0.55
Mar	0.75	0.74	0.74	0.73	0.75	0.74	0.73	0.72	0.74	0.73	0.71	0.70	0.74	0.71	0.70	0.68
Apr	0.70	0.70	0.69	0.69	0.70	0.70	0.69	0.68	0.70	0.68	0.67	0.66	0.69	0.67	0.66	0.64
May	0.82	0.81	0.80	0.80	0.81	0.81	0.80	0.79	0.81	0.79	0.78	0.76	0.80	0.78	0.76	0.74
Jun	0.90	0.89	0.88	0.88	0.89	0.88	0.88	0.87	0.89	0.87	0.86	0.84	0.88	0.86	0.83	0.81
Jul	0.96	0.95	0.94	0.94	0.96	0.95	0.94	0.93	0.95	0.93	0.91	0.90	0.95	0.92	0.89	0.87
Aug	0.83	0.82	0.81	0.81	0.83	0.82	0.81	0.80	0.82	0.80	0.79	0.77	0.82	0.79	0.76	0.74
Sep	0.89	0.89	0.88	0.88	0.89	0.88	0.88	0.87	0.89	0.87	0.86	0.85	0.88	0.86	0.84	0.82
Oct	0.68	0.67	0.67	0.66	0.68	0.67	0.66	0.65	0.67	0.66	0.64	0.63	0.67	0.64	0.62	0.60
Nov	0.30	0.30	0.29	0.29	0.30	0.30	0.29	0.29	0.30	0.29	0.28	0.27	0.29	0.28	0.27	0.26
Dec	0.33	0.33	0.33	0.33	0.33	0.33	0.33	0.32	0.33	0.32	0.31	0.31	0.33	0.31	0.30	0.30
Annual	0.67	0.67	0.66	0.66	0.67	0.66	0.66	0.65	0.67	0.65	0.64	0.63	0.66	0.64	0.62	0.61

3.3.2. OPTIMIZATION OF THE COLLECTOR PARAMETERS

The second sets of simulations are conducted to study the effect of collector design parameters on the monthly and annual solar fractions as well as collector characteristic factors. A theoretical flat-plate collector is modeled within the same forced circulation (indirect) system. It is assumed that the absorber plate is coated with a selective coating (e.g. Black-Chrome or Black-Copper), glazing is a single plate low iron glass, and both back and sides of the collector are insulated with 5 (cm) thickness Rock Wool insulation with the density of 24 (kg/m^3). Moreover, from the actual data, the wind velocity is considered to be 15 (km/hr), the winter values. In this model, the optimized parameters from the previous section have been used as constants, i.e., A_c = 6 (m^2), $\dot{m}$ = 180 (kg/hr), V_c = 390 (lit), H_t = 1.6 (m), C_p = 3.8 (kJ/kg °C), $2L$ = 6 (m), and hot water supplied at 60°C with daily consumption of 246 (lit/day). Additional parameters, used in this set of simulation runs, are listed in Table 3-9.

Table 3-8: Range of the Studied Design Parameters for Second Sets of the Simulations

Design Parameters	Range of Parameters
δ_p	0.1–1.5 (mm)
k (Copper)	393 (W/m.K)
k (Aluminum)	221 (W/m.K)
k (Steel)	45.3 (w/m.K)
$t_{insulation}$	5 cm
$k_{insulation}$ (Rock Wool)	0.04 (W/m.K)
U_b	0.9 (W/m^2.K)
U_{side}	0.12 (W/ m^2.K)
C_B	20 (kJ/hr.m^{2}K/kJ)
$h_{f,i}$	100—4000 (W/ m^2.K)
$D_{r,i}$ (Copper, type "L": ASTM B88)	0.008–0.0254 (m)
$D_{r,o}$	0.00953–0.0289 (m)
A_c $(l \times w)$	6 (m^2)
n	4–24
$\dot{m}/A_c$	30 (kg/hr.m^2)
V_c/A_c	65 (lit/m^2)
C_p	3.8 (kJ/kg^{o}C)
α_p (selective surface)	0.97
ε_p (selective surface)	0.1
Glass thickness	4 (mm)
τ_g (low iron glass)	0.91
ε_g	0.88
$(\tau\alpha)_n$	0.88
V (wind)	4.2 (m/sec)

3.3.2.1. The Effect of the Absorber Plate Material

The variation of the monthly and annual solar fractions and the collector efficiency is studied for three different absorber plate materials: Copper, Aluminum, and Steel with 1 (mm) thickness. In this case, collector is 2×3 meters, inside diameter of the tubes is 24.5 (mm), and the number of riser tubes (n) is 10. The monthly variation of the solar fractions for different plate material is shown in Figure 3-13. It is found that the solar fraction and the collector efficiency increases as the thermal conductivity of the absorber plate increases. The variation of the solar fraction is large for the smaller values of the thermal conductivity. The dependency of the solar fraction on the k weakens for

greater values of the k. For instance, replacing plate material from copper to aluminum reduces the annual solar fraction and the collector efficiency by 1% and 1.2%, respectively. By changing the plate material from copper to steel the annual solar fraction and the collector efficiency are reduced by 9.4% and 10.6%. These results, for the forced system, are in good agreement with the previously published data, such as Shariah et al. (1999), for the thermosyphon systems.

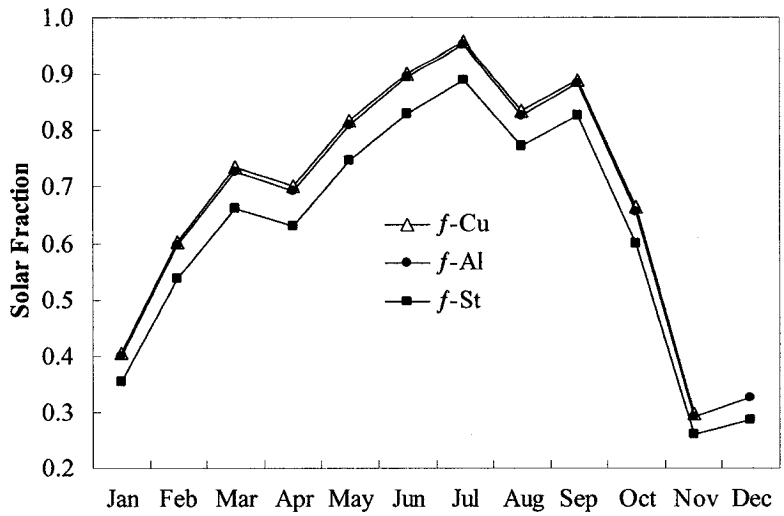

Figure 3-13: Monthly Solar Fraction for Different Absorber Plate Material: 1-Copper (Cu), 2-Aluminum (Al), 3-Steel (St)

The annual values of the solar fraction, the collector efficiency (η), the heat removal factor (F_R), and the collector efficiency factor (F') for these three plate materials are depicted in Figure 3-14. From the results it can be seen that f, η, F_R, and F' decreases with a decrease in thermal conductivity (k). By changing the plate material from copper to aluminum, f, η, F', F_R, are reduced, respectively, by only 1.5%, 1.2%, 1.2%, and 1.2%. By changing the copper plate to steel, f, η, F', F_R are reduced by 9%, 10.6%, 10.3% and 10%, respectively. Similarly, the variation of the characteristic factors is significant for the smaller values of the thermal conductivity but it becomes insignificant as k increases. The above results indicates that fabrication of commercial collectors with copper

absorber plate, which is more expensive, is not really necessary and an aluminum absorber plate can have similar performance to that of copper. The overall heat loss coefficient (U_L), for the studied materials, is found to be in range of 12.80 to 12.87 (kJ/hr.m^2.K), which indicates the negligible effect of the k on the U_L. The results also showed that the minimum monthly values of f, η, and U_L; occurring in November, are respectively 56%, 8.5%, and 8.1% smaller than their annual values. Maximum values of f, and U_L, occurring in July, are respectively 44% and 6.6% greater than their annual values. The differences between the maximum and minimum values of the remaining studied parameters with the annual ones were negligible.

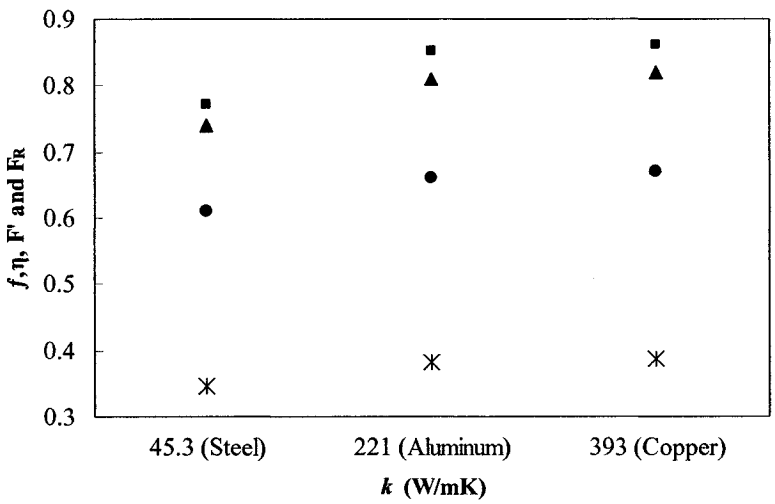

Figure 3-14: Variation of the annual f (•), η (*), F' (■), and F_R (▲) versus the Thermal Conductivity of Plate (k)

3.3.2.2. The Effect of the Absorber Plate Thickness

The effect of the absorber plate thickness (δ_p) on the performance of the system is studied over a range of δ_p varying from 0.1 to 1.5 (mm). The collector specifications are 2×3 meters aluminum plate, inside diameter of the tubes is 24.5 mm, and the number of the riser tubes (n) is 10. The variations of the annual solar fraction as well as the collector characteristic factors with the plate thickness are presented in Figure 3-15. Figure 3-16

also shows the variation of the monthly solar fraction for different plate thicknesses. The results show that the solar fraction and the collector characteristics factors are improved by increasing the plate thickness. The plots show that the improvement of these factors is very significant as δ_p increases from 0.1 to 0.4 (mm). This influence weakens as the thickness reaches to the values around 0.5 to 0.8 (mm), and then for the thicker plates rate of improvement becomes very small. Results show that the solar fraction (f), collector efficiency (η), collector efficiency (F') and heat removal (F_R) factors increased by 15.7%, 17.3%, 16% and 15.3%, respectively, as δ_p increased from 0.1 (mm) to 0.5 (mm). Whereas, when δ_p increased from 0.5 (mm) to 1 (mm), f, η, F', F_R increased, respectively by 2.3%, 2.6%, 2.6%, and 2.5%. It is concluded that the plate thickness in the range of 0.6 to 0.8 (mm) is sufficient for the residential applications and thicker plates seems to be not economical. The thickness of 0.8 (mm) is selected for the subsequent parametric studies. It was also observed that the influence of δ_p, in this studied range, is negligible on the U_L. As δ_p increased from 0.1 (mm) to 1.5 (mm), U_L decreased from 12.92 to 12.80 (kJ/hr.m^2.K). The results also showed that the minimum monthly values of f, η, and U_L; occurring in November, are respectively 56%, 9.5%, and 8.2% smaller than their annual values. Maximum values of f, and U_L, occurring in July, are respectively 46% and 6.6% greater than their annual values. The differences between the maximum and minimum values of the remaining studied parameters with the annual ones were negligible.

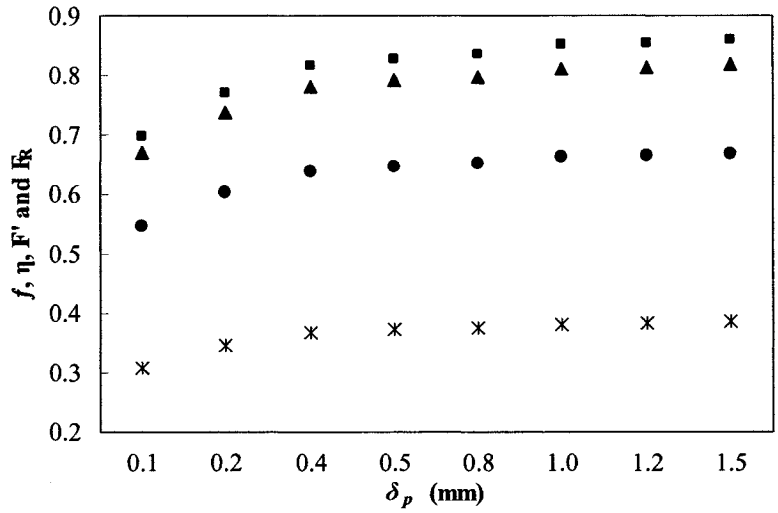

Figure 3-15: Variation of the annual f (•), η (*), F' (■), and F_R (▲) versus the Absorber Plate Thickness (δ_p)

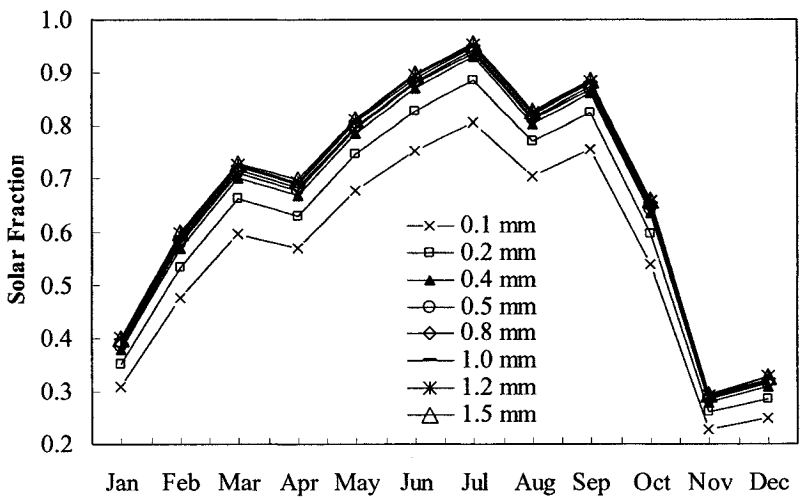

Figure 3-16: Variation of the Monthly Solar Fraction with the Absorber Plate thickness

3.3.2.3. The Effect of the Riser Tube Diameter

For the same collector with 6 (m^2) area, 10 riser tubes, and aluminum absorber plate with 0.8 (mm) thickness, the effect of the riser tube diameter ($D_{r,i}$) is studied over a variety of available commercial type "L" copper tube sizes, which are 8 mm, 8.64 mm, 13.84 mm, 16.92 mm, 19.94 mm, and 25.4 mm. The results indicating the variation of the annual solar fraction, collector efficiency, and the collector characteristic factors are

shown in Figure 3-17. The results show that the solar fraction, the collector efficiency and the collector characteristics factors improve as the size of riser tubes increases; however, this increment is about 5% between an 8 (mm) and 25.4 (mm) pipe, and it is less than 2.5% between 13.84 (mm) and 25.4 (mm) pipe. It can be concluded that the riser tube diameter –in this range– has no significant influence on the solar fraction and other collector characteristic factors. Therefore, considering scaling problems inside the tubes, cost, fabrication difficulties, and capacity to carry the maximum flow rate, tubes with 13.84 mm to 19.94 mm inside diameters seems to be more feasible. It is worth mentioning that tubes with diameter smaller than 8 (mm) will results in very low solar fractions and high pressure drop; thus, they are not recommended. It was also found that the impact of $D_{r,i}$, is negligible on the U_L. As $D_{r,i}$ increased from 8 to 25.4 (mm), U_L decreased from 12.84 to 12.81 (kJ/hr.m^2.K). The results also showed that the minimum monthly values of f, η, and U_L; occurring in November, are respectively 56%, 9%, and 8.15% smaller than their annual values. Maximum values of f, and U_L, occurring in July, are respectively 45% and 6.6% greater than their annual values. The differences between the maximum and minimum values of the remaining studied parameters with the annual ones were negligible.

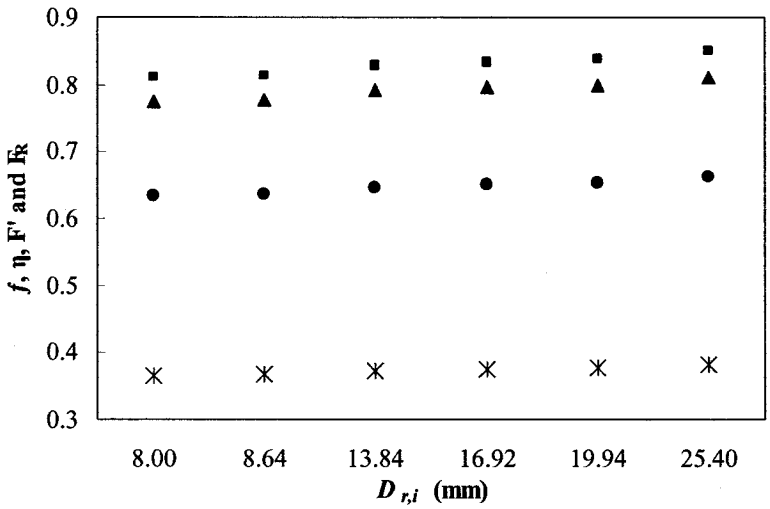

Figure 3-17: Variation of the annual f (•), η (*), F' (■), and F_R (▲) versus Riser Tube Diameter ($D_{r,i}$)

3.3.2.4. The Effect of the Number of the Risers

The number of riser tubes is one of the important parameters of a flat-plate collector design. For a fixed collector width, increasing the number of risers reduces distance between riser tubes and vise versa since $w = n \times W$. To study the effect of the number of risers, a $l = 3$ by $w = 2$ meters collector with aluminum absorber plate ($\delta_p = 0.8$ mm) is considered. The tubes is considered to be with $D_{r,i} = 13.84$ mm. The number of the risers varied from $n = 4$ to $n = 24$ corresponding to the tube distancing values varying from W= 50 (cm) to $W = 8.33$ (cm). The variation of the solar fraction, the collector efficiency and characteristic factors with the number of the tubes are presented in Figure 3-18. Result show that the annual solar fraction of the system as well as collector efficiency and collector characteristic factors increases with the number of riser tubes. However, the percentage increase of these parameters is higher as n increases from 4 to 9. For n above 9 the percentage increase of these parameters becomes relatively small. For instance, the increase in the annual solar fraction and heat removal factor is about 43% and 34%, respectively, as n increased from 4 to 8. Whereas f, and F_R increased only

7.7% and 8.6% as n increased from 9 to 16. It is found that the reduction of the overall heat loss coefficient by increasing the number of tubes is insignificant. As n increased from 4 to 24, U_L only reduced from 13 to 12.74 (kJ/hr.m^2.K). The results also showed that the minimum monthly values of f, η, and U_L; occurring in November, are respectively 54-60%, 6-16%, and 8-8.6% smaller than their annual values. Maximum values of f, and U_L, occurring in July, are respectively about 48% and 6.8% greater than their annual values. The differences between the maximum and minimum values of the remaining studied parameters with the annual ones were negligible.

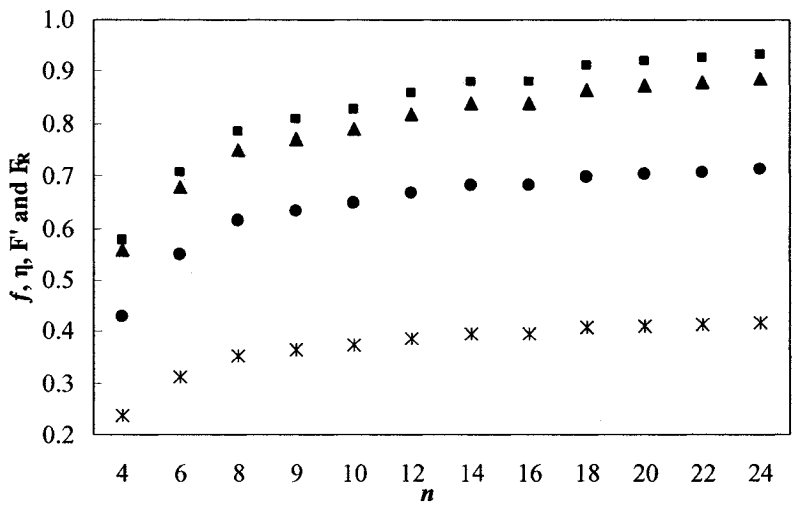

Figure 3-18: Variation of the annual f (•), η (*), F' (■), and F_R (▲) versus Number of Riser Tubes (n)

The monthly variation of the solar fractions is presented in Table 3-10. It is concluded that a collector with n equal to 14 or 18 –corresponding to tube spacing values of W = 14.3 (cm) or W = 11.1 (cm) – could yield sufficient performance for our application. It is important to note that the number of tubes, on the other hand, can be affected by the collector's aspect ratio and greater numbers are not necessarily yield to a higher performance. This is studied in the next section.

Table 3-9: Variation of the Monthly and Annual Solar Fraction with Number of Riser Tubes for a 3×2 meters collector with $D_{r,i}$ = 13.84 (mm)

n	4	6	8	9	10	12	14	16	18	20	22	24
Jan	0.23	0.31	0.36	0.37	0.39	0.40	0.42	0.42	0.43	0.44	0.44	0.45
Feb	0.37	0.48	0.54	0.56	0.58	0.60	0.62	0.62	0.64	0.64	0.65	0.65
Mar	0.48	0.60	0.67	0.69	0.71	0.73	0.75	0.75	0.77	0.78	0.78	0.79
Apr	0.45	0.57	0.64	0.66	0.68	0.70	0.72	0.72	0.73	0.74	0.75	0.75
May	0.54	0.68	0.76	0.78	0.79	0.82	0.83	0.83	0.85	0.86	0.86	0.86
Jun	0.60	0.76	0.84	0.86	0.88	0.90	0.91	0.91	0.93	0.93	0.93	0.94
Jul	0.64	0.82	0.90	0.92	0.94	0.96	0.97	0.97	0.98	0.98	0.99	0.99
Aug	0.56	0.71	0.78	0.80	0.81	0.83	0.85	0.85	0.86	0.87	0.87	0.87
Sep	0.60	0.76	0.83	0.85	0.87	0.89	0.90	0.90	0.91	0.92	0.92	0.92
Oct	0.43	0.54	0.61	0.63	0.64	0.66	0.68	0.68	0.70	0.70	0.71	0.71
Nov	0.17	0.23	0.26	0.28	0.28	0.30	0.30	0.30	0.32	0.32	0.32	0.33
Dec	0.19	0.25	0.29	0.30	0.31	0.33	0.34	0.34	0.35	0.36	0.36	0.37
Annual	0.43	0.55	0.61	0.63	0.65	0.67	0.68	0.68	0.70	0.70	0.71	0.71

3.3.2.5. The Effect of the Collector's Aspect Ratio

The dimension of the collector can be confined by architectural geometry of the building, thus, affecting the aspect ratio of the collector. The change in the aspect ratio can be attained by either changing the tube spacing when the tube number is fixed, or by altering the tube number when tube spacing is maintained constant. Considering $A_c = l \times w = l \times n \times W$, the aspect ratio, R, can be defined as $R = l / w = l /(n\mathrm{W}) = A_c/(nW)^2$. The collector is of same specification in previous section. In the first case, the number of riser tubes is kept constant equal to 14 and the aspect ratio is varied from R = 0.2 to 5 by changing the tube spacing from W = 39.1 to 7.8 (cm), respectively. The result for the first case is depicted in Figure 3-19. The results show that for a constant tube number, the annual solar fraction, the collector efficiency, and the collector's characteristic factors increased with an increase in the aspect ratio (i.e. either increase of tube length or decrease of tube spacing). The percentage increase is large for aspect ratios less than 1, but fort R above 1.2, the percentage increase becomes small. For instance, the annual

solar fraction is increased 34% as R increase from 0.2 to 1.2, yet it is increased only 5.7% as R increased from 1.2 to 5. For the studied range of aspect ratios, U_L is only varied between 12.8 and 13.1 (kJ/hr.m^2.K). The results also showed that the minimum monthly values of f, η, and U_L; occurring in November, are respectively 54-58%, 5.7-14%, and 8.2% smaller than their annual values. Maximum values of f, and U_L, occurring in July, are respectively about 40-48% and 6.7% greater than their annual values. The differences between the maximum and minimum values of the remaining studied parameters with the annual ones were negligible. The result indicates that the aspect ratios between R = 1.5 to 2 corresponding to the tube spacing between W = 14.3 to 12 (cm) yield adequate performance of the system. Nevertheless, since the difference between the value of the parameters corresponding to R = 1 and 1.2 with those of corresponding to R = 1.5 is very small, these aspect ratios, also, can be used confidently in case of architectural limitations. From the results it can also be concluded that as long as R is between 1.25 and 2 (i.e. tube spacing is between 15.6 to 12 cm) the system has the lowest heat loss and thus highest performance.

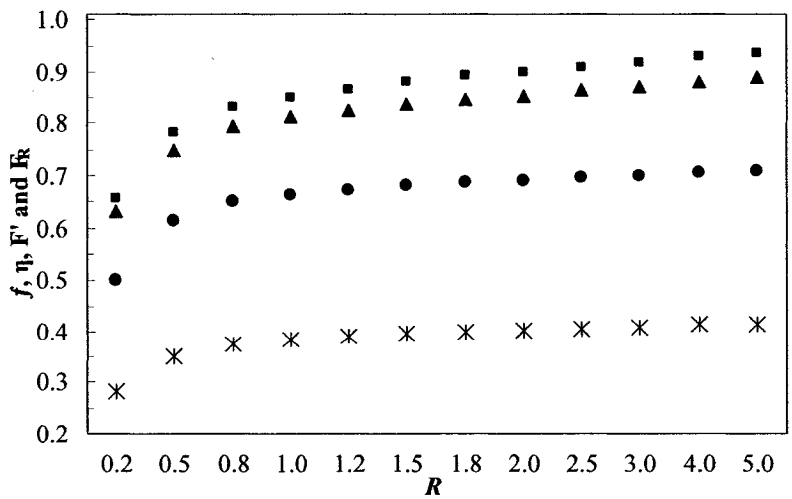

Fig 3-19: Variation of the annual f (•), η (*), F' (■), and F_R (▲) versus Collector Aspect Ratio (R) for Constant n=14

In the second case, the tube spacing is kept constant at W = 14.3 (cm), where altering the aspect ratio changed the number of tubes. Since smaller aspect ratios (below 0.8) have insufficient performance and higher aspect ratios have lager U_L, the simulation is conducted for the R values between 0.5 and 18. The result, for the second case, is depicted in Figure 3-20. The result show that increasing the collector aspect ratio decreases the annual solar fraction, the collector efficiency and the characteristic factors decreases. These changes for the solar fraction and collector characteristic factors, however, are almost negligible (i.e. less than 1%). Therefore, for the tube diameter and spacing within the optimum values and constant collector area, reduction of tube number will not affect performance of the system, appreciably, as long as tube length increases. In other word, system performance and collector efficiency increases by either increasing the tube length (i.e. increasing the aspect ratio) or reducing the tube number when the area and tube spacing is kept constant. Increasing the aspect ratio, in this case, increases the flow velocity inside each tube which, in turn, improves the heat transfer rate inside the tubes. Even though the collector flow rate is very small (0.0083 kg/sec.m^2) and results showed that the difference between the solar fraction of a collector will 4 riser tubes and 10.3 meters length (R = 18) and a collector with 14 risers and 3 meters length (R = 1.5) is only 2%, a narrow and long collector with less tubes can results high pressure drops and high friction losses which, in practice, reduces the performance dramatically. For example increasing flow rate from 30 to 50 (kg/hr.m^2) causes 5% reduction of annual solar fraction and 3% reduction in collector efficiency for R = 12 or 18. Considering results from section 3.4.2.4, the tube number less than 4 or R grater than 9 is not recommended. In other word, if the aspect ratio needs to be increased tube spacing has to

be reduced from the optimum value corresponding to R = 1.5. Selecting an adequate aspect ratio needs a balance between all of the parameters, and a reasonable pressure drop inside each tube as well as economical considerations.

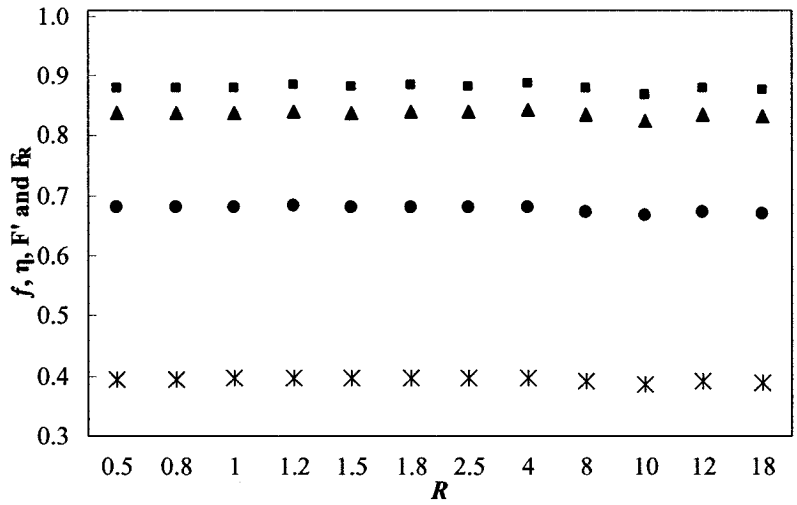

Figure 3-20: Variation of the annual f (•), η (*), F' (■), and F_R (▲) versus the Collector Aspect Ratio (R) for Constant W=14. 3 (mm)

In this case as R varied between 0.5 and 18, U_L only varied between 12.77 and 13.2 (kJ/hr.m^2.K). The results also showed that the minimum monthly values of f, η, and U_L; occurring in November, are respectively 55%, 7.8%, and 8.2% smaller than their annual values. Maximum values of f, and U_L, occurring in July, are respectively about 42.3% and 6.6% greater than their annual values. The differences between the maximum and minimum values of the remaining studied parameters with the annual ones were negligible.

3.3.2.6. The Effect of Heat Transfer Coefficient inside the Tubes

The effect of heat transfer coefficient inside the tubes ($h_{f,i}$) was studied for the collector with 6 (m^2) area, 0.8 (mm) thick aluminum absorber plate, 13.84 (mm) ID riser tubes, 14.3 (cm) tube spacing and R = 1.5. $h_{f,i}$ was varied from 100 and 300 (w/m^{2}K) for

laminar flows and 1000- 1500 (W/m^{2}K) for turbulent flows (Duffie and Beckman, 1991). The variation of the annual solar fraction, the collector efficiency and characteristic factors are presented in Figure 3-21. The plate is also considered to be coated with a selective coating and the contact between the plate and the tubes is very good (i.e. $1/C_B$ = 0.05 hr.mK/kJ for unit length). The results show that the solar fraction, collector efficiency and characteristic factors increased with an increase in $h_{f,i}$. Plots show that the percentage increase is large for smaller value of $h_{f,i}$ i.e. when the flow is in laminar range. For $h_{f,i}$ above 1000 (W/m^{2}K) i.e. in the turbulent regime, the percentage increase becomes smaller. The results also showed that the overall heat loss coefficient decreased slightly as $h_{f,i}$ increased (i.e. from 13.05 to 12.78 kJ/hr.m^2.K).

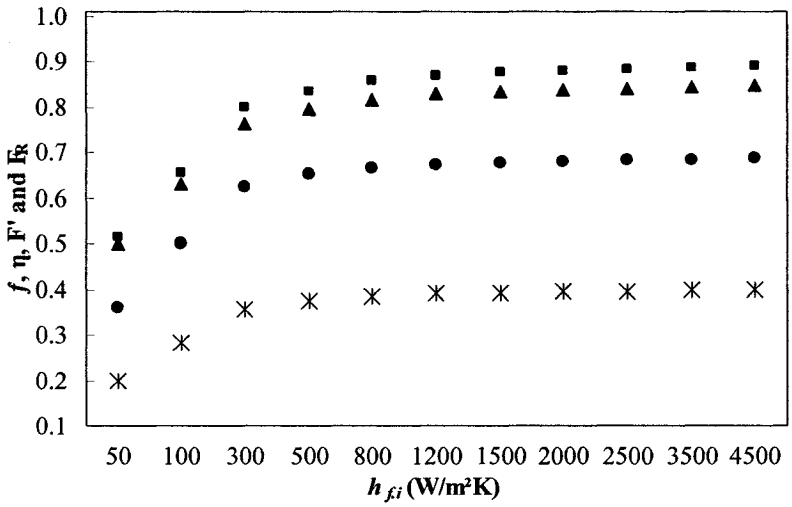

Figure 3-21: Variation of the annual f (•), η (*), F' (■), and F_R (▲) versus Heat Transfer Coefficient Inside the Tube ($h_{f,i}$) when $\varepsilon_p = 0.1$ and $(1/C_B) = 0.05$

The results also indicated that the minimum monthly values of f, η, and U_L; occurring in November, are respectively 55-60%, 8-18%, and 8-8.7% smaller than their annual values. Maximum values of f, and U_L, occurring in July, are respectively about 42-50% and 6.6-7% greater than their annual values. The differences between the maximum and

minimum values of the remaining studied parameters with the annual ones were negligible.

3.4. CONCLUSION OF THIS CHAPTER

To optimize the design parameters of a solar water heating system with flat-plate collector that provides hot water requirements of a one family house in Montreal one direct and one indirect system were modeled. Two sets of simulations were conducted. The first set was to determine the optimum values of the system parameters and the second set to determine the optimum values of the collector design parameters alone. From the simulation results it was concluded that:

- A 6 (m^2) collector, with superior values of $F_R(\tau\alpha)_n$ and $F_R U_L$, is appropriate for this application.
- Comparing simulation results with those obtained from f-chart method shows that the f-chart can be used to estimate the required collector area and the annual solar fraction but it is not adequate to estimate the monthly fractions.
- Degradation of the solar fractions from direct to indirect system is due to the incorporation of the additional heat exchanger but not due to replacing water to glycol solution. The reduction of solar fractions is about 6 to 15.5%. Percentage of the glycol solution in water has small effect on the solar fractions.
- The annual and monthly solar fractions are the highest and the supplied auxiliary heating energy is the lowest when the auxiliary heater is installed in series –outside the main storage tank– and before tempering valve. When the auxiliary heater is located in series but after tempering valve or when it is located inside the tank, solar fractions are lower and delivered auxiliary energy is greater.

- Both the solar fraction and the collector efficiency increases rapidly as the collector flow rate increases. After reaching to the optimum value of the flow rate around 30 ($kg/hr.m^2$) the solar fraction and the collector efficiency decreases with a further increase in flow rate.
- The solar fraction increase as the tank volume increase up to certain values. The optimum volumes found to be around 55-65 (lit/m^2). Larger tanks, above 80 (lit/m^2), results in higher heat loss from the tank to the surroundings that reduces the system performance.
- The solar fraction increases with an increase in the heat exchanger effectiveness up to values around 0.6-0.7. It decreases slightly with a further increase in the effectiveness.
- The solar fraction increases with the tank height. The percentage increase is sharp when the tank height passes the dimensions corresponding to horizontal tank to those of vertical one. The percent increase of the solar fraction with the tank height is small for tank height greater than 1.2 (m).
- The annual solar fraction decreases as the length of the pipes connecting the collector to the heat exchanger increases or as the size of the pipes increases. Contrarily, the collector efficiency increases as the pipes' length and diameter increases. Pipe diameters of 25.4 or 38.3 (mm) with total pipe length ($2L$) less than 10 (m) are sufficient for our application.
- The solar fraction, the collector efficiency, and the collector characteristic factors increase with an increase in the thermal conductivity of the absorber plate. Replacing absorber plate material from steel to aluminum has very significant effect on the

collector and system performance but changing it from aluminum to copper has not significant effect.

- The solar fraction, the collector efficiency, and the collector characteristic factors increase with an increase in the absorber plate thickness. The percentage increase in the system performance is large as the thickness increases up to 0.6 (mm). Further increase of the plate thickness slightly improves the system performance. Plate thickness around 0.8 (mm) is found to be adequate for this application.
- The percentage increase in the solar fraction, the collector efficiency, and the collector characteristic factors is small for the riser tubes diameters ($D_{r,i}$) greater than 8 (mm). However considering less pumping requirements, fabrication troubles, erosion, and cost; the pipe diameter of 13.84 (mm) found to be appropriate for our application.
- Changing the number of riser tubes can affect either the tube distancing or collector width, which influences the collector and system performances. For a constant collector width, as the number of riser tubes increases, the solar fraction, the collector efficiency, and the collector characteristic factors improves. Dependency of these factors on the tube number is strong when the tube number is small. When the tubes are more than 12 or 14, the influence of the tube number on the collector and the system performance becomes weak.
- The aspect ratio of the collector can be changed by either changing the tube number for fixed tube spacing or tube spacing for the fixed tube number. For a constant tube number as the aspect ratio increases (either the tube length increases or the tube distance decreases) the solar fraction, the collector efficiency, and the collector

characteristic factors increase continuously. The percentage increase of these parameters for aspect ratios less than 1 is large, and for aspect ratios greater than 1.2, is small. When the tube spacing is kept constant, altering aspect ratio will change the tube number and the tube length. However if the tube diameter and spacing is within the obtained optimum values, reduction of the tube numbers, as the aspect ratio increases and tube length increases, has very small effect on the performance. Aspect ratios around 1.5 found to be suitable for our application.

- Variation of the most of the collector's parameters influences the overall heat transfer coefficient slightly. However replacing selective coating with non-selective one increase U_L drastically.
- Increasing the heat transfer rate between the tube wall and the fluid has very significant effect on the system performance when the flow changes the regime from laminar to turbulent. For a fully turbulent flow inside the tubes, the percentage increase in the solar fraction, the collector efficiency, and the collector characteristic factors is small with an increase in heat transfer coefficient.
- Based on the calculated optimum values presented in Table 3-11, the optimal monthly solar fractions that can be achieved with such a system in Montreal are shown in Figure 3-22. This system can supply 85-97%, and 30-62% of the hot water load in hot and cold seasons, respectively, by solar energy. Annual solar fraction of this system is 68%.

Table 3-10: Optimum Parameters- Indirect Forced Circulation System

Parameters	Value
A_c	6 (m^2)
C_p	3.8 (kJ/kgK)
δ_p	0.6–0.8 (mm)
k (Aluminum)	221 (W/m.K)
$t_{insulation}$	5 cm
$2L$	6-16 (m)
$D_{r,i}$	13.8–19.9 (mm)
ε_{HX}	0.7
n	14
W	14.3 (cm)
$\dot{m}/A_c$	30 ($kg/hr.m^2$)
V_c/A_c	65 (lit/m^2)
α_p	0.97
ε_p	0.1
Glass thickness	4 (mm)
τ_g	0.91
ε_g	0.88

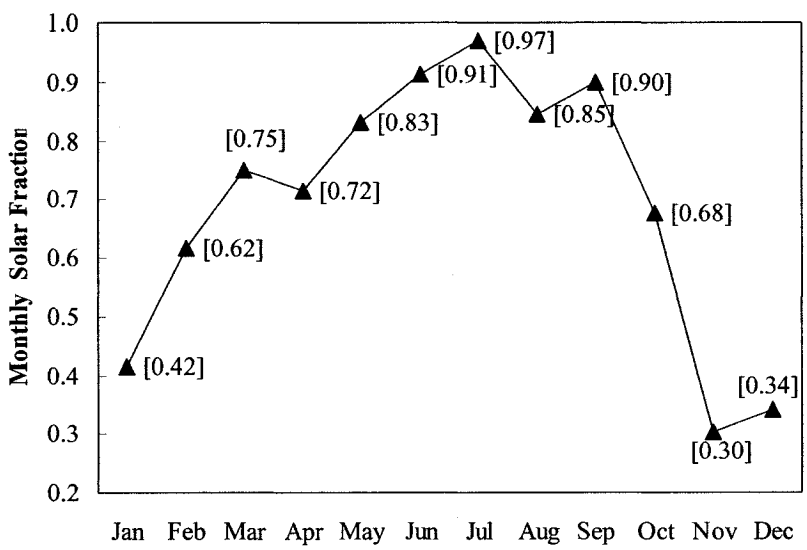

Figure 3-22: Monthly Solar Fractions, $f(\bullet)$ for Calculated Optimum Design Parameters- ***Indirect Forced Circulation System***

CHAPTER 4

EXPERIMENTAL STUDY OF THE THERMAL PERFORMANCE OF THE FLAT-PLATE COLLECTORS

4.1. INTRODUCTION

One of the major shortcomings of the flat-plate collectors in cold climate is high thermal losses from the absorber plate to the surrounding, which causes the reduction of useful energy gain, q_u, according to Equation 2.34. Several methods to suppress thermal losses that have already been widely studied are mentioned in section 1.3.3. Alternatively, by increasing the collector efficiency factor, F', the useful energy gain will increase, that in turn, results a cooler plate. Thus, the cooler the plate the lower the heat losses from the plate to the surroundings would be. In order to increase the collector's efficiency factor, augmentation of the heat transfer coefficient from the collector tubes' wall into the water, according to Equation 2.35, can be an option. The enhancement of heat transfer rate in the solar collectors could have a significant impact on the overall performance of the solar water heating systems.

Enhancement of heat transfer rate of the forced convection between the pipe wall and flow has been studied and widely employed in the double pipe or shell-and-tube heat exchangers, boilers, and gas turbines by means of different techniques. Passive techniques such as extending or coating the heat transfer surfaces, using various devices to swirl or augment the flow, adding projections in the inner surface of the pipe to increase the roughness, inserting helical ridges and/or grooves into the inner surface of pipe, or twisting the pipe itself have been very successful techniques. In situations where manufacturing and maintenance difficulties as well as cost are important concerns,

installing flow augmentation devices (i.e. turbulators) are preferred rather than finned or modified surfaces.

Most of the passive methods are used to increase heat transfer coefficient ($h_{f,i}$) by disrupting boundary layer, increasing the effective Reynolds number, and increasing the temperature and velocity gradient. Enhancement of heat transfer rate with passive methods, however, is associated with additional frictional and pressure losses due to secondary flows. One of the methods to enhance heat transfer coefficient is by generating the swirling flow inside a pipe. This can be achieved by three methods: (a) by introducing a tangential flow into the pipe through single or multiple entrances pipes at the different angles to the pipe axis, tangential nozzles, and snails; (b) by installing axial or radial guide vanes; or (c) by rotating the tube directly (Gupta et al., 1984). A simple twisted metal strip or a coiled wire (e.g. spring) can generate swirl inside the tube. Tangential entrance or a single vane installed at the pipe inlet results in a decaying swirl flow which in turn reduces the heat transfer and pressure drop with the distance from the pipe entrance. To create a non-decaying swirling flow, turbulators has to be installed at certain intervals within the pipe to generate swirls continuously and to keep heat transfer rate and pressure drop constant along the pipe.

Smithberg and Landis (1964) analytically and experimentally studied heat transfer characteristics, velocity distribution and friction losses of a fully developed turbulent flow inside a pipe with twisted strip turbulators, under isothermal and forced convection condition. The results that were obtained for different twist pitch to pipe diameter showed that velocity profile is helical indicating vortex formation in the core. They also presented equations to predict heat transfer coefficients and friction losses for tube with twisted

strip turbulators. They recommended twisted tapes as inexpensive but effective way to increase Nusselt number in heat exchangers. Thorsen and Landis (1968) experimentally and theoretically studied friction and heat transfer characteristics of air flowing inside a tube with twisted tape turbulator over a variety of pitch-to-diameter ratios and Reynolds numbers. They developed an analytical model that predicts fraction and heat transfer characteristics of a swirl flow more direct and inclusive than Smithberg and Landis' (1964) model. Narezhnyy and Sudarev (1971) studied the effect of a helical bent turburaltor placed only at the pipe inlet, and found that the increase of pressure drop was not as significant as the enhancement of heat transfer rate. Hong and Bergles (1976) experimentally determined the heat transfer coefficient of electrically heated tube with two twisted strips. For a fully developed laminar flow, they found that Nusselt number is a function of the twist ratio, Reynolds number and Prandtl number, and it is nine times larger than that of the tube without turbulators under similar heating conditions. They also initiated that swirl flow increases the fraction factor mostly at large Reynolds numbers. Malsliyah and Nandakumar (1976) obtained heat transfer characteristics of an internally finned tube with forced convection, fully developed laminar flow and uniform heat flux. They found that the Nusselt number is higher than that for the smooth pipe, and is a function of fin length and thickness. They also found that for any fin geometry, there is an optimum fin number for the maximum heat transfer. Junkhan et al. (1985) experimentally studied the effect of different turbulators installed at the tube inlet of a fire tube boiler, and found that the transferred heat to the water is increased considerably. Yildiz et al. (1998) studied the effect of a twisted strip profile that used as the turbulator inside a concentric double-pipe heat exchanger where hot air passed inside and cold

water passed outside the tube. They found 100% increase in the Nusselt number due to this modification. They stated that the rate of heat transfer can be increased further by increasing pitch number of the twists, and also that the pressure drop due to this turbulator, is relatively high but negligible compared to enhancement of the heat transfer rate. Dumuş et al. (2002) used a snail at the inlet of the inner pipe of a concentric double pipe heat exchanger to generate swirling flow. The effect of snail on the heat transfer rate and pressure drop was studied. They found that the Nusselt number was increased from 85% to 200% in a counter flow exchanger with 15^{o} to 75^{o} swirling angles, respectively. Promvonge and Eiamsa-ard (2006) studied the impact of a snail at the tube inlet as swirl flow generator, and conical nozzles with different pitch (distance between nozzles) arrangements inside the pipe as reverse flow generators. They found that application of snail and conical nozzles increased heat transfer rate by 278% and 206% respectively. The combined effect of both snail and nozzles were about to 316% increase in the heat transfer rate. They, however, observed very high pressure drops and found that the Nusselt number increases as pitch number decreases and Reynolds number increases. Naphon et al. (2006) applied mechanically helical ribs with different heights and pitches on the outer surface of a copper tube and studied the effect of these ribs on the heat transfer rate in a double pipe heat exchanger with hot and cold water flows. They observed significant increase in heat transfer rate and pressure drop in the presence of ribs.

In all of the above mentioned studies, the test pipe was subjected to a uniform heat flux or constant wall temperature boundary condition that was attained by means of electrical heater, wrapped around the pipe, or hot water flowing around the tube.

Moreover the geometry of the tested sections was basically an individual straight pipe. The flat-plate collectors, on the other hand, have pipe-and-fin geometry. That is, the flat-plate fins are externally attached to the pipes. Moreover, the heat transfer mode to the collector is mainly radiation and partly convection. Because of this particular geometry and the modes of heat transfer neither the heat flux nor the wall temperature are uniform over the entire geometry. Therefore, the results from these previous studies cannot be applied directly to the solar collectors. Furthermore, in solar collectors, the solar irradiance that warms water is limited or low. Therefore, in order to warm water from inlet to desired outlet temperature, flow rates needs to be kept very small. These flow rates are typically much less than the range of flow rates studied in those previous studies.

In solar collectors, high temperature gradient throughout the pipe results in a large variation of density. Low flow velocities, which make flow properties strongly depend on the temperature gradient, along with influence of gravitational forces causes the generation of the free convection inside the tubes that combines with existing forced convection. Thus, the convection inside the collector tubes is of mixed type.

When a horizontal tube walls is heated uniformly or kept at constant temperature, the water adjacent to the side walls is warmer, and consequently lighter, than the bulk fluid in the core of the pipe. Buoyancy forces moves water upwards and by continuity the fluid at the center downwards. Combination of these two cross sectional currents (secondary flow) with that of axial forced flow creates two spiral vortices that are moving forward along the pipe (in helical pattern). As a result of this combined convection (free and forced) the heat transfer coefficient values becomes relatively higher than those of

theoretical values restricted to the constant property fluids. The velocity profile is also highly affected by this secondary flow. However, when a solar collector is heated by radiation, the flow pattern is much more complicated than that of a uniformly heated individual pipe since upper surface of the tube is also subjected to the direct radiation and it is warmer than the lower surfaces. This maintains a stable light fluid always at the top of the pipe which could hardly mix with the colder core fluid. Thus the secondary flows runs at the lower sections of the tube.

Combined laminar free and forced convection in horizontal straight tubes have been extensively studied. Ede (1961) experimentally recorded new values of local heat transfer coefficient over a variety of Reynolds numbers, pipe diameters and fluid typs. He compared his results with the conventional correlations. He found that his recorded data are far higher than those values predicted by basic theory due to effect of free convection. Faris and Viskanta (1969) conducted an analytical study to estimate the average Nusselt number for a range of Grashof and Prandtl numbers for and compared the results with those of available experimental data. Bergles and Simonds (1971) performed an experimental study and combined their data with other existing values and correlations to substantiate the effected of free convection on the Nusselt number. They found that with a reasonable heating rate, the heat transfer coefficient can be improved by 3-4 times than those of predicted by constant property formulas. Newell and Bergles (1970) performed an analytical study to analysis the effect of free convection on horizontal pipe with uniform heat flux and presented the correlations for heat transfer and pressure drop pipe wall temperature differences between top and bottom. Morcos and Bergles (1975) experimentally studied the effect of property variation on heat transfer and pressure drop

for laminar flow in horizontal pipe. They found that Nusselt number is mainly depends on Rayleigh number, Prandtl number and dimensionless tube wall paramters. They also presented correlations for Nusselt number and friction factor. Similar studies concerning the combined free and forced convection in horizontal heated pipes were conducted by Mori and Futagami (1967), Siegwarth et al. (1969), Shannon and Depew (1968), and McComas and Eckert (1966). Among which, only very few works such as Iqbal (1966) and Barozzi et al. (1985) are found that concerned the mixed convection effects in solar collector geometry where in both case the models were heated by electrical wires.

Several passive heat transfer heat transfer enhancement techniques have been reported in the literature and discussed previously for straight tubes, which have shown to increase the heat transfer rate. However, as mentioned earlier due to the dissimilar geometry, boundary condition and convection modes, the results from these studies cannot be directly applied for solar collectors. Therefore, the present study is aimed at conducting a detailed experimental investigation of different passive heat transfer enhancement techniques in flat-plate solar collectors.

4.2. EXPERIMENTAL SETUP AND PROCEDURE

The experimental facility is depicted schematically in Figure 4-1. The main Features of this system are:

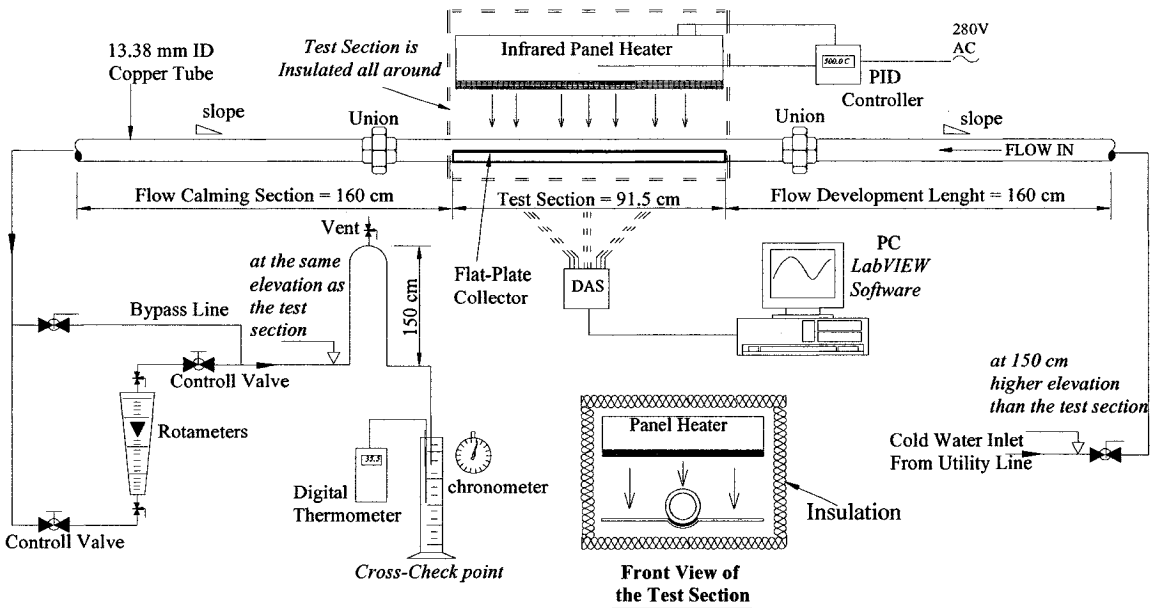

Figure 4-1: Schematic of the Experimental Setup

- *A single-tube flat-plate solar collector*: Tested model is a flat-plate collector with 0.145 (m^2) of area. Solar collector is made of 1.1 (mm) thick copper plate and 13.38 (mm) ID type M copper tube (see Figure 4-2). Tested section of the collector is 915 (mm) long. Tube was soldered to the plate by lead and entire collector was painted with high temperature black matt color.
- *A panel heater*: To supply thermal energy to the test section by means of radiation a high temperature infrared panel heater (Omega QF-063610-T) is used. The heater is as same dimensions as the collector (i.e. 915×152 mm) and was installed above and parallel to the collector. The distance from the face of collector to the face of heater was set equal to 50 (mm). The heater has the maximum density of 15500 (W/m^2)

with output wavelength between 2.5 to 6 microns. It is 2160 Watt, 240 Volt and its face is black quartz-ceramic cloth.

- *PID controller*: To keep the heater at constant temperature an autotune PID temperature controller (Micro Omega CN77000) is used. Input temperature to the controller was taken from the center of heater, using a K type *Chromega-Alomega* thermocouple with ±0.4°C accuracy. Controller has the accuracy of the ±0.5°C.
- *Data acquisition system*: To collect the plate, tube, ambient, and water outlet and inlet temperatures a National Instrument (N1 SCX1-1000) data acquisition system with a 16 channel card (PCI-6063-E) is used. System was hooked to a PC using *LabWIEW 7Express* software. Sample reading rate was 100 Hz.
- *Entrance and Exit Length*: To ensure that the flow is fully developed before entering into the test section and it is also calm while leaving the test section two 13.38 (mm) ID straight copper pipes, 1600 (mm) long, are installed on both sides of the test section.
- *Rotameters*: Two Rotameters, one in range of 4.5 to 577 (ml/min) (Omega FL-1448-G) and other (Omega FL-1502-A) in range of 548 to 5488 (ml/min) were installed in parallel to adjust and measure water flow rates. Since the flow rates were very small, it was experienced that installing the rotameters in the outlet of the test section minimized the fluctuation of the flow rate, from the set point, and eliminated the air bubbles. Control valves were installed before and after the flow meters to facilitate accurate flow control and complete filling of the test section.
- *Thermal insulation*: Thermal insulation (Reflectix R-4) with radiation reflective surfaces were used to insulate the test section (as shown in Fig. 4-1) to reduces

thermal and radiative losses. It was to ensure that the most part of the radiative energy, emitted from the heater, is absorbed by the collector.

- A digital thermometer a chronometer, and a measuring cylinder is used to cross check the flow rate and outlet temperature of the water. This was to make sure that data reading from the rotameters and outlet thermocouple is accurate.
- *Thermocouples*: Thermocouples used to measure water, plate and pipe wall temperatures were type T copper-constantan with the accuracy of ±0.1°C. The thermocouples were simultaneously calibrated before starting the test. In addition, every day before warming up the system, thermocouples were simultaneously examined with ambient air temperature and cold water run.
- *Heat Flux Sensor*: To measure amount of the radiation, received on the plate's surface two thin film heat flux sensors (Omega HFS-4) were used according to Omega's procedures; however, despite of the manufacture's claim, these sensor were not able to measure radiation accurately. Therefore, the values obtained from these sensors are not presented in here. Using these sensors, for this purpose, is not recommended.

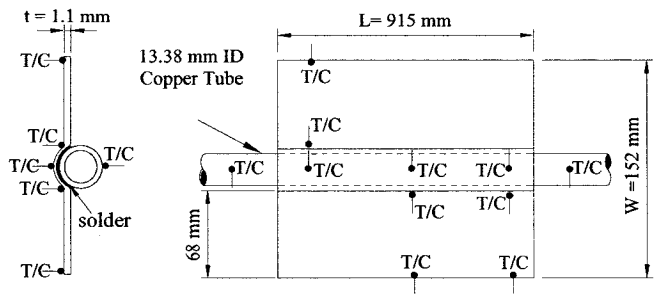

T/C : Thermocouple

(Location of the thermo-couples is identical for all of the other models)

Figure 4-2: Solar Collector Basic Model and Location of the Thermocouples

To investigate the effect of passive heat transfer augmentation methods in solar water heating application, four models were designed and fabricated for this purpose, that are:

- *Model # 1*: It is the basic model which is being used in all of the conventional solar water heating system with flat-plate collector. It consists of a circular copper tube (13.38 mm ID) and a copper plate (fin) connected to the plate as shown in Figure 4-3. This model is used to obtain reference data.
- *Model # 2*: In this model a twisted strip was inserted inside the collector's tube to induce swirl flow inside the tube. The twisted strip was made of 1 (mm) thick copper plate, and in such a way that fits inner diameter of the tube. Two length of the twisted strips were considered. One short (25% of the test section's length) and the other full length. The detailed sketch of the model is shown in Fig. 4-3.
- *Model # 3*: In this model a coli-spring wire made of copper was inserted inside the collector's tube to introduce a helical surface roughness (elements). This was to induce turbulence and swirl flow inside the tubes. Both short and full length coil have been tested. The detailed sketch of the model is shown in Fig. 4-3.
- *Model # 4*: In this model conical shape ridges (diverging nozzles) made of brass were installed every 152 (mm) to generate longitudinal vortices inside the tube. The detailed sketch of the model is shown in Fig. 4-3.

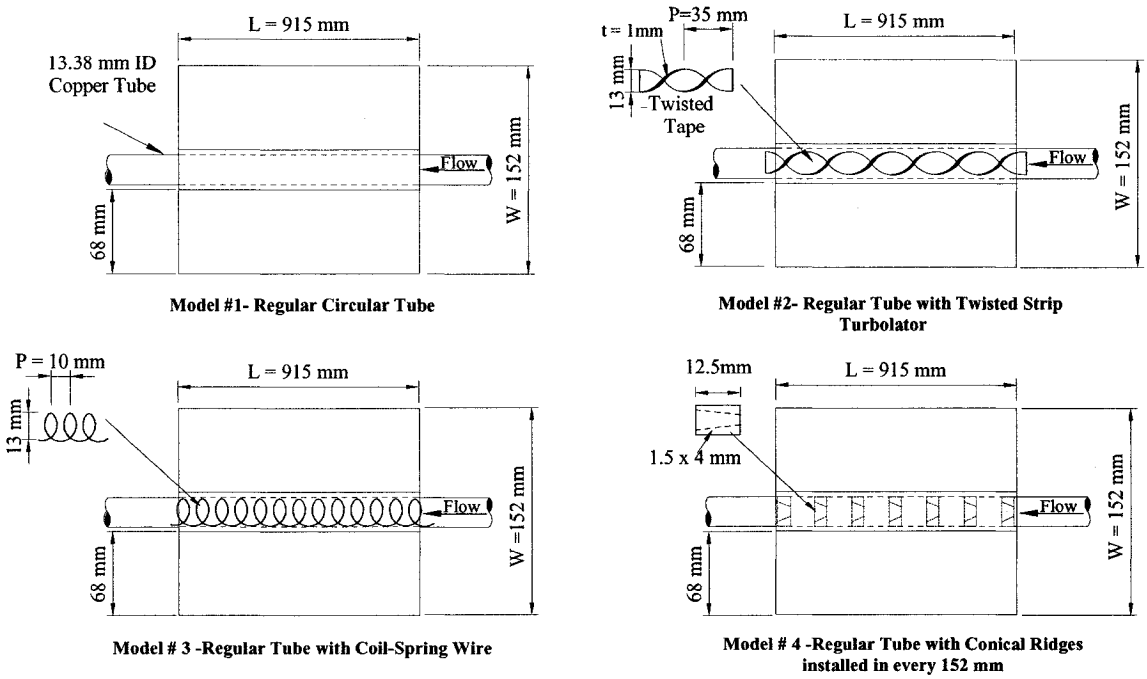

Figure 4-3: Solar Collector Models, Base and with Different Heat Enhancement Devices

4.2.1. The Experimental Conditions

Each model was tested for two different heater's surface set temperatures, 400°C and 300°C. It was estimated that in these heater set temperatures and with 50 (mm) gap between model and heater, the average absorber plate temperature is comparable with those of obtained from the sun. Considering actual operating condition, City water supplied through utility line was used as the working fluid. The temperature of the city water at inlet to the test section was varied from test to test. Water was pressurized by building's booster pumps. Using an open water circuit each model was tested over a wide range of flow rates, which were 0.14, 0.21, 0.29, 0.37, 0.47, 0.55, 0.57, 1.1, 2.2, 3.3, and 4.4 (lit/min). For each run, inlet and outlet temperature of water was measured by thermocouples which were directly inserted inside the tube. Plate temperature at six location (tip and base of the plate at the center and 50 mm from the both sides of the plate), and tube wall temperature at different axial locations (in the top and bottom of the

pipe wall) were measured using thermocouples attached directly to the surfaces, as shown in Fig.4-2. Every day before starting the tests, system was run with maximum flow to discharge the air from inside the system. System was also installed with slight slop towards the inlet point to facilitate air removal from the system. Moreover, to ensure that the test section along with entrance and exit pipe length is completely fill with water all the time during the tests and to trap air bubbles (which is unavoidable in an open circuits) somewhere else than the test section, the entire system were located at an elevation 1500 (mm) lower than the water supply line and discharge point of the system (see Fig. 4-1). For each experimental run, after setting flow rate and heater set temperature, the data acquisition was started 15 minutes after keeping system at that condition to ensure steady condition (equilibrium) was obtained. Then, the data was acquired for 10 minutes at sampling rate of 100 Hz. Each run was repeated twice at the different times to ensure repeatability of every experiment.

A large number of tests were conducted to optimize the experimental setup. For instance test section with or without the insulation, test section with or without extra straight pipes for flow development, and flow meters before and after the test section. It was found that test section with insulation, developed flow, and with flow meters located at the exit of the test section, yields to steadier conditions and consistency in obtained data.

4.3. DATA REDUCTION

The average inlet and outlet water temperatures as well as average plate and tube surface temperatures were obtained by time-averaging in 10 minutes of data for each test.

All properties of the water are calculated in bulk water bulk temperature where $T_{f,avg}$ computed as:

$$T_{f,avg} = \frac{T_{f,out} + T_{f,in}}{2} \tag{4.1}$$

The average pipe wall, plate tip, and plate base temperatures were obtained by averaging temperatures at three axial locations for each one. Moreover, as mentioned earlier, each run was repeated twice and the average values based on both repeated runs for each case are presented hereinafter. The average heat transfer rate (i.e. energy input) per unit length of the tested models was calculated based on the overall enthalpy increase of the water inside the tube, following Barozzi et al. (1985) as:

$$q_l = \dot{m} c_p (T_{f,out} - T_{f,in}) / L \tag{4.2}$$

Therefore, average wall heat flux was approximated as:

$$q_W = q_l / \pi D \tag{4.3}$$

Since the inlet water temperature varied from test to test, all temperature readings were normalized (dimensionless form) to supersede the effect of inlet water temperature, following Habib and Negm (2001) and Chou and Lien (1991) as:

$$\theta = \frac{T - T_{in}}{q_l / (\pi k_f)} \tag{4.4}$$

It was found that the absolute values of outlet, plate, and tube temperatures are function of the inlet water temperature; however, the amount of increase of the water temperature (ΔT) is a weak function of the inlet water temperature and difference between outlet and inlet temperature, for a certain flow rate and heater set temperature, was almost the same for different inlet temperatures. From the averaged pipe wall, plate tip and plate base temperatures, the average non-dimensional temperatures were computed using above equation as $\theta_{Avg\text{-}Pipe}$, $\theta_{Avg\text{-}Tip}$, $\theta_{Avg\text{-}Base}$, and $\Delta\theta_{water}$.

Radiation, exchanged between the collector and heater is estimated by:

$$q_{rad} = A_c \sigma F_{ph-c} (T_{ph}{}^4 - T_c^4)(\frac{1}{\varepsilon_{ph}} + \frac{1}{\varepsilon_c} - 1)^{-1} \quad (4.5)$$

where $F_{ph\text{-}c}$ is the shape factor between the absorber plate and panel heater, A_c is the collector's area, T_{ph} and T_c, and ε_{ph}, and ε_c are the panel heater and absorber's surface temperatures and emissivities, respectively. Values of local and mean Nusselt number are calculated using below equations following Barozzi et al. (1985) and Piva et al. (1995)

as: $$Nu_x = q_W D/(T_W - T_{f,b})k_f \quad (4.6)$$

and $$Nu_m = (1/x)\int_0^x Nu_x dx \quad (4.7)$$

where $T_{f,b}$ is local bulk fluid temperature and is calculated as below:

$$T_{f,b} = T_{f,in} + (q_l \cdot x)/(\dot{m} c_p) \quad (4.8)$$

The dimensionless parameters used in this study are computed as:

Reynolds number: $$Re = UD/\nu \quad (4.9)$$

Grashof number: $$Gr = g\beta D^3 (T_W - T_{f,b}) / \nu^2 \quad (4.10)$$

Prandtl number: $$Pr = \nu/\alpha \quad (4.11)$$

Rayleigh number: $$Ra = Gr.Pr \quad (4.12)$$

Richardson number: $$Ri = Gr/Re^2 \quad (4.13)$$

Incropera et al.(2007). Following Morcos and Bergles (1975) and Barozzi et al. (1985) the modified form of Grashof number, based on the supplied heat flux is:

$$Gr_q = g\beta D^4 q_W /(\nu^2 k_f) \quad (4.14)$$

therefore modified Rayleigh and modified gradient Richardson numbers can be written as: $$Ra_q = Gr_q.Pr \ , \ Ri_q = Gr_q/Re^2 \quad (4.15)$$

Following Bonnefoi et al. (2004), the flux Richardson number in terms of supplied heat flux, in axial direction (i.e. flow direction) is computed as:

$$Ri = g\beta\Delta T_{water} \times L/U^2 \tag{4.16}$$

4.4. RESULTS AND DISCUSSION

Figures 4-4 and 4-5 shows the actual temperature rise of the water ($\Delta T_{water} = T_{f,out} - T_{f,in}$) versus Reynolds number for all models, and for both heater set temperature of 400 and 300 (°C), respectively. In both cases, it can be seen that as Reynolds number increases, ΔT_{wate} decreases. As shown in Figure 4-4, for flow rates around 0.1 to 0.2 (lit/min), which is close to the optimum flow rate for flat-plate collector (see Chapter 3), absolute temperature rise (ΔT) of 50 to 55 (°C), from the inlet water temperature, was achieved when the heater was set at 400 (°C). These values are consistence with the actual values that can be achieved with this type of collectors in summer. These results also indicate that ΔT is identical for all of the models, in each flow rate and heater set temperature.

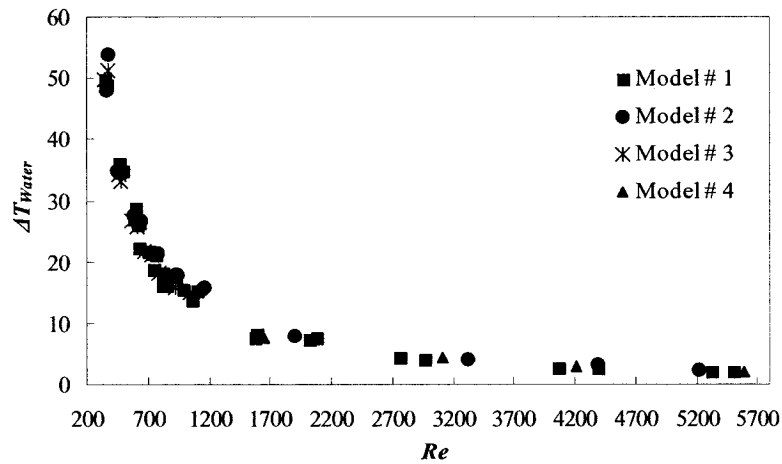

Figure 4-4: Temperature Rise of the Water (°C) versus Reynolds Number for Heater Set Temperature of 400°C- All Models

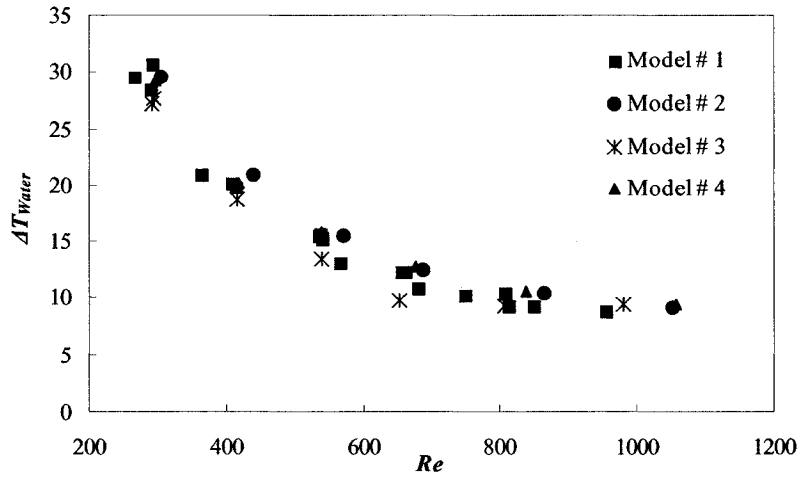

Figure 4-5: Temperature Rise of the Water (°C) versus Reynolds Number for Heater Set Temperature of 300°C- All Models

In Figures 4-6 and 4-7, variation of dimensionless forms of the temperature rise is presented versus Reynolds number. In these figures the effect of inlet water temperature is eliminated using dimensionless forms of the ΔT. However, it can be seen that dimensionless temperature rise, $\Delta\theta_{water}$, follows the same trend as Figures 4-4 and 4-5. From repeating the tests with different inlet water temperatures it was also found that the absolute and dimensionless temperature rise of the water is only function of the flow rate and supplied energy but it is independent of the inlet water temperature.

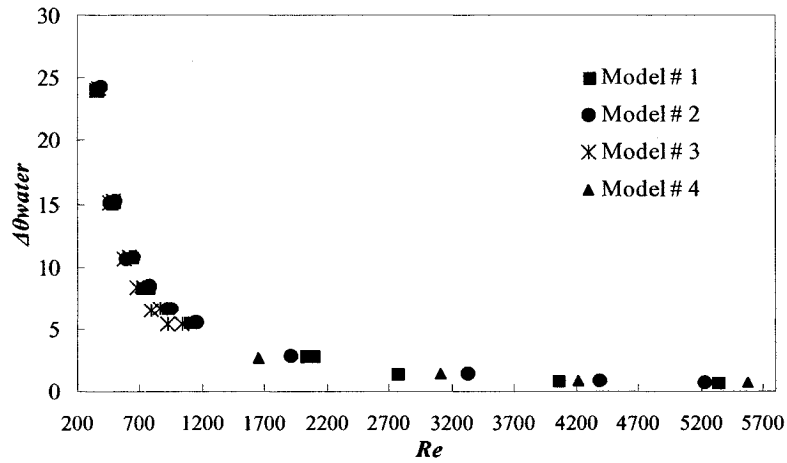

Figure 4-6: Dimensionless Temperature Rise of the Water (°C) versus Reynolds Number for Heater Set Temperature of 400 °C- All Models

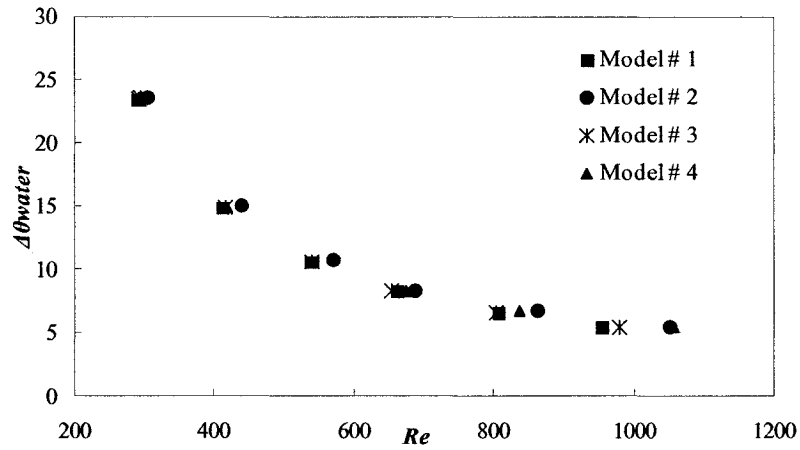

Figure 4-7: Dimensionless Temperature Rise of the Water (°C) versus Reynolds Number for Heater Set Temperature of 300 °C- All Models

In Figures 4-8 and 4-9 the variation of the dimensionless plate base temperatures at 400 and 300 (°C) heater set temperatures versus Reynolds number (i.e. flow rates) are presented, respectively. Figures 4-10 and 4-11 shows the variation of the dimensionless plate tip temperatures at 400 and 300 (°C) heater set temperatures versus Reynolds number, respectively. These results indicates that the average base and tip temperatures of the absorber plate decreases as Reynolds number increases, that is, the removed heat from the system increases as the flow rate increases according to equation 4.2. The results also shows that the average base and tip temperatures are similar for all of the models, in each flow rates, and the variation of the temperatures follows identical trend for all models. Contrarily to our expectations, it can be seen that the application of these passive methods has insignificant effect on the enhancement of the heat transfer, for both heater set temperatures (i.e. supplied heat fluxes) and in the range of studied flow rates. For Model # 3 a slight degradation of the heat transfer can be found since plate tip and base temperature are somehow higher than those for Model # 1.

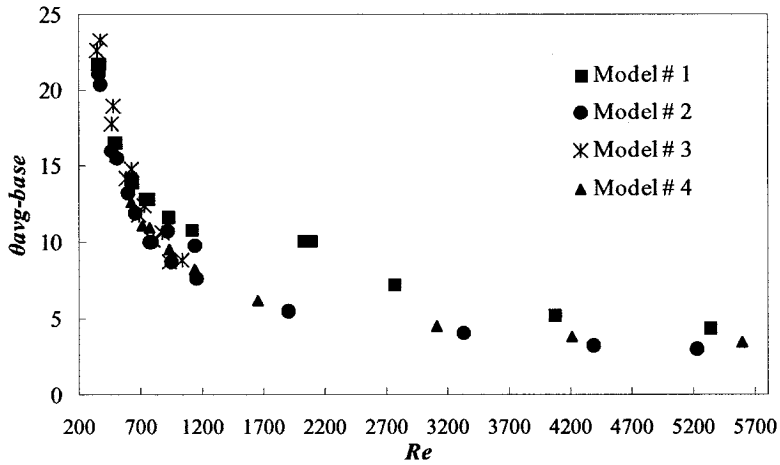

Figure 4-8: Dimensionless Average Plate Base Temperature (°C) versus Reynolds Number for Heater Set Temperature of 400 °C- All Models

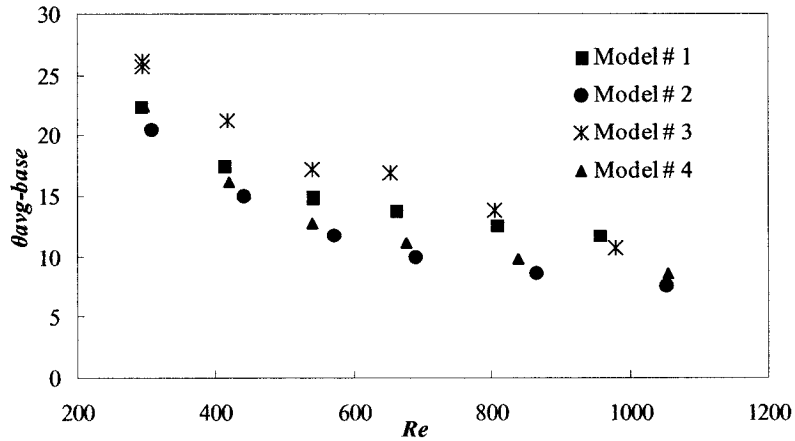

Figure 4-9: Dimensionless Average Plate Base Temperature (°C) versus Reynolds Number for Heater Set Temperature of 300 °C- All Models

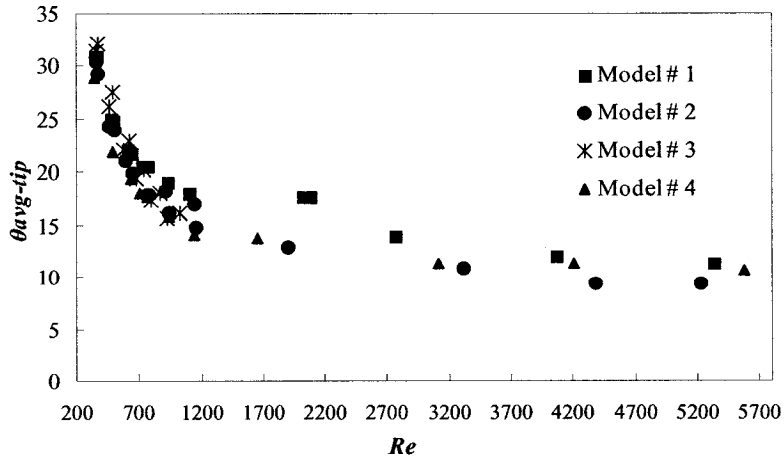

Figure 4-10: Dimensionless Average Plate Tip Temperature (°C) versus Reynolds Number for Heater Set Temperature of 400 °C- All Models

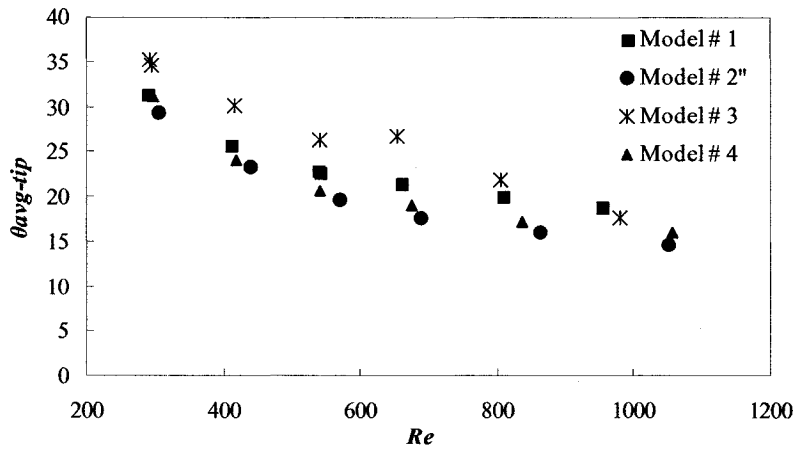

Figure 4-11: Dimensionless Average Plate Tip Temperature (°C) versus Reynolds Number for Heater Set Temperature of 300 °C- All Models

Figures 4-12 and 4-13 present the average wall heat fluxes (q_W) versus Reynolds number for all models, and for heater set temperature of 400 and 300 (°C). Although the heater surface temperature was kept at constant values, however, the results shows increase of the average wall heat flux with Reynolds number. This is because as the Reynolds number increased, the average plate temperature decreased (see Figures 4-8, 9, 10, and 11) resulting higher exchange of radiation between the plate and the heater surfaces' according to Equation 4.5.

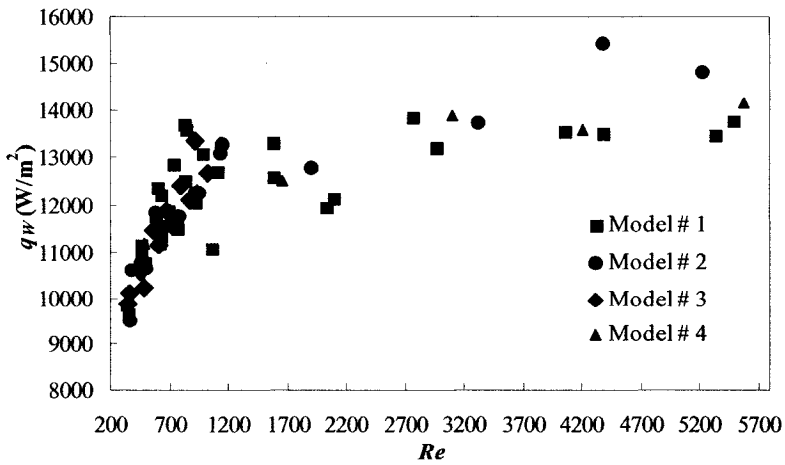

Figure 4-12: Average Wall Heat Flux (W/m^2) versus Reynolds Number for Heater Set Temperature of 400 °C- All Models

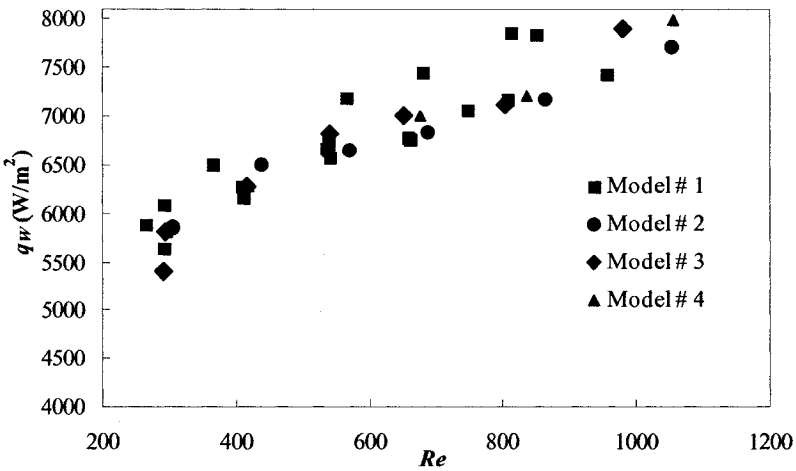

Figure 4-13: Average Wall Heat Flux (W/m^2) versus Reynolds Number for Heater Set Temperature of 300 °C- All Models

To make side-by-side comparison, Figure 4-14 and 4-15 present variation of the normalized water temperature rise, average plate base, average plat tip and average pipe wall temperatures of the basic model, in dimensionless forms, for heater set temperature of 400 and 300 (°C), respectively. It is obvious that by decreasing Reynolds number (i.e. flow rate) all values increases. From the figures it can be found that average plate base temperatures and average pipe wall temperatures are almost equal for any flow rate. In the studied range the instantaneous collector efficiencies are estimated to be around 43-50% using Equation (4.2) divided to Equation (4.5) times L.

The results showed that the average values of the absolute and dimensionless temperature increase of water, and dimensionless plate base and tip temperatures are almost identical for all of the models. Therefore, to investigation the heat transfer behavior of this system, hereinafter, the basic model (i.e. Model # 1) is set for further investigation and measurements. It can be expected that the values of the dimensionless parameters (*Nu, Gr, Ra, Ri*) for the basic model can be generalized for the modified geometry models, for each flow rate and each heater set temperature.

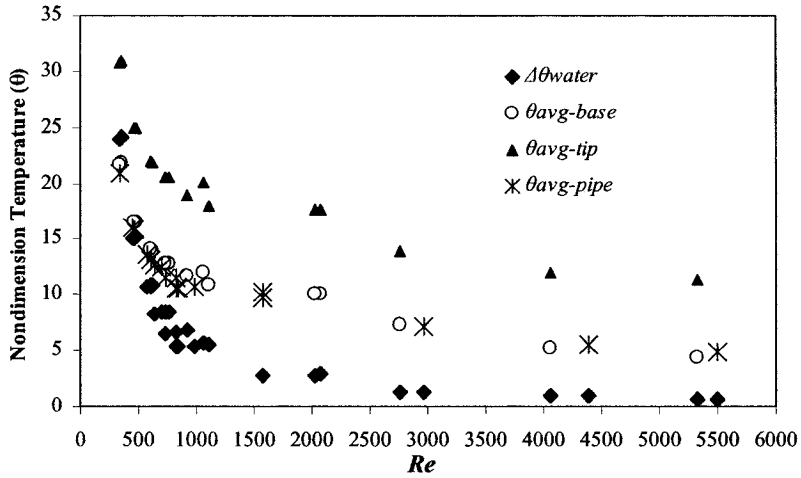

Figure 4-14: Dimensionless Water Temperature Rise, Average Pipe Wall, Plate Tip, and Plate Base Temperatures (°C) versus Reynolds Number for Heater Set Temperature of 400 °C- Basic Models

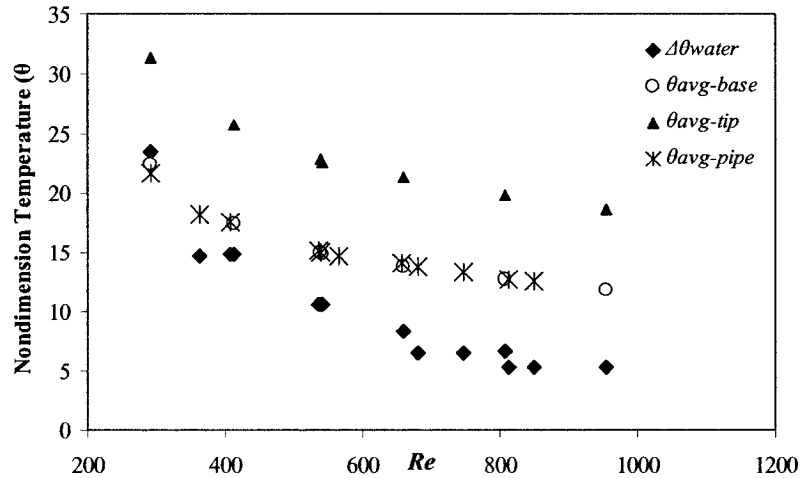

Figure 4-15: Dimensionless Water Temperature Rise, Average Pipe Wall, Plate Tip, and Plate Base Temperatures (°C) versus Reynolds Number for Heater Set Temperature of 300 °C- Basic Models

To analyze the nature of the heat transfer phenomenon in our experimental setup that deals with combined free and forced convection inside the tube, first parameter that is considered is Grashof number. Grashof number presents the ratio of the buoyancy forces to viscous forces. Grashof number is a measure of intensity of natural convection and has a similar rule as Reynolds number in forced convection. The combined effect of the free and forced convection appears, generally, when $Gr/Re^2 \approx 1$. When $Gr/Re^2 >> 1$ the effect of free convection is dominant and Nusselt number–the dimensionless convection

heat transfer measure at the surface– is only function of *Gr* and *Pr* numbers; whereas, for $Gr/Re^2 \ll 1$ forced convection is dominant and Nusselt number is only function of *Re* and *Pr* numbers (Incropera, 2007). Figure 4-16 and 4-17 presents the variation of the Grashof (*Gr*), which is based on temperature difference between pipe wall and bulk flow, and modified Grashof (Gr_q) numbers, which is based on supplied heat flux, with Reynolds number for heater set temperatures of 400 and 300 (°C), respectively.

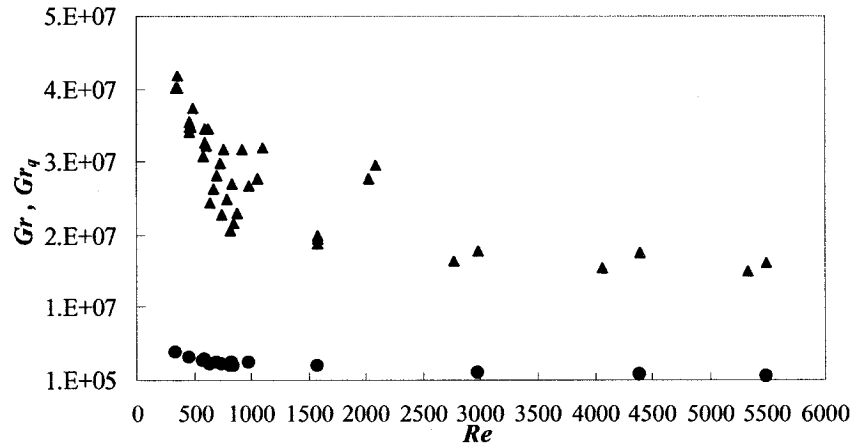

Figure 4-16: Variation of Grashof (•) and Modified Grashof (▲) Numbers versus Reynolds Number for Heater Set Temperature of 400 °C

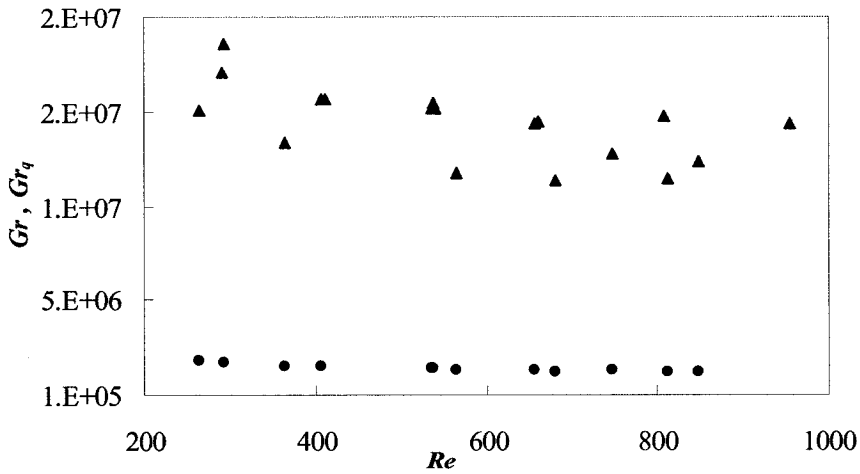

Figure 4-17: Variation of Grashof (•) and Modified Grashof (▲) Numbers versus Reynolds Number for Heater Set Temperature of 300 °C

From the figures it can been seen that for any Reynolds number, modified Grashof number and Grashof numbers are in range of 10^7 and 10^5, respectively. The values of the

Grashof number increases as Reynolds number decreases. Comparing Grashof number with their pertinent Reynolds numbers shows that for any cases, even high Reynolds number, always Gr and $Gr_q >> Re^2$ which indicates that in our studied range free convection is dominant (White, 1991). Domination of the free convection is stronger for lower Reynolds numbers, as expected.

In density stratified flows, gravity forces that manifest themselves in buoyancy force forms are very important. Richardson number (gradient Richardson number) is another parameter that determines the domination of the free convection effects relative to the forced convection. Gradient Richardson number is related to the ratio of buoyancy to inertial forces and can be expressed as:

$$Ri = -g\frac{d\rho_0 / dz}{\rho_o (dU/dz)^2} = g\beta\frac{dT/dz}{(dU/dz)^2} \tag{4.17}$$

Critical value of the gradient Richardson number, above which shear flows are linearly stable, is 0.25; however, when $Ri>>1$ the stratification is much more stronger than fluid motion (i.e. sheer forces are ineffective) (Majda and Shefter, 1998). Alternatively, flux Richardson number (Ri_f), which is related to gradient Richardson number, is defined as the rate of removal of energy by buoyancy forces to energy production by shear forces (Turner 1973). The critical value of the Ri_f is same 0.25. For $Ri_f > 1$ buoyancy removes energy from the fluid at much higher rate than its production by shear forces. As a result turbulence suppresses. Therefore when Richardson numbers (whether flux or gradient Richardson number) is above unity, shear forces are ineffective and heat transfer is almost entirely due to free convection. Figures 4-18 and 4-19 shows the variation of the modified gradient Richardson number (Ri_q) and flux Richardson number in axial

coordinate (*Ri*) versus Reynolds number, respectively for heater set temperature values of 400 and 300 (°C), respectively.

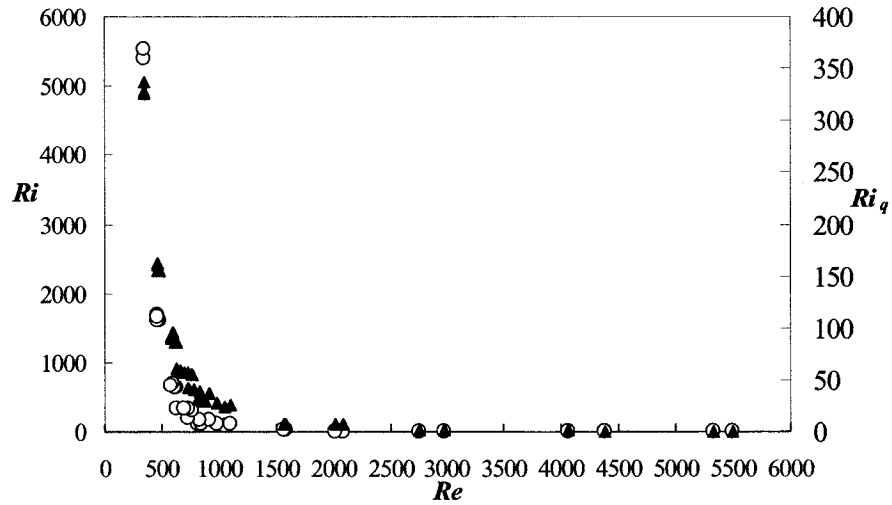

Figure 4-18: Variation of Flux Richardson (○) and Modified Gradient Richardson (▲) Numbers versus Reynolds Number for Heater Set Temperature of 400 °C

Results show that for both heater set temperature cases, and for any Reynolds numbers with in the range studied here, the Richardson numbers are above the critical value of 0.25, indicating that at the condition studied in the present study, the flows were linearly stable. For lower flow rates, Richardson numbers (as large as 5500 for *Ri* and 340 for Ri_q) is significantly larger than unity indicating the intensity of the buoyancy forces and stability of shear forces or, in other word, indicating that the forced convection is negligible and the heat transfer is due to free convection. The minimum values of *Ri* and Ri_q are above 0.5. Therefore introducing turbulence by means of shear production will be unsuccessful and it will be easily damped by buoyancy forces. Increase in stability for stratified flows reduces the turbulent intensity. That is why none of the passive methods applied in this study, that are based on shear production caused any heat transfer augmentation.

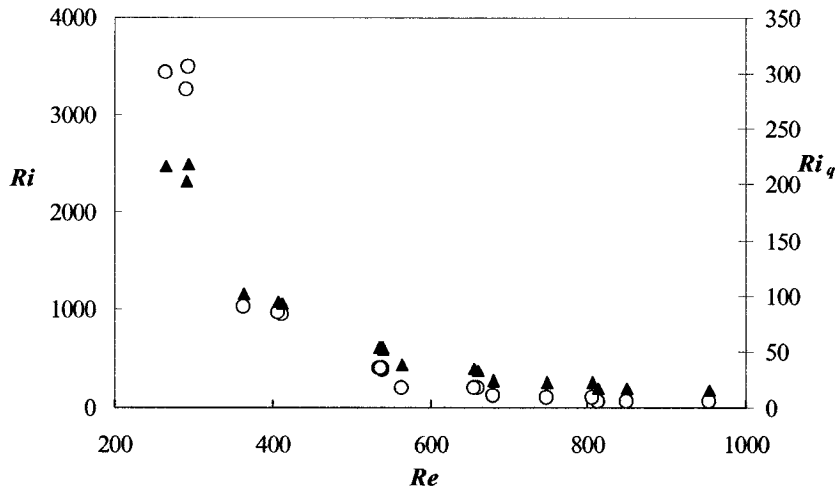

Figure 4-19: Variation of Flux Richardson (○) and Modified Gradient Richardson (▲) Numbers versus Reynolds Number for Heater Set Temperature of 300 °C

Values of the Richardson and modified Richardson numbers for both heater set temperatures of 400 and 300 (°C), and for the Reynolds numbers in laminar range are presented in logarithmic scale in Figure 4-20.

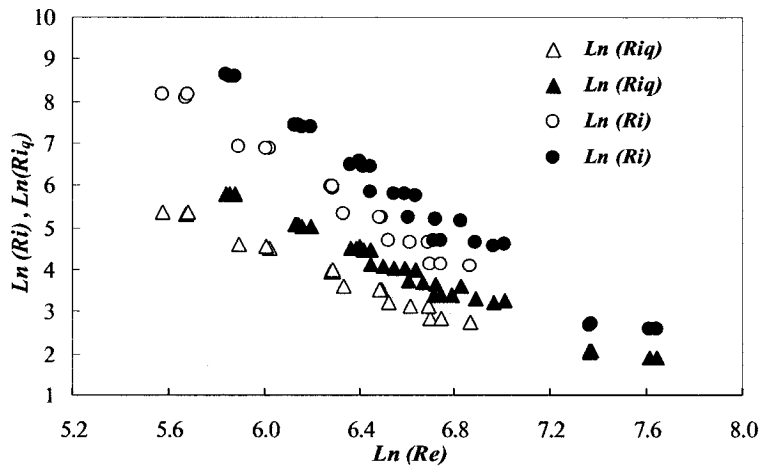

Figure 4-20: Variation of Flux (Ri) and Modified Gradient (Ri_q) Richardson Numbers versus Reynolds Number in Logarithmic Scale for Heater Set Temperature of 400 °C (▲,•) and 300 °C (Δ , o)

Another important parameter which is a measure of generation and perturbation of free convection, or transition form laminar to turbulent flow in free convection boundary layer, is the Rayleigh number (*Ra*). Rayleigh number is a measure of relative amount of the viscous and buoyant forces. The onset of free convection occurs at Ra_c

=1708, which is considered as the critical Rayleigh number. Beyond this critical value the flow becomes unstable and for $Ra > 10^5$ transition to turbulence begins. Beyond $Ra > 10^6$–10^7 the flow becomes fully turbulent (Busse, 1978). The structure of this turbulence is fundamentally different from that generated by the shear flow. According to Incropera et al. (2007) when $1708 < Ra < 5\times10^4$, fluid motion is composed of regularly spaced roll cells, while for Raleigh numbers above this range, the cells collapse and fluid motion becomes turbulent. Bennefoi et al. (2004) have also indicated the instability of flow and generation of thermo-convective structure (transversal and longitudinal roll) for Rayleigh numbers above 1708, for thermally stratified Poiseuille–Bénard flows. In the present study, as Figure 4-20 and 4-21 shows, values of Rayleigh and modified Rayleigh number are in range of 10^6 to 10^8.

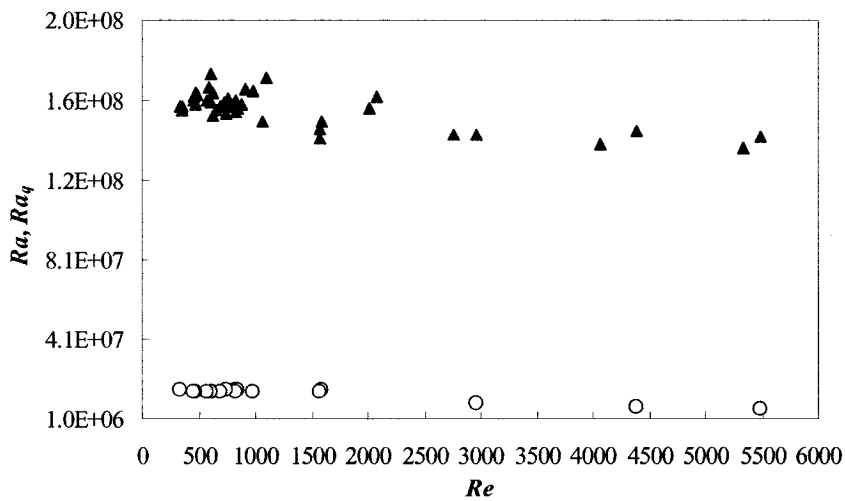

Figure 4-21: Variation of Rayleigh (○) and Modified Rayleigh (▲) Numbers versus Reynolds Number for Heater Set Temperature of 400 °C

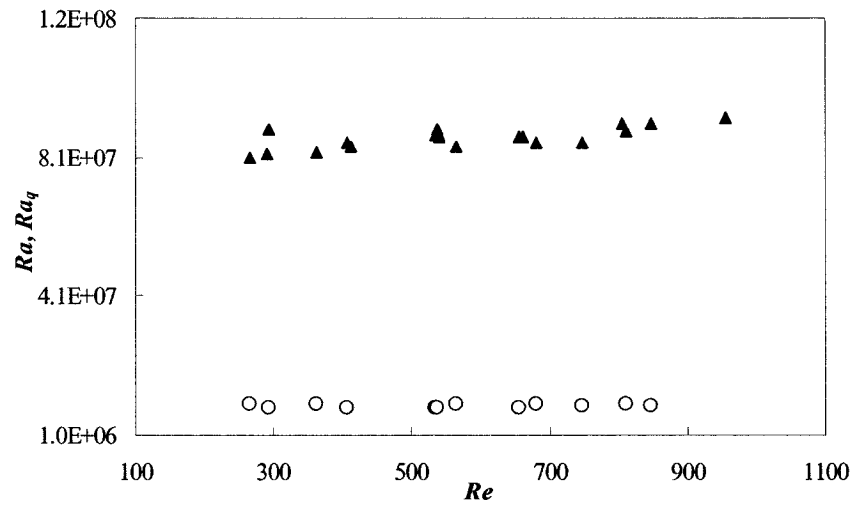

Figure 4-22: Variation of Rayleigh (○) and Modified Rayleigh (▲) Numbers versus Reynolds Number for Heater Set Temperature of 300 °C

Most of the previous experimental studied have used similar geometry (e.g. straight horizontal tube alone) and similar method in imposing thermal energy into the test section (e.g. either heat source surrounded uniformly all around the pipe or tested section heated from below, upward, in case of rectangular ducts). Therefore, good agreements have been reported between their measurements and correlation. In our case, not only heat source, heating direction, and module's geometry were dissimilar to these studies but also the range of *Ra* and *Gr* numbers in the present study are significantly higher than the correlation limits in previous studies. Therefore, it is impossible to validate our data with available correlations. However, in Figures 4-23 and 4-24, values of average Nusselt numbers from the given data are compared with two correlations that are suggested for mixed laminar convection in horizontal pipes with uniform heat fluxes, for heater set temperature of 400 and 300 (°C), respectively. These correlations are Ede (1961) and Siegwarth et al.(1969). Correlation of Ede (1961) for fully developed flow of water in horizontal tube with uniform heat flux is:

$$Nu = 4.36\ (1+ 0.06\ (Ra/Pr)^{0.3}) \tag{4.18}$$

and correlation of Siegwarth et al.(1969) for constant viscosity and infinite Prandtl number is:

$$Nu = 0.471\ (Ra)^{1/4} \tag{4.19}$$

This correlation in modified from is given in Barozzi (1985), which used in Figures 4-18 and 4-19, as:

$$Nu = 0.629\ (Ra_q)^{1/5} \tag{4.20}$$

Two other famous correlations of Morcos and Bergles (1975), that is valid for $3\times10^4 < Ra < 10^6$ and Brown and Thomas (1965) that is valid for $4\times10^4 < Gr < 480\times10^4$ have lower range compared to our *Gr* and *Ra* values.

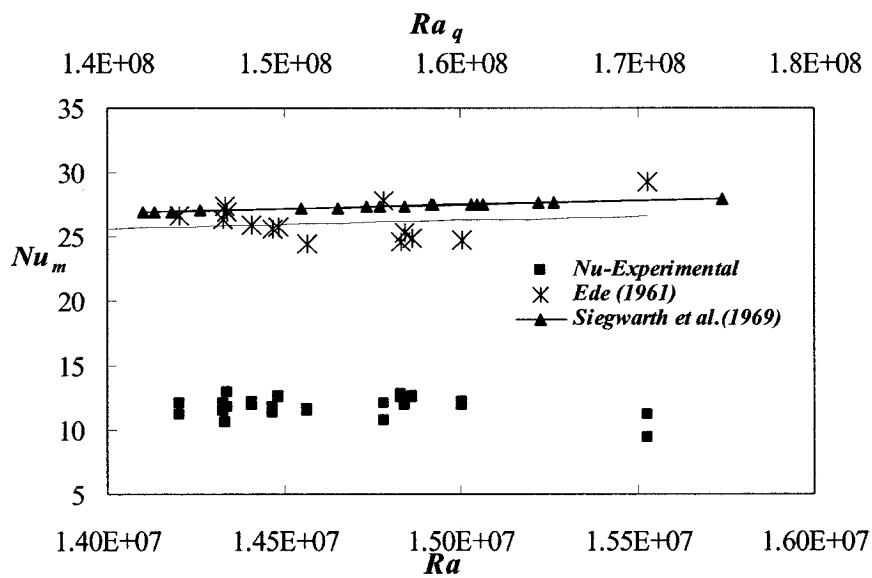

Figure 4-23: Comparison of Average Measured Nusselt Numbers with Ede (1961) and Siegwarth et al. (1969) Correlations for Heater Set Temperature of 400 °C

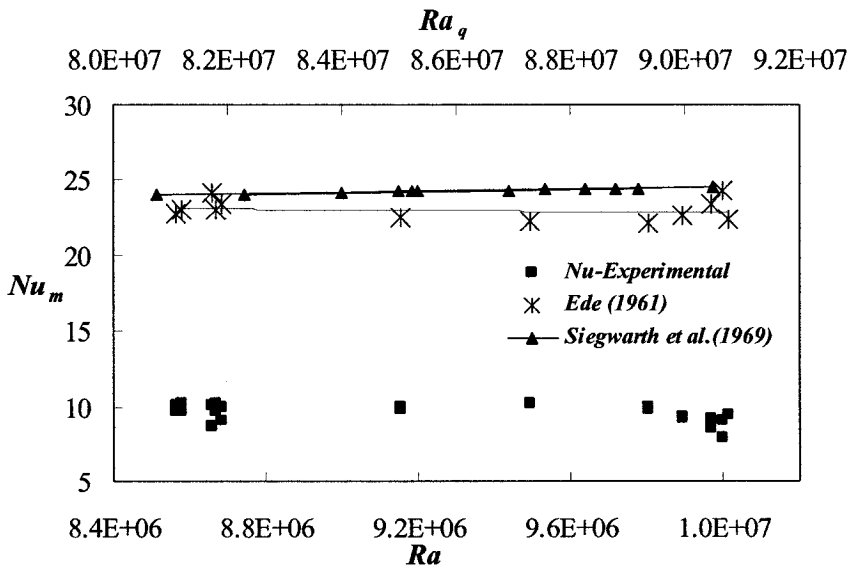

Figure 4-24: Comparison of Average Measured Nusselt Numbers with Ede (1961) and Siegwarth et al. (1969) Correlations for Heater Set Temperature of 300 °C

From Figures 4-22 and 4-23, it can be concluded that the obtained Nusselt numbers are much higher than the theoretical value of the Nusselt number (i.e. 4.36) for horizontal tube with uniform heat flux, where effect of free convection and secondary flow are not taken into account (i.e. $Gr = 0$). Due to combined free and forced convection effects our measured Nusselt numbers are 100 – 135% higher than the theoretical value. Although our measured Nusselt numbers follows the same trend as the correlations of Ede (1961) and Siegwarth et al. (1969); however, there is no good agreement between our measurements and these correlations, which were developed for a simple straight tube geometry that is heated uniformly by electrical wires. In the experimental study of Barozzi et al. (1985) test section was similar to our study (i.e. flat-plate collector); however, heat was imposed to the models by means of electrical elements longitudinally inserted inside the absorber plate to provide uniform heat flux. They reported values of local Nusselt numbers, in the range of 5 to 10 for various flow rates and heat fluxes. Our

values, somehow, are closed to their values because of the similar geometry. Nevertheless, in our case, along with upward heating of the tube by the absorber plate, there is downward heating of the pipe's upper surface directly by radiation causing different heat transfer behavior that can not be properly predicted by available correlations and can not be validated by previous works.

4.5. CONCLUSION

The impact of free convection on the heat transfer between a horizontal tube wall and fluid in the forced circulation systems is very important and complex. When the flow rates are low, but temperature difference between pipe wall and bulk fluid temperature is significantly high, buoyant forces coupled with axial flow of the fluid creates a three dimensional motion. This combined effect of free and forced convection affects the velocity profile and the heat transfer coefficient inside the tube from which strong buoyant forces results improvement of Nusselt numbers.

In the present study, the effect of free convection on fully developed forced laminar flow in horizontal tube (of a flat-plate solar collector) with modified geometry is experimentally investigated. The study covered a wide range of low Reynolds number and high values of Grashof and Rayleigh numbers. Onset of secondary flow, due to buoyant forces has been discovered since the values of Nusselt numbers were significantly higher than that of theoretical constant property value (i.e.4.36). It was, moreover, found that due to high temperature difference between the tube wall and water and also due to low flow rates, buoyant forces are much stronger than shear forces. This results in domination of the free convection to forced convection heat transfer modes. Domination of the free convection, in turn, causes ineffectiveness of any heat transfer

augmentation passive methods that are based on introduction or increase of shear forces. Strong buoyant forces, either destruct shear production or highly turbulent the laminar flow, that make mechanical turbulence or vortices generation devices ineffective. In the present study several passive heat transfer enhancement methods applied onto a flat-plate collector, nevertheless, no improvement of heat transfer has been witnessed for variety of flow rates and heat inputs. In addition, no previous experimental study, within the literature, has been found to investigate combined effect of free and forced convection in such a complex geometry where heat is provided non-uniformly around the tube partly by downward radiation and partly upward conduction. This is very complex problem that requires more investigation, including flow visualization, theoretical study and extraction of the correlation formulas for Nusselt number.

CHAPTER 5

CONCLUSIONS AND RECOMMENDATIONS FOR THE FUTURE WORKS

5.1. OVERALL CONCLUSION

Solar energy, as the most abundant and cost-effective source of renewable energy, can be utilized even in the cold climates like Canada. In the present research, the possibility of utilizing solar energy for domestic water heating in the residential units is investigated for Montreal area. An indirect forced circulation solar water heating system is proposed and modeled for the cold climate. Using TRNSYS program, all important design parameters are studied and optimum values are determined. The solar fraction is used as the optimization parameter. The optimization included both the system and the collector design parameters that consists of required collector area, fluid type, collector mass flow rate, storage tank volume and height, heat exchanger effectiveness, size and length of connecting pipes, absorber plate material and thickness, number and size of the riser tubes, tube spacing; and the collector's aspect ratio.

An indoor experimental facility was also developed to evaluate the thermal performance of solar collectors. An attempt was made to increase the collector efficiency factor by improving the heat transfer coefficient between the tubes of the collector and the water. For this purpose, several passive heat transfer enhancement method were applied inside the tubes and studied. In this study, twisted strips were inserted inside the tubes to introduce swirl flow and tangential velocity component near the tube wall. Coil-spring wires were inserted to enhance turbulence by introducing helical surface roughness. Finally, diverging nozzles (conical ridges) inserted inside the tubes to generate vortices. The performance was analyzed based on the heat transfer to the

collector fluid for a wide range of flow rates and for two different incident radiant heat fluxes. The convection heat transfer mechanism inside the collector that is influenced by thermal stratification, buoyancy fluxes and shear flow, was investigated based on pertinent dimensionless parameters. For the flow rates that are typically used in the solar flat-plate collectors, values of Grashof, modified Grashof, Rayleigh, modified Rayleigh, and gradient Richardson numbers are found to be as high as 4×10^{6}, 4×10^{7}, 1.5×10^{7}, 1.6×10^{8}, 340, respectively. These results show that for the given geometry and configuration, free convection is the dominant heat transfer mode, forced convection is negligible, and the flow is thermally turbulent. Therefore, application of the any heat transfer enhancement method that is based on the production of shear forces is ineffective. The present study provides the first detailed thermal analysis to investigate the heat transfer augmentation in flat-plate solar collectors. The results have highlighted the complexity of the heat and fluid interactions, which need further in depth investigations.

5.2. FUTURE WORKS

Despite of the extensive investigations on solar water heating systems, there is a scarcity of the literature concerning solar water heating systems for the cold climates. Therefore, more theoretical and experimental investigations seem to be necessary. For instance, simulations can be conducted for other systems that can also be operated in the cold climate, such as drain-back systems with water or antifreeze as the working fluid, or the systems operated with phase-changing fluids. The long term performance of the present system can also be experimentally investigated in the actual outdoor conditions. Moreover, despite the extensive literature on the effect of combined free and forced

convection heat transfer inside the horizontal, vertical and inclined tubes, no work has been found that was focused on the investigation of mixed convection in solar collectors. Due to the specific geometry, flow rate range and heat transfer mechanism associated with solar collectors, the general trends observed in mixed convection through straight pipes cannot be implemented directly in solar collectors. Thus, there is a need to develop improved correlations for solar collectors. Furthermore, no significant work using advanced measurement and flow visualization methods, such as PIV and infrared imagery has been found even for uniformly heated horizontal tubes. Thus, these advanced techniques can also be used to study complex flow and thermal interactions in such applications.

5.3. CONTRIBUTION

The work presented in this thesis is preliminary which can be extended to an extensive future works on solar thermal systems for cold climate, in particular, the investigation of thermo-fluid behavior in such a complicated regime which is still poorly understood. An extensive literature review is conducted to summarize most of the related previous investigations on this subject. This review can be used to get ideas for further research. Contrary to most of the previously published studies that are focused on the natural circulation (thermosyphon) systems suitable for hot or moderate climates, a forced circulation system is modeled and all design parameters are optimized. This design can be used as a preliminary step towards the design and construction of efficient solar water heating systems for residential units in the cold climate. In the previous studies concerning the heat transfer enhancement devices, only an individual straight pipe was subjected to a uniform heat flux or constant wall temperature boundary condition. In

the present study, a flat-plate solar collector module is used to study the effect of modified geometry in the augmentation of the heat transfer rate from the tubes of the collector into the working fluid. In this setup the heat transfer mode to the collector is mainly radiation and partly convection, and because of this particular geometry and the modes of heat transfer, neither the heat flux nor the wall temperature are uniform over the entire geometry. Furthermore, flow rates, in this study, were kept very small which are typically much less than the range of flow rates studied in those previous studies. In addition no detailed study on the thermal behavior inside a solar collector has been reported in the literature.

REFERENCES

Abdel-Khalik, S.I.(1976), "Heat Removal Factor for a Flat-Plate Solar collector with a Serpentine Tube," *Solar Energy*, Vol.18, No.1, pp.59-64.

Abdullah, A.H., Abou-Ziyan, H.Z. and Ghoneim, A.A. (2003), "Thermal Performance of Flat Plate Solar Collector Using Various Arrangements of Compound Honeycomb," *Energy Conversion & Management*, Vol.44, pp. 3093-3112.

Abou-Ziyan, H.Z. and Richards, R.F. (1997), "Effect of Gap Thickness on a Rectangular-Cell Compound-Honeycomb Solar collector," *Solar Energy*, Vol.60, No.5,pp. 271-280.

Akyurt, M. (1984), "Development of Heat Pipes for Solar Water Heating," *Solar Energy*, Vol.32, No.5, pp. 625-631.

ASHRAE Handbook, *2005 Fundamentals*, Chapter 21, ASHRAE, Atlanta, GA, (2005).

ASHRAE Handbook, *2003 HVAC Application*, Chapter 33, ASHRAE, Atlanta, GA., (2003).

AMETEK Inc. *Solar Energy Handbook, Theory and Application.* 2nd ed. Chilton Book Company, Radnor, PA. (1984).

Babbitt, Harold E., *Plumbing*, 3rd ed., McGraw Hill, New York, (1960).

Barozzi, G.S., Zanchini, E., and Mariotti, M. (1985), "Experimental Investigation of Combined Forced and Free Convection in Horizontal and Inclined Tubes," *MECCANICA*, Vol. 20, pp. 18-27.

Baughn, J.W. and Young, M.F. (1984), "The Calculated Performance of a Solar Hot Water System for a Range of Collector Flow Rates," *Solar Energy*, Vol.32, No.2, pp. 303-305.

Becker, B.R. and Stogsdill K.E. (1990), "A Domestic Hot Water Use Database," *ASHRAE Journal*, Vol. 32 (9): pp. 21-25.

Beckman, W.A., Klein, S.A., and J.A.Duffie, *Solar Heating Design by the f-Chart Method*, John Wiley, New York, (1977).

Bonnefoi, C., Abid, C, Medale, M., and Papini, F. (2004),"Poiseuille-Benard Instability in a Horizontal Rectangular Duct Water Flow," *Int. Journal of Thermal Sciences*, Vol. 43, pp. 791-796.

Bergles, A.E. and Simonds, R.R. (1971), "Combined Forced and Free Convection for Laminar Flow in Horizontal Tubes with Uniform Heat Flux," *Int. Journal of Heat and Mass Transfer*, Vol. 14, pp. 1989-2000.

Bickle, L.W. (1975), "Passive Freeze Protection for Solar Collectors," *Solar Energy*, Vol. 17, No. 6, pp. 373-374.

Bliss, R.W. (1959), "The Derivations of Several 'Plate-Efficiency Factors' Useful in the Design of Flat Plate Solar Heat Collectors," *Solar Energy*, Vol. 3, pp. 55-64.

Buckless, W.E., and Klein, S.A. (1980), "Analysis of Solar Domestic Hot Water Heaters," *Solar Energy*, Vol.25, No. 5, pp. 417-424.

Brown, A.R. and Thomas, M.A. (1965),"Combined Free and Forced Convection Heat Transfer for Laminar Flow in Horizontal Tubes," *Jour. Mechanical Engineering Science*, Vol. 7, No.4, pp. 440-448.

Busse, F.H. (1978), "Non-Linear Properties of Thermal Convection," *Rep. Prog. Physics*, Vol. 41, UK.

Cathro, K., Constable, D. and Solaga, T. (1984), "Silica Low-Reflection Coating for Collector Covers, by a Dip-Coating Process," *Solar Energy*, Vol.32, No.5, pp. 573-579.

Chiou, J.P. (1982), "The Effect of Non-uniform Fluid Flow Distribution on the Thermal Performance of Solar collector," *Solar Energy*, Vol. 29, No. 6, pp. 487-502.

Chou, F.C. and Lien, W.Y. (1991),"Effect of Wall Heat Conduction on Laminar Mixed Convection in the Thermal Entrance Region of Horizontal Rectangular Channel," *Wärme- und Stoffübertragung*, Vol.26, pp. 121-127.

Chow, S.P. and Harding, G.L. (1985), "Effect of antireflection coating on the transmittance of glass tubular and plane double glazed covers for flat plate collectors," *Solar Energy*, Vol. 34, No.2, pp.183-186.

Chun, W., Kang, Y.H., Kwak, H.Y. and Lee, Y.S. (1999), "An Experimental Study of The Utilization of Heat Pipes for Solar Water Heaters," *Applied Thermal Engineering*, Vol.19, pp. 807-817.

Cooper, P.I. (1979), "The Effect of Inclination on the Heat Loss from Flat-Plate Solar Collectors," *Solar Energy*, Vol.27, No.5, pp. 413-420.

DeWinter, F. (1975), "Heat Exchanger Penalties in Double-Loop Solar Water Heating System." *Solar Energy*, Vol.17, pp. 335.

Duffie, J.A., and Beckman, W.A., *Solar Engineering of the Thermal Processes*, 2nd ed. John Wiley & Sons Inc., New York, (1991).

Durmuş, A., Durmuş. A., and Esen, M. (2002), "Investigation of Heat Transfer and Pressure Drop in a Concentric Heat Exchanger with Snail Entrance," *Applied Thermal Engineering*, Vol. 22, pp. 321–332.

Durmuş, A. (2004), "Heat Transfer and Exergy Loss in Cut Out Conical Turbulators," *Energy Conversion & Management*, No. 45, pp. 785-796.

Eaton, C.B. and Blum, H.A. (1975), "The Use of Moderate Vacuum Environment as a Means of Increasing the Collection Efficiencies and Operating Temperatures of a Flat-Plate Solar Collector," *Solar Energy*, Vol.17, pp.151-158.

Ede, A.J. (1961), "The Heat Transfer Coefficient for Flow in a Pipe," *Int. Journal of Heat and Mass Transfer*, Vol. 4, pp. 105-110.

Edlin, F. F. (1958), "Plastic Glazing for Solar Energy Application," *Solar Energy*, Vol. 2, No. 2, pp. 3-5.

Eisenmann, W., Vajen, K. and Ackermann, H. (2004), "On the Correlations between Collector Efficiency Factor and Material Content of Parallel Flow Flat-Plate Solar Collector," *Solar Energy*, Vol.76, pp. 381-387.

Environment Canada web site: http://www.climate.weatheroffice.ec.gc.ca/climate_normals/stnselect_e.html (Consulted in 2006).

Esen, M. and Esen, H. (2005), "Experimental Investigation of a Two-Phase Closed Thermosyphon Solar Water Heater," *Solar Energy,* Vol. 79, pp. 459-468.

Faris, G.N. and Viskanta, R. (1969), "An Analysis of Laminar Combined Forced and Free Convection Heat Transfer in a Horizontal Tube," *Int. Journal of Heat and Mass Transfer*, Vol. 12, pp. 1295-1309.

Fanney, A.H. and Klein, S.A. (1988), "Thermal Performance Comparisons for Solar Hot Water Systems Subjected to Various Collector and Heat Exchanger Flow Rates," *Solar Energy*, Vol.40, No.1, pp. 1-11.

Francken, J.C. (1984), "On the Effectiveness of a Flat Plate Collector," *Solar Energy*, Vol. 33, pp. 363-366.

Furbo, S. and Jivan Shah, L. (2003), "Thermal Advantages for Solar Heating Systems with a Glass Cover with Antireflection Surfaces," *Solar Energy*, Vol.74, pp.513-523.

Garg, H.P. and Datta, G. (1984), "The Top Loss Calculation for Flat Plate Solar Collectors," *Solar Energy*, Vol. 32, No.1, pp. 141-143.

Gani, R. and Symons, J.G. (1979), "Cover Systems for High Temperature Flat-Plate Solar Collectors," *Solar Energy*, Vol.22, No.6, pp. 555-561.

Ghamari, D.M. and Worth, R.A. (1992), "The Effect of Tube Spacing on the Cost-Effectiveness of a Flat-Plate Solar Collector," *Renewable Energy*, Vol. 2, No. 6, pp. 603-606.

Gilbert Associates Inc. EPRI EA-4006, Research Project 1101-1, Electric Power, Research Institute, Palo Alto, CA.,(1985)

Gombert, A., Glaubitt, W., Rose, K., Dreibholz, J., Blasi, B., Heinzel, A., Sporn, D., Doll, W., and Wittwer, V. (2000), "Antireflective Transparent Covers for Solar Devices," *Solar Energy*, Vol. 68, No. 4, pp. 357-360.

Groenhout, N.K., Behnia, M. and Morrison, G.L. (2002), "Experimental measurement of heat loss in an advanced solar collector," *Experimental Thermal and Fluid Science*, Vol. 26, pp. 131-137.

Gupta, A.K., Lilley, D.G. and Syred, N. (1984). *Swirl Flows*., England, Abaccus Press; 1984.

Gutierrez, G., Hincapie, F., Duffie, A. and Beckman, W.A. (1974), "Simulation of Forced Circulation Water Heaters; Effect of Auxiliary Energy Supply, Load Type and Storage Capacity," *Solar Energy*, Vol. 15, No. 4, pp. 287-298.

Haberl, J. S. (2004),"Literature Review of Uncertainty of Analysis Methods (F-Chart Program)," Texas Engineering Experiment Station (TEES), Texas A&M University System, ESL-TR-04/08-04.

Habib, M.A. and Negm, A.A.A (2001),"Laminar Mixed Convection in Horizontal Concentric Annuli with Non-Uniform Circumferential Heating," *Heat and Mass Transfer*, Vol. 37, pp. 427-435.

Hahne, E.(1985), "Parameter Effects on Design and Performance of Flat Plate Solar Collector," *Solar Energy*, Vol.34, No.6, pp.497-504.

Hammad, M. (1995), "Experimental Study of The Performance of a Solar Collector Cooled by Heat Pipe," *Energy Conversion & Management*, Vol. 36, No. 3, pp. 197-203.

Hendron, R. (Feb. 2005),"Building America Research Benchmark Definition," Publication No. NREL/TP-550-37529, Colorado.

Hiller, C.C. (1998), "New Hot Water Consumption Analysis and Water-Heating System Sizing Methodology," *ASHRAE Transactions: Symposia. SF-98-31-3.*

Hollands, K.G. and Lightstone, M.F.(1989), "A Review of Low-Flow, Stratified-Tank Solar Water Heating System," *Solar Energy*, Vol.43, No.2, pp.97-105.

Hollands, K.G. and Stedman B.A. (1992), "Optimization of an Absorber Plate Fin Having a Step-Change in Local Thickness," *Solar Energy*, Vol. 49, No. 6, pp. 493-495.

Hollands, K.G.T. (1965), "Honeycomb Devices in Flat Plate Solar Collectors," *Solar Energy*, Vol. 9, No. 3, pp. 159-64.

Hong, S.W., and Bergles, A.E. (1976), "Augmentation of Laminar Flow Heat Transfer in Tubes by Means of Twisted-Tape Insert," *Trans. of ASME, Series C, Journal of Heat Transfer*, Vol. 98, No.1, pp. 251-256.

Hottel, H.C., and Woertz, B.B. (1942), "Performance of Flat Plate Solar Heat Collectors," *Trans. ASME*, Vol. 64 pp.91-104.

Hottel, H.C. and Unger, T.A. (1959), "The Properties of a Copper Oxide-Aluminum Selective Black Surface Absorber of Solar Energy," *Solar Energy*, Vol. 3, No.3, pp. 10-15

Hussein, H.M.S., Mohamad, M.A. and El-Asfouri, A.S. (1999), "Optimization of a Wickless Heat Pipe Flat Plate Solar Collector," *Energy Conversion & Management*, Vol.40, pp. 1949-1961.

Hussein, H.M.S., El-Ghetany, H.H. and Nada, S.A. (2006), "Performance of Wickless Heat Pipe Flat Plate Solar Collectors Having Different Pipes Cross Sections Geometries and Filling Ratios," *Energy Conversion & Management*, Vol. 47, pp. 1539-1549.

Incropera F.P., De Witt D.P., Bergman TH.L., and Lavine A.S. (2007), *Fundamentals of Heat and Mass Transfer*, 6th ed. John Wiley & Sons, NY.

Iqbal, M. (1966), "Free-Convection Effects Inside Tubes of Flat-Plate Solar Collectors," *Solar Energy*, Vol. 10, No. 4, pp. 207-211.

Iqbal, M. (1979*a*), "A study of Canadian diffuse and total solar radiation data –I, Monthly average daily horizontal radiation," *Solar energy*, Vol. 22, pp. 81-86.

Iqbal, M. (1979*b*), "Optimum Collector Slope for Residential Heating in Adverse Climates," *Solar Energy*, Vol.22, No. 1, pp.77-79.

Jordan, U. and Vajen, K. (2000), "Influence of the DHW Load Profile on the Fractional Energy Saving: A Case Study of a Solar Combi-System with TRNSYS Simulation," *Solar Energy*, Vol. 69(suppl.), pp. 197-208.

Jones, G.F. and Lior, N. (1994), "Flow Distribution in Manifolded Solar Collectors with Negligible Buoyancy Effects," *Solar Energy*, Vol. 52, No. 3, pp. 289-300.

Joudi,Kh.A., and A.M. Witwit, A.M. (2000), "Improvements of gravity assisted wickless heat pipes," *Energy Conversion & Management,* Vol. 41, pp. 2041-2061.

Junkhan, G.H., Bergles, A.E., Nirmalan, V., and Ravigururajan T. (1985), "Investigation of Turbulators for Fire Tube Boilers," *Trans. of ASME, Journal of Heat Transfer,* No. 107, No. 2, pp. 354–360.

Kalogirou, S.A. and Papamaracou, C. (2000), "Modeling of a Thermosyphon Solar Water Heating System and Simple Model Validation," *Renewable Energy*, Vol. 21, pp. 471-493.

Kautsch, P., Dreyer, J. and Hengsberger, H. (2002), "Thermisch-hygrisches Verhalten von Glas Doppelfassaden unter Solarer Einwirkung," Bundesministerium für Erergie und Umwelttechnologien, Wien.

Kettleborough, C.F. (1959), "Experimental Results on Thermostatically Controlled Solar Water Heaters," *Solar Energy*, Vol.3, No.1, pp. 55-58.

Kempton, Willett (1987), "Residential Hot Water: A Behaviorally-Driven System," *Energy Efficiency: Perspectives on Individual Behavior,* American Council for an Energy-Efficient Economy, Washington, D.C.

Kern, J. and Harris, I. (1975), "On the Optimum Tilt of a Solar Collector," *Solar Energy*, Vol.17, No.2, pp. 97-102

Kena, J.P. (1983), "The Thermal Trap solar collectors," *Solar Energy*, Vol.31, No.3, pp. 335-338.

Khalifa, A. N. (1999), "Thermal Performance of Locally Made Flat Plate Solar Collectors Used as Part of a Domestic Hot Water System," *Energy Conversion & Management*, Vol. 40, pp. 1825-1833.

Khan, E. U. (1967), "Evaluation of Bond Conductance in Various Tube-in-Strip Types of Solar Collectors," *Solar Energy*, Vol. 11, No.2, pp. 95-97.

Kikas, N.P. (1995), "Laminar Flow Distribution in Solar System," *Solar Energy*, Vol.54, No.4, pp. 209-217.

Klein, S.A. et al. (2004), TRNSYS Version. 16, Solar Energy Laboratory, University of Wisconsin-Madison, Website: http://sel.me.wisc.edu/trnsys.

lein, S.A., Beckman, W .A. and Duffie, J. A. (1976), "A Design Procedure for Solar Heating Systems," *Solar Energy*, Vol. 18, No. 2, pp. 113-127.

Klein, S.A. (1975), "Calculation of flat-plate collector loss coefficient," *Solar Energy*, No. 17, pp. 79-80.

Kokoropoulos P., Salam E., Daniels F. (1959), "Selective Radiation Coating. Preparation and High Temperature Stability," *Solar Energy*, Vol. 3, No. 4, pp. 19-23.

Lenel, U.R. and Mudd, P.R. (1984), "A Review of Material for Solar Heating System for Domestic Hot Water," *Solar Energy*, Vol. 32, No. 1, pp. 109-120.

Liu, B.Y.H. and Jordan, R. (1963), "The Long-Term Average Performance Of Flat-Plate Solar-Energy Collector," *Solar Energy*, Vol. 7, No.2, pp.53-74.

Lu, S.M., Li, Y.C.M. and Tang, J.C. (2003), "Optimum Design Of Natural-Circulation Solar-Water-Heater by the Taguchi Method," *Energy*, Vol.28, pp. 741-750.

Lutz, James (2005), "Estimating Energy and Water Losses in Residential Hot Water Distribution Systems," Lawrence Berkeley National Laboratory, LBNL57199, CA.

Malhorta, A., Garg, H.P. and Palit, A. (1981), "Heat loss Calculation of Flat Plate Solar Collector," *Thermal Energy*, Vol. 2, No. 2.

Malsliyah, J.H. and Nandakumar, K. (1976), "Heat Transfer in Internally Finned Tubes," *Trans. of ASME, Series C Journal of Heat Transfer*, Vol. 98, No. 1, pp. 257-261.,

Majda, A.J. and Shefter, M. (1998), "The Instability of Stratified Flow at Large Richardson Numbers," *Applied Mathematics*, Vol. 95, pp. 7850-7853.

Marcoux, C., and Dumas, C. (2004), "Température de l'eau dans l'aqueduc de Montréal. http://www.ashrae-mtl.org/text/f_ashrae.html (Consulted in Aug. 2006).

Mathioulakis, E. and Belessiotis, V. (2002), "A New Heat-Pipe Type Solar Domestic Hot Water System," *Solar Energy*, Vol. 72, No. 1, pp. 13-20.

Maure, D. and Galanis, N. (1979), "Solar Radiation Data for Quebec," *Solar Energy*, Vol. 23, pp. 309-314.

McComas, S.T. and Eckert, E.R.G. (1966), "Combined Free and Force Convection in a Horizontal Circular Tube," *Journal of Heat Transfer, Trans. of the ASME*, Vol 88, pp. 147-153.

Mills, D. and Morrison, G.L. (2003), "Optimization of Minimum Backup Solar Water Heating System," *Solar Energy*, Vol. 74, pp. 505-511

Michaelides, I.M. and Wilson, D.R. (1997), "Simulation Studies of the Position of the Auxiliary Heater in Thermosyphon Solar Water Heating Systems," *Renewable Energy*, Vol. 10, No. 1, pp. 35-42.

Michaelides, I.M. and Wilson, D.R. (1996), "Optimum Design Criteria for Solar Hot Water System," *Renewable Energy,* Vol. 9, Issues 1-4, pp. 649-652.

Morrison, G.L. and Braun, J.E. (1985), "System Modeling and Operation Characteristics of Thermosyphon Solar Water Heaters," *Solar Energy*, Vol. 34, No.4/5, pp. 389-405.

Morcos S.M., and Bergles, A.E. (1975), "Experimental Investigation of Combined Forced and Free Laminar Convection in Horizontal Tubes," *Journal of Heat Transfer, Trans. of the ASME*, Vol 97, pp. 212-219.

Mori, Y. and Futagami, K. (1967), "Forced Convection Heat Transfer Uniformly Heated Horizontal Tubes," *Int. Journal of Heat and Mass Transfer*, Vol. 10, pp. 1801-1813.

Mutch, J.J. (1974), "Residential Water Heating: Fuel Conservation, Economics and Public Policy," *RAND Report*, R-1498.

NAHB Research Center, Inc. (2002), "Domestic Hot Water System Modeling for the Design of Energy efficient Systems," Marlboro, MD.

Naphon, P., Nuchjapo, M., and Kurujareon, J. (2006), "Tube Side Heat Transfer Coefficient and Friction Factor Characteristics of Horizontal Tubes with Helical Rib," *Energy Conversion & Management*, No. 47, pp. 3031–3044.

Narezhnyy, EG., and Sudarev, AV. (1971), "Local Heat Transfer in Air Flowing in Tubes with a Turbulence Promoter at the Inlet," *Int. Journal of Heat and Mass Transfer,* No. 2–3, pp.62–66.

Newell, P.H. and Bergles, A.E. (1970), "Analysis of Combined Free and Forced Convection for Fully Developed Laminar Flow in Horizontal Tubes," *Journal of Heat Transfer, Trans. of the ASME*, Vol 92, pp. 83-89.

Perlman, M. and Mills, B.E. (1985), "Development of Residential Hot Water Patterns," *ASHRAE Transactions*, Vol. 91, Part 2A, pp. 657-679. ASHRAE, Atlanta, GA,

Piva, S., Barozzi, G.S., and Collins, M.W. (1995),"Combined Convection and Wall Conduction Effects in Laminar Pipe Flow: Numerical Predictions and Experimental Validation Under Uniform Wall Heating," *Heat and Mass Transfer*, Vol. 30, pp. 401-409.

Plante, R.H. (1983), *Solar Domestic Hot Water: A Practical Guide to Installation and Understanding*, New York, John Wiley & Sons.

Pluta, Z. and Pomierny, W. (1995), "The Theoretical and Experimental Investigation of the Phase-Change Solar Thermosyphon," *Renewable Energy*, Vol.6, No.3, pp. 317-321.

Promvonge, P., and Eiamsa-ard, S. (2006), "Heat Transfer Enhancement in a Tube with Combined Conical-Nozzle Inserts and Swirl Generator," *Energy Conversion & Management,* No. 47, pp. 2867–2882.

Rao, S.K. and Suri, R.K. (1969), "Optimization of Flat-Plate Solar Collector Area," *Solar Energy*, Vol. 12, pp. 531-535.

Reddy, KS. and Kaushika, ND. (1999), "Comparative Study of TIM Cover Systems for Integrated-Collector-Storage Solar Water Heaters," *Solar Energy Materials and Solar Cells*; Vol.58, pp. 431-446

Rommel, M. and Moock, W. (1997), "Collector Efficiency factor F' for Absorbers with Rectangular Fluid Ducts Containing the Entire Surface," *Solar Energy*, Vol. 60, Nos. 3/4, pp. 199-207.

San Martin, R.L. and Fjeld, G.J. (1975), "Experimental Performance of Three Solar Collectors," *Solar Energy*, Vol. 17, No. 6, pp. 345-349.

Shannon, R.L. and Depew, C.A. (1968), "Combined Free and Forced Laminar Convection in a Horizontal Tube with Uniform Heat Flux," *Journal of Heat Transfer, Trans. of the ASME*, Vol 90, pp. 353-357.

Shariah, A.M. and Ecevit, A. (1995), "Effect of Hot Water Load Temperature on the Performance of a Thermosyphon Solar Water Heater with Auxiliary Electric Heater," *Energy Conversation & Management*, Vol. 36, No. 5, pp. 289-296.

Shariah, A.M. and Löf, G.O.G (1996), "The Optimization of Tank-Volume-to-Collector-Area Ratio for a Thermosyphon Solar Water Heater," *Renewable Energy*, Vol. 7, No.3, pp. 289-300.

Shariah, A.M. and Löf, G.O.G (1997), "Effects of Auxiliary Heater on Annual Performance of Thermosyphon Solar Water Heater Simulated under Variable Operating Conditions," *Solar Energy*, Vol. 60, No. 2, pp. 119-126.

Shariah, A. and Shalabi, B. (1997), "Optimal Design for a Thermosyphon Solar Water Heater," *Renewable Energy*, Vol. 11, No. 3, pp. 351-361.

Shariah, A.M., Rousan, A., Rousan, Kh.K. and Ahmad, A.A. (1999), "Effect of Thermal Conductivity of Absorber Plate on the Performance of a Solar Water Heater," *Applied Thermal Engineering*, Vol. 19, pp.733-741.

Shariah, A., Al-Akhra, M.A. and Al-Omari, I.A. (2002), "Optimizing the Tilt Angle of Solar Collectors," *Renewable Energy*, Vol. 26, pp. 587-598.

Shing-An, W. (1974), "An Experimental Study of Corrugated Steel Sheet Solar Water Heater," *Solar Energy*, Vol. 23, pp. 333-341.

Siebers, D. L. and Viskanta, R. (1977), "Comparison of Predicted Performance of Constant Outlet Temperature and Constant Mass Flow Rate Collectors," *Solar Energy*, Vol. 19, No. 4, pp. 411-413.

Siegwarth, D.P. ,Miksell, R.D., Readal, T.C., and Hanratty, T.J. (1969)," Effect of Secondary Flow on the Temperature Filed and Primary Flow in a Heated Horizontal Tube," *Int. Journal of Heat and Mass Transfer*, Vol. 12, pp. 1535-1552.

Smithberg, E., and Landis, F. (1964), "Friction and Forced Convection Heat-Transfer Characteristics in Tube with Twisted Tape Swirl Generators," *Trans. of ASME, Series C, Journal of Heat Transfer*, Vol. 86, No. 1, pp. 39-49.

Soin, R.S., Sangameswar, R, Rao, D.P. and Rao, K.S. (1979), "Performance of Flat Plate Solar Collector with Fluid Undergoing Phase Change," *Solar Energy*, Vol.23 No.1,pp. 69-73.

Soin, R.S., Raghuraman, S. and Murali, V. (1987), "Two-Phase Water Heater: Model and Long term Performance," *Solar Energy*, Vol.38, No.2, pp. 105-112.

Thorsen, R. and Landis, F. (1968), "Friction and Heat Transfer Characteristics in Turbulent Swirl Flow Subjected to Large Transverse Temperature Gradient," *Trans. of ASME, Series C, Journal of Heat Transfer*, Vol. 90, No. 1, pp. 87-97.

Tiris, Ç., Tiris, M. and Türe, ie (1995), "Effects of Fin Design on Collector Efficiency," *Energy*, Vol.20, No.10, pp.1021-1026.

Tiwari, R.C., Kumar, A., Gupta, S.K. and Sootha, G.D. (1991), "Thermal Performance of Flat-Plate Solar Collectors Manufactured in India," *Energy Conversation & Management*, Vol. 31, pp. 309-313.

Tripanagnostopoulos, Y., Souliotis, M. and Nousia, TH. (2000), "Solar Collectors with Colored Absorbers," *Solar Energy*, Vol. 68, No. 4, pp. 343-356.

Turner, J.S. (1973), *Buoyancy Effects in Fluids*, Cambridge At The University Press, UK.

Uhlemann, R. and Bansal, N.K. (1985), "Side-by-Side Comparison of a Pressurized and a Non-Pressurized Solar Water Heating Thermosyphon System," *Solar Energy*, Vol. 34,No. 4/5, pp. 317328.

Usibelli, A. (1984), "Monitored Energy Use of Residential Water Heaters," Lawrence Berkeley National Laboratory, LBNL7873.

U.S. Department of Energy, *Household Energy Consumption and Expenditures19937, Part 1: National Data*, Washington, DC: Energy Information Administration.DOE/EIA-0321/1(1993).

US Department of Energy, Energy Efficiency and Renewable Energy, *A Consumer's Guide to Energy Efficiency and Renewable energy: Sizing a Solar Water Heating System.* (Consul. in April 2006) http://www.eere.energy.gov/consumer/your_home/water_heating

Wang, X.A. and Wu, L.G. (1990), "Analysis and Performance of Flat-Plate Solar Collector Arrays," *Solar Energy*, Vol. 45, No. 2, pp. 71-78.

Weitbrecht, V., Lehmann, D. and Richter, A. (2002), "Flow Distribution in Solar Collector with Laminar Flow conditions," *Solar Energy*, Vol. 73, No. 6, pp. 433-441.

Whiller, Austin (1964), "Thermal Resistance of the Tube-Plate Bond in Solar Heat Collectors," *Solar Energy*, Vol. 8, No. 3, pp. 95-98.

Whillier, A. and Saluja, G. (1965), "Effect of Materials and Construction Details on The Thermal Performance of Solar Water Heaters," *Solar Energy*, Vol. 9, No.1, pp.21-26.

White, F.M. (1991), *Viscous Fluid Flow*, 2nd ed., McGraw Hill, NY.

Wijeysundera, N.E. and Iqbal, M. (1991), "Effect of Plastic cover thickness on Top Loss Coefficient of Flat-Plate Collectors," *Solar Energy*, Vol.46, No.2, pp.83-87.

Wilcox, B.A. and Barnaby, S. (1977), "Freeze Protection for Flat-Plate Collectors Using Heating," *Solar Energy*, Vol.19, No.6, pp. 745-746.

Wongsuwan, W. and Kumar, S. (2005), "Forced Circulation Solar Water Heater Performance Prediction by TRNSYS and ANN," *International Journal of Sustainable Energy*, Vol. 24, No. 2, pp. 69–86.

Xinian, J, Zhen, T., Junsheng, L, and Hougchuan, G. (1994), "Theoretical and Experimental Studies on Sequential Freezing Solar Water Heaters," *Solar Energy*, Vol. 53, No. 2, pp. 139-146.

Yeh, H.M., Ho, C.D. and Yeh C.W. (2003), "Effect of Aspect Ratio on the Collector Efficiency of Sheet-And–Tube Solar Water Heaters with the Consideration of Hydraulic Dissipated Energy," *Renewable Energy*, Vol. 28, pp. 1575-1586.

Yildiz, C., Bicer, Y., and Pehlivan, D. (1998), "Effect of Twisted Strips on Heat Transfer and Pressure Drop in Heat Exchangers," *Energy Conversion & Management*, Vol. 39, No. 3/4, pp. 331-336.